NASA Technical Memorandum 4051

# Design and Testing of a High Power Spacecraft Thermal Management System

Michael E. McCabe, Jr.
*Goddard Space Flight Center*
*Greenbelt, Maryland*

Jentung Ku
*OAO Corporation*
*Greenbelt, Maryland*

Steve Benner
*TS Infosystems, Inc.*
*Lanham, Maryland*

National Aeronautics
and Space Administration

**Scientific and Technical
Information Division**

**1988**

# Preface

This report presents the design and test results of an ammonia hybrid capillary pumped loop thermal control system which could be used for heat acquisition and transport on future large space platforms and attached payloads such as those associated with the NASA Space Station. The High Power Spacecraft Thermal Management (HPSTM) system can operate as either a passive, capillary pumped, two-phase temperature control system, or as a mechanically pumped loop.

The system consists of an evaporator section, a condenser section, liquid and vapor transport lines, a mechanical pump, and a reservoir. In the evaporator section, heat is applied to three parallel cold plates, each with a surface area of 0.186 $m^2$. The applied heat could represent the heat dissipated by a payload, instrument, or electronics which would be mounted to the plate. Within each plate are four capillary pumps. These pumps serve the dual functions of evaporating the liquid ammonia and circulating the fluid through the loop. All pressure head is provided by capillary action, precluding the need for a mechanical pump. Vapor from the evaporator flows through 10 meters of tubing to the condenser section. There, the heat is rejected in a tube-in-shell heat exchanger. Liquid is returned to the evaporator section via 10 meters of aluminum tubing.For mechanically pumped (hybrid) operations, a mechanical pump in the liquid line and in series with the capillary pumps increases the flow and heat transport capacity of the system.

Testing has shown that in the capillary-mode, the HPSTM evaporators can acquire a total heat load of between 600 W and 24 kW, with a maximum heat flux density of 4.3 $W/cm^2$. With the mechanical pump circulating the ammonia, a heat acquisition potential of 52 kW (9 $W/cm^2$ heat flux density) has been demonstrated for 15 minutes without an evaporator failure. These results represent a significant improvement over the maximum heat transport capacity previously displayed in other capillary systems. The hybrid system still retains the proven capillary capabilities of temperature control, heat load sharing and flow control between evaporator plates, rapid power cycling, and pressure priming recovery of deprimed evaporators. Results of a computer model of pressure drops across the capillary pumps agree closely with actual differential pressure transducer data.

LIST OF FIGURES

LIST OF TABLES

# 1 INTRODUCTION

## 1.1 Future Thermal Requirements

Future spacecrafts will have significantly more challenging thermal design requirements than those of past and present systems. Temperature control of the next generation of space platforms and large spacecrafts such as NASA's Space Station will require thermal systems that can acquire, transport, and reject many kilowatts of heat over distances up to 100 meters in length to keep on-board equipment and instruments within their allowable temperature range, while not overburdening the craft with excessive weight penalties and costs. Many studies have shown that two-phase thermal systems which utilize an evaporation-condensation cycle are significantly more efficient than conventional single-phase loops for managing large heat loads and long transport lengths, and offer a nearly uniform temperature throughout the loop regardless of the heat load.

## 1.2 Capillary Pumped Thermal Control Systems

Two-phase heat transport systems which utilize the surface tension forces established in a fine-pore polyethylene wick to circulate the system's working fluid, precluding the need for a mechanical pump, have proven performance characteristics that are capable of meeting thermal requirements defined for platforms and attached payloads on the NASA Space Station. The Capillary Pumped Loop (CPL) has evolved over the past four years, and has exhibited up to an 8 kW heat load capacity over a 10 meter transport distance in a one-g environment (1-3). A small-scale CPL experiment has twice been flight tested aboard the Space Shuttle, verifying thermal control capability in a microgravity environment (4). The CPL systems tested to date have exhibited characteristics which include high heat flux densities (<1 $W/cm^2$), temperature and fluid flow control among multiple parallel evaporators, pressure priming evaporator recovery, and the capacity to share heat between evaporators.

## 1.3 Hybrid Thermal Control Systems

One advantage of utilizing a totally passive thermal control loop such as the CPL is that there are no moving parts within the system. Such a thermal system would be desirable in an application where vibrations must be minimized, or on an autonomous, free-flying platform. All pressure required to circulate the working fluid is established by capillary action in the evaporator section. The maximum pressure head which can be developed by capillary action dictates the maximum flow rate and heat load capacity of the thermal system.

For some spacecrafts, the normal operating mode may be such that the passive thermal system will always be adequate for temperature control. However, the thermal system may become subjected to a heat load greater than the capillary limit, either because of the evolutionary growth of the spacecraft, or due to a sudden, short-term spike in the power system which must be transported from the heat source to the radiator. For such a situation, a mechanical pump can be installed in a CPL system to increase its heat load handling capacity by augmenting the capillary pumps with an additional source of pressure head.

The feasibility of operating a system that can be run as either a capillary pumped loop or a hybrid loop was the main objective of the HPSTM test program. The system was designed to manage heat loads up to 10 kW steady-state in the capillary-mode, with a transient demonstration power of 50 kW in the hybrid configuration, using anhydrous ammonia as the working fluid.

The HPSTM system was built for the United States Air Force (AFWAL,Thermal Technology Group , Wright Patterson Air Force Base) by the OAO Corporation, under a subcontract from the Boeing Aerospace Company. After some initial testing by OAO, the loop was loaned to NASA/Goddard Space Flight Center (GSFC) for one year for hardware modifications and additional testing. The results of this latest test program, performed by GSFC and OAO personnel at the OAO Heat Pipe Laboratory from September,1987 to January,1988 are presented in this report.

# 2 SYSTEM DESIGN AND OPERATING PRINCIPLES

The HPSTM system is a capillary pumped loop installed with a mechanical pump to accommodate higher heat loads than experienced by other CPL systems built to date. In order to understand the operational characteristics of the HPSTM, one must first know the principles behind the CPL.

## 2.1 The Capillary Pumped Loop

The design of a CPL, illustrated in Figure 2-1, consists of an evaporator, a vapor transport line, a condenser and subcooler ,a liquid line, and a reservoir. The CPL is a continuous loop, with vapor and liquid flowing in the same direction. The system operates as follows: when heat is applied to the evaporator, liquid evaporates from the saturated ultra-high molecular weight polyethylene wick and flows through the vapor line to the condenser zone, where the heat is removed. Flow in the condenser consists initially of high-speed vapor flow plus a liquid wall film which subsequently becomes "slug" flow. The fluid passes

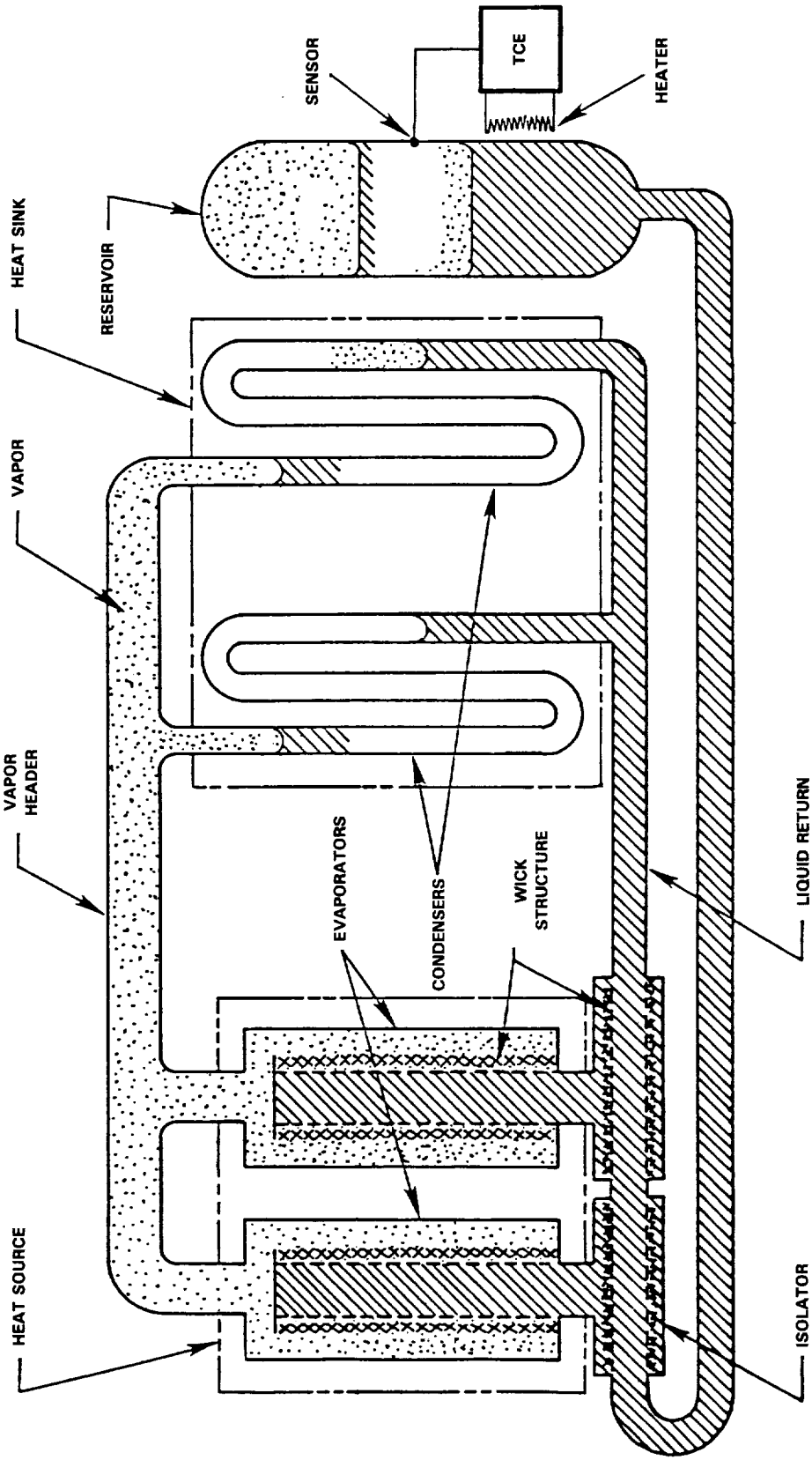


Figure 2-1. Capillary Pump Loop Design

through a subcooler to ensure complete condensation of all vapor bubbles as well as to provide enough subcooling to the fluid to prevent any vaporization before the liquid reaches the evaporators. A liquid return line connects the subcooler to the evaporators, completing the loop.

The CPL is different from the heat pipe in that the wick structure is only required in the evaporator section. Also, the self-regulating nature of the parallel capillary pumps eliminates the need for flow-control valves. Using smooth-walled tubing in the remainder of the system without valves reduces the pressure losses in the system. With a lower pressure drop, higher heat transport limits are attainable than are possible with heat pipes. In the CPL as well as in heat pipes, the meniscus naturally adjusts to establish the pumping head needed to match the flow losses associated with the applied heat load and condenser conditions.

## 2.2 The Hybrid Capillary Pumped Loop

The HPSTM system is a CPL which was designed so that it could be operated in either the purely passive mode or in the hybrid configuration ,whereby a positive displacement gear pump in a bypass to the liquid return line augments the flow capability of the capillary evaporators. The HPSTM system tested in this program is illustrated in Figure 2-2. It consists of three evaporator cold plates with four capillary pump evaporators on each cold plate, a condenser and integral subcooler, a reservoir which acts as a saturation temperature controller and fluid inventory manager, a gear pump and thermal flowmeter in the liquid line bypass for the hybrid operating configuration, and 10 meters (32.8 ft) each of smooth-walled aluminum liquid and vapor transport lines. A manually-controlled flow bypass valve is used to switch operating modes between the capillary and mechanically-pumped configurations. A photograph of the actual system is shown in Figure 2-3. The evaporator plates are in the foreground, while the condenser is in the background.

### 2.2.1 Evaporator Section

In the evaporator section, four 0.609 m (2 ft) active length aluminum capillary evaporator pumps were metallurgically bonded to a 1.9 cm (.75 in) thick aluminum plate to achieve the cold plate configuration shown in Figure 2-4. Each cold plate has a separate isolator and minor vapor header. The isolator, shown in Figure 2-5, consists of a stainless steel tube swaged around the same type of porous tubular wick used in the evaporator pump, though with a 20 micron average pore size. Each isolator is fed with liquid from the liquid return line as shown in Figure 2-2. The purpose of the isolator is to prevent vapor back flow to the inlet of any other evaporator pump from a deprimed evaporator,

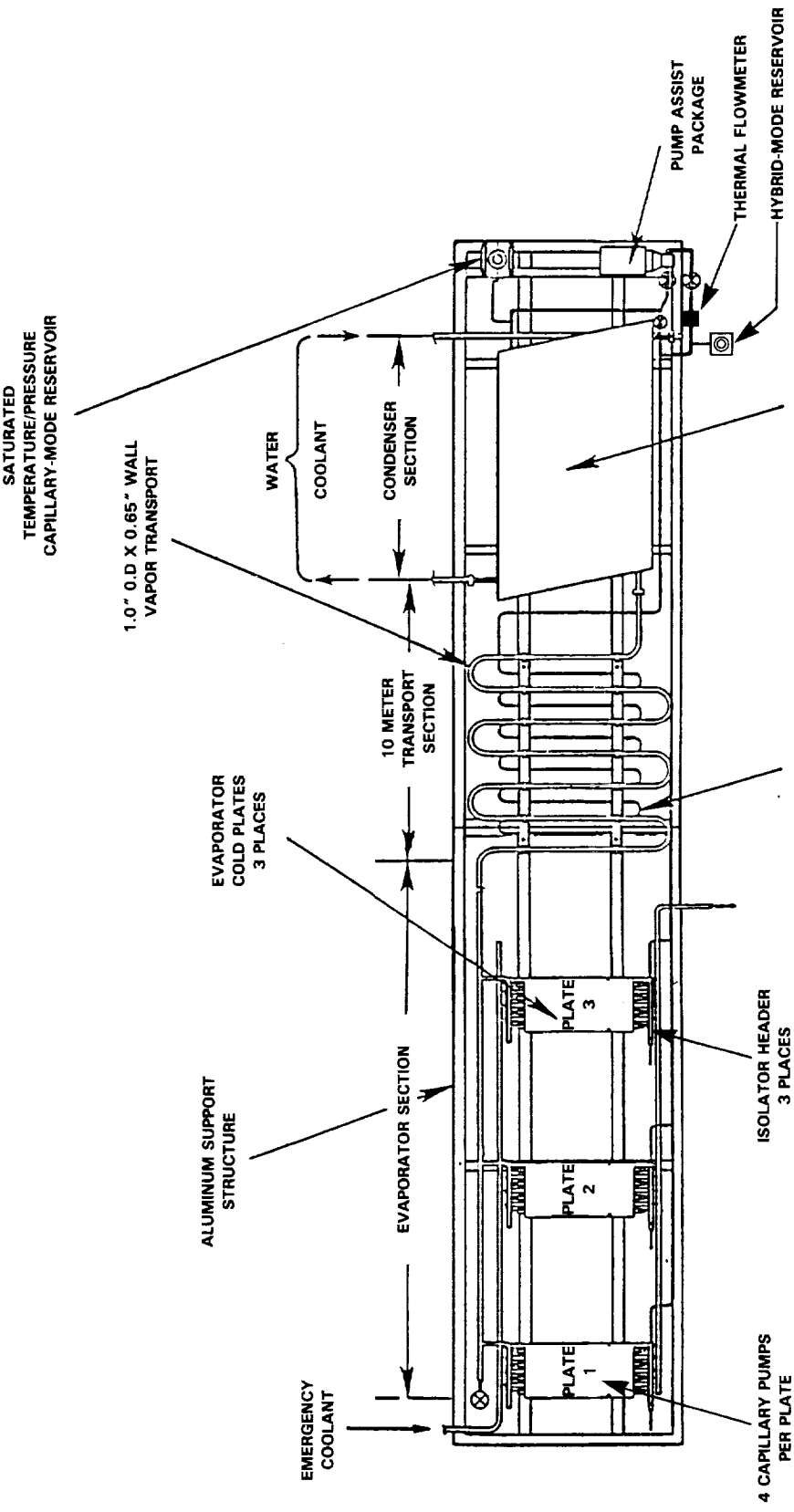


Figure 2-2. High Power Spacecraft Thermal Management (HPSTM) System

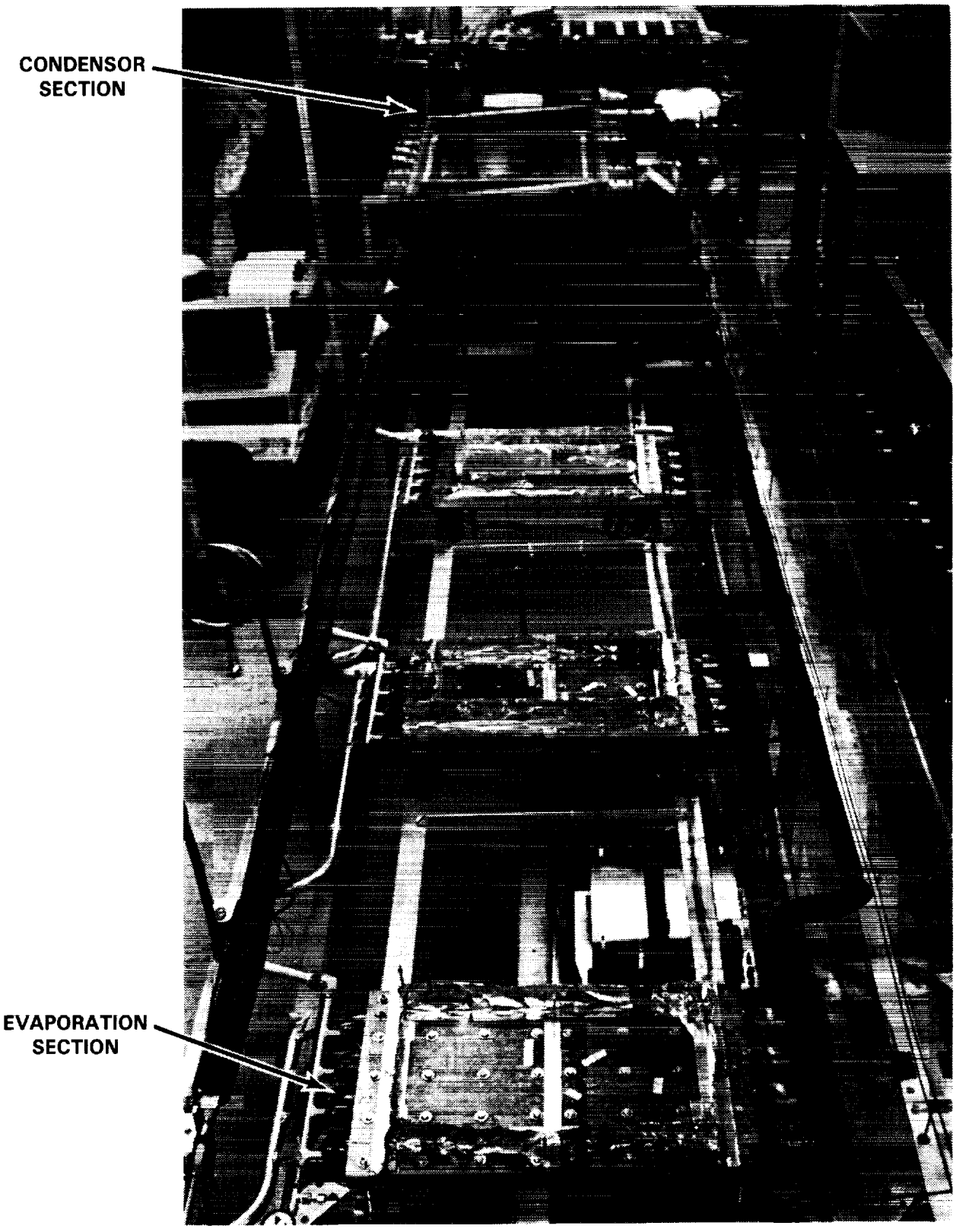


Figure 2-3. HPSTM CPL Demonstration System

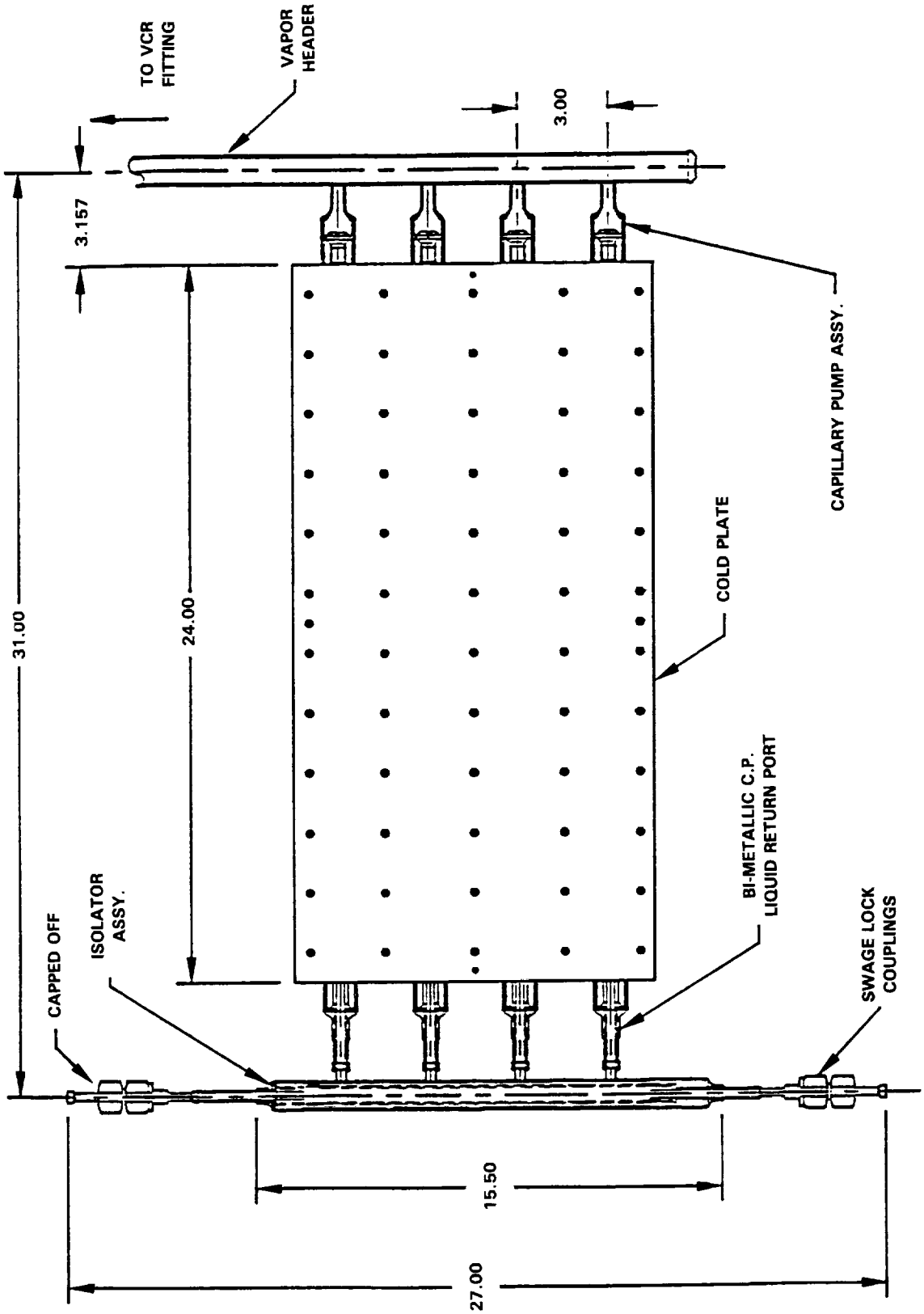


Figure 2-4. HPSTM Evaporator Plate Assembly

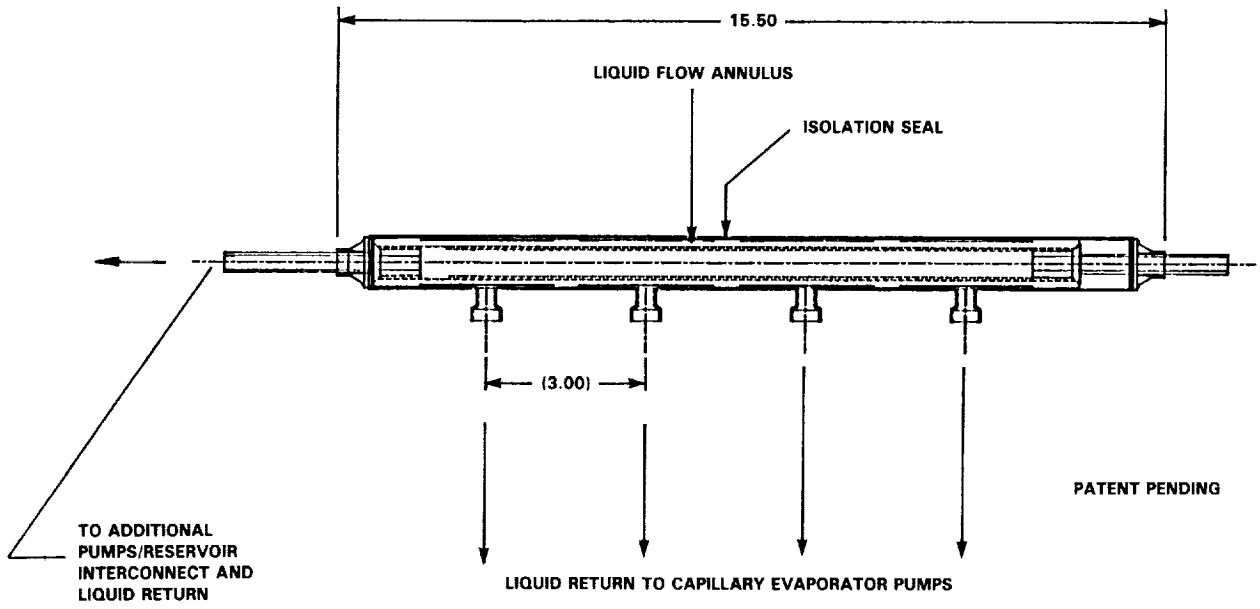


Figure 2-5. Isolator Assembly

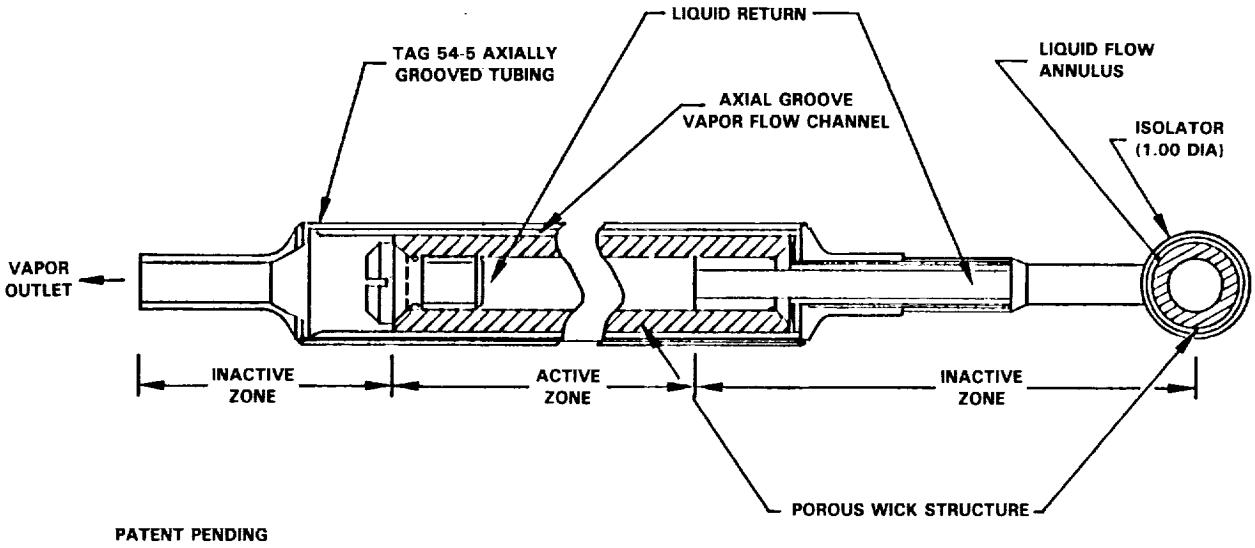


Figure 2-6. Capillary Pump Evaporator

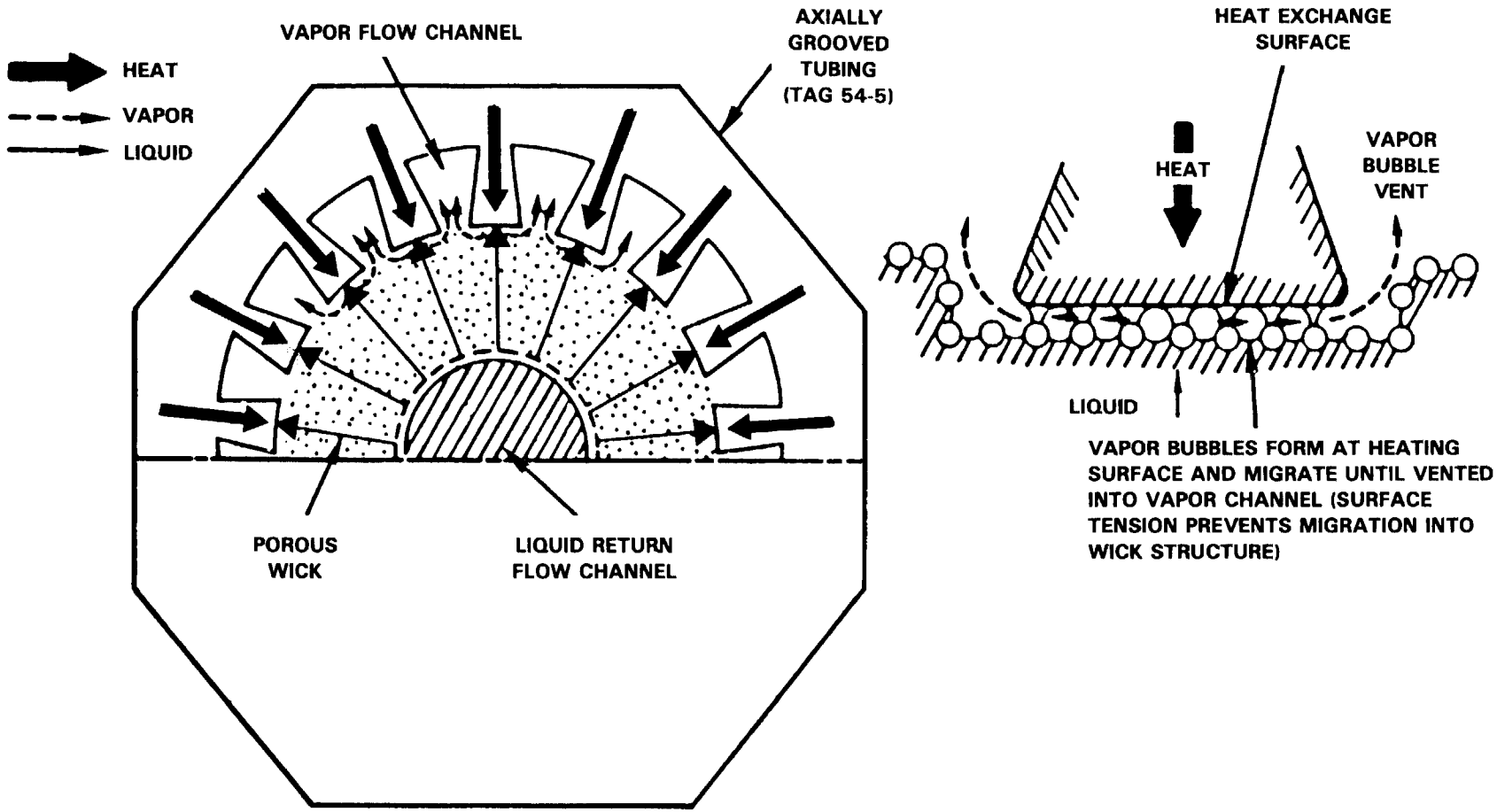


Figure 2-7. CPL Evaporator Heat and Fluid Transfer

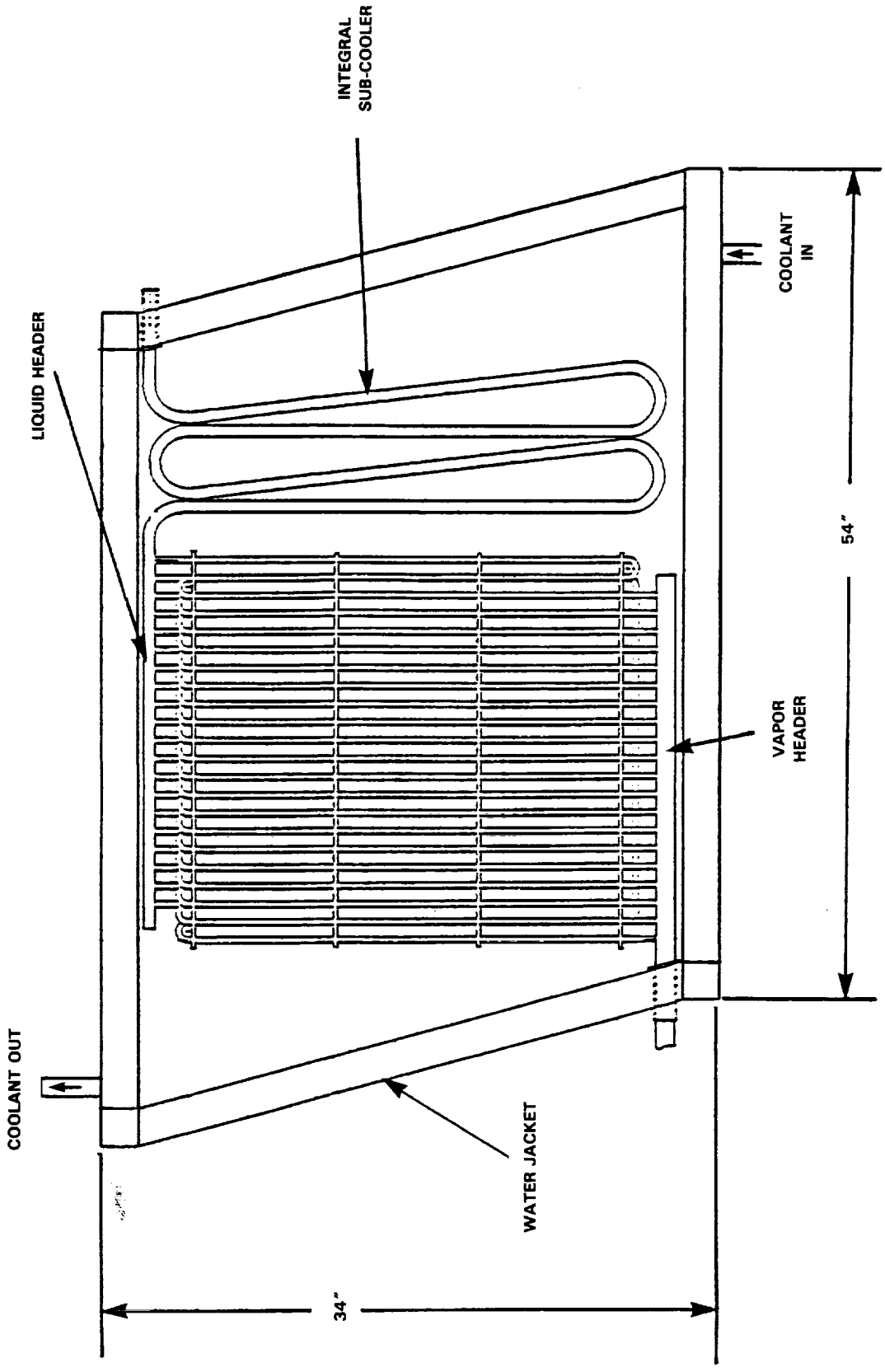


Figure 2-8. HPSTM Condenser Heat Exchanger

and to keep any non-condensible gases from migrating into the capillary pump. If a capillary pump stops circulating fluid while heat is still being applied, any liquid in that pump and its inlet will vaporize. The wicked isolator allows liquid to pass through the pores on route to the capillary pump when the pump is operating normally, and it also blocks the vapor from flowing back into the inner annulus of the isolator section when the pump has failed, thereby preventing other pumps from failing because one pump has become vapor locked. The isolator/capillary pump configuration is illustrated in Figure 2-6.

A cross-section of the capillary evaporator pump is presented in Figure 2-7. Liquid ammonia fills the center and wets the porous wick. When heat is conducted from the outer surface of the pump to the heat exchange surface, vapor bubbles begin to form. Surface tension of the liquid prevents the vapor from flowing back into the pump, so the bubbles migrate into the vapor flow channels. These channels empty into the pump vapor outlet, and from here, the vapor exits the capillary pump and enters the vapor header.

### 2.2.2 Condenser Section

The HPSTM system utilizes a 50/50 mixture of ethylene glycol and water to cool the condenser tubing by forced convection in a tube-in-shell heat exchanger arrangement. The condenser tubing is illustrated in Figure 2-8. The condenser is made of 20 parallel, multi-pass, internally- finned tubes. Each of the condenser tubes begins at a welded interface to the 2.54 cm OD x 0.165 cm wall (1 in x 0.065 in) vapor transport section and ends at a welded interface to the 1.59 cm OD x 0.165 cm wall (0.625 in x 0.065 in) liquid header section. The subcooler is an extension of the condenser, and consists of multiple paths of 1.59 cm OD x 0.165 cm smooth wall tubing within the antifreeze-cooled jacket. The cooling jacket is made of aluminum channel frame which is bolted to an aluminum cover on top and bottom.

### 2.2.3 Transport Lines

Both the vapor and liquid transport lines use smooth-walled tubing. The vapor header in the HPSTM is constructed of 2.54 cm OD x 0.165 cm wall aluminum tubing, and is 10 meters in length. The vapor header is also designed to accommodate a spacing of 1 meter between the adjacent cold plate centerlines. The system's liquid line consists of 10 meters of aluminum tubing also, and is 1.59 cm OD x 0.165 cm wall. All transport tubing is insulated with armorflex insulation to minimize the heat transfer with the environment.

### 2.2.4 Mechanical Pump And Thermal Flowmeter

When the assistance of the mechanical pump in the HPSTM is required, the flow is bypassed from its normal route through the pump and thermal flowmeter as shown in Figure 2-2. A positive displacement Micro gear pump, model 114/56C, augments the capillary pumps. A variable speed controller allows for the manual adjustment of the pump speed.

To measure the mass flow rate delivered by the Micro pump, a thermal flowmeter was constructed and installed downstream of the pump. This flowmeter consists of an aluminum block which is mounted to the bypass tubing. Electrical strip heaters with a total capacity of 500 W were epoxied to the top surface of the block. A digital wattmeter measured the heat input to the block, and two thermocouples were wired to measure the temperature difference between two points 0.15 meters upstream and downstream of the block. The entire arrangement was insulated with 1.27 cm thick nomex felt.

The thermal meter was used to calculate flow rate by using the equation for sensible heating. The mass flow rate was calculated by dividing the heat input to the block by the product of the temperature difference into and out of the block and the specific heat of liquid ammonia, taken at the average of the block inlet and outlet temperatures. While this was a crude method for measuring flow, the calculated flow rate during the hybrid operations at least led to a good estimate for the flow at a given pump speed. The analysis of the test data showed that the flowmeter readings were very close to the actual flow rates. However, it is very difficult to estimate the percent of accuracy, given the limitations of such a measuring device.

### 2.2.5 Reservoir

Control of the HPSTM saturation temperature was maintained by controlling its reservoir temperature. The reservoir is an accumulator used for fluid inventory and operating temperature control. Distribution of the liquid between the reservoir and the loop is maintained by a pressure balance between these two elements. Any change in loop operating temperature due to variations in condenser blockage, which can be caused by changes in evaporator heat load, sink temperature, or other factors, will result in a pressure imbalance in the loop. A pressure variation will cause fluid to be displaced into or out of the reservoir, until equilibrium is restored.

The temperature of the liquid-vapor interface in the reservoir will control the saturation temperature in the loop as long as three conditions are met. First, the reservoir must be of sufficient volume to accommodate the range of liquid displacement required to maintain any variations in operating conditions. Therefore, the reservoir must at least be able to

hold all the fluid which could fill the condenser. Second, the reservoir must always contain two phases, liquid and vapor. Finally, the condenser must always be partially filled with liquid.

Two separate control reservoirs were used during different portions of the HPSTM test program. For the capillary pumped testing, a 0.00378 $m^3$ (one gallon), 304L stainless steel"Whitey" pressure vessel was used as the system reservoir. Its location in the loop can be seen in the Figure 2-2, plumbed directly into the liquid return line where it exits the subcooler. For the hybrid testing, a larger, 0.00567 $m^3$ (1.5 gallon) reservoir was plumbed into the bypass line as seen in Figure 2-2. This accumulator was set in a frame and placed on a digital scale so that the exact charge within the bottle would be known at all times.

# 3 FACILITY HARDWARE DESCRIPTION

The HPSTM system for this part of the test program included not only the thermal hardware previously described but also a data acquisition system, a power system, a cooling system, and a safety system. The data and power systems were provided by the GSFC. The cooling system was built by the OAO Corporation. Elements of the safety system were supplied by both the GSFC and OAO.

## 3.1 Data Acquisition System Description

A schematic of the data acquisition system is displayed in Figure 3-1. Data was collected using a NEFF data acquisition system , at a scan rate of 1,000 channels per second. The data system was interfaced with a Microvax II computer by a general purpose interface bus. Temperature readings from 118 thermocouples, pressure measurements from two absolute and one differential pressure transducers, and powers to the reservoir and 12 evaporator pumps were measured and displayed on the terminal every second and stored on the computer's hard disk every five seconds. For the hybrid testing, the exit quality, ratio of vapor mass flow to total mass flow, of fluid leaving the evaporator section, mass flow rate measured by the thermal flowmeter, and amount of evaporator heating which was used to bring the liquid ammonia up to the saturation temperature (sensible heating) were calculated and displayed every second, but were not stored on the disk. A Brothers printer and Hewlett-Packard plotter were connected to the Microvax computer to allow for real-time data printouts and data reduction. Two CRT's displayed all of the data.

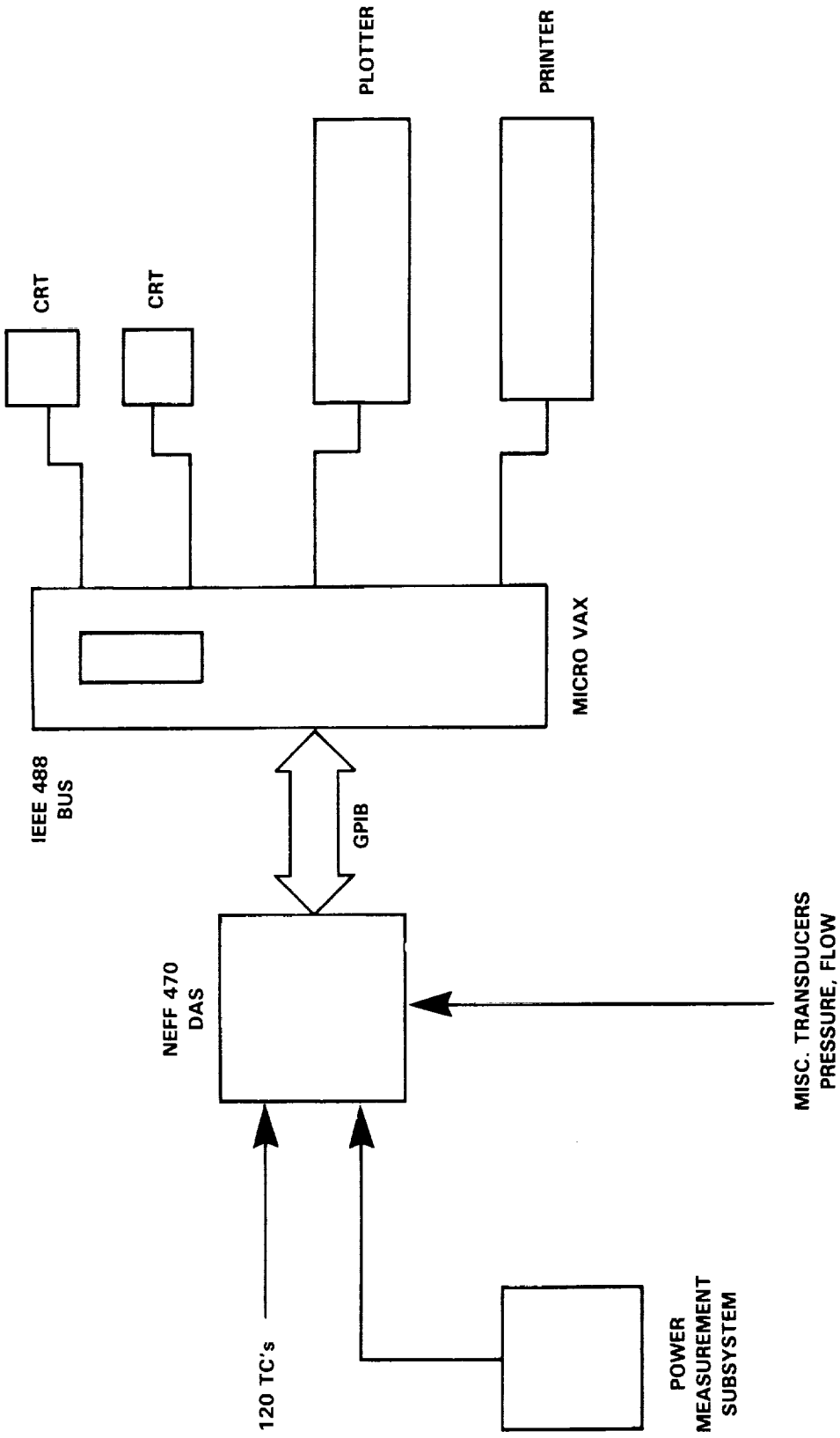


Figure 3-1. HPSTM Data Acquisition System

## 3.2 Power Distribution System Description

The power distribution system consisted of a centralized power distribution unit (PDU) which delivered power to a panel of 12 variacs, one for each capillary evaporator pump, and 13 power transducers (the extra transducer being used for the reservoir heater). Power to the power distribution unit entered at 480 VAC and was then dispersed to twelve 208 VAC circuits. Each identical circuit was then connected to a corresponding variac, which allowed each evaporator to be powered up to 5.4 kW (65 kW potential).

As shown in Figure 3-2, cartridge heaters were inserted in the evaporator cold plates above the capillary pumps. Since each pump is 0.61 meters long and each heater is 0.305 meters long, the heaters were placed end-to-end within the plate. Six heaters were used for each capillary pump (72 heaters in the system), and each set of six was controlled by one variac. This way, each pump was heated the same way both axially and radially. During all of the tests performed during this program, all four evaporator pumps on a particular plate were heated with the same load.

## 3.3 Cooling System Description

The condensers of the HPSTM were cooled by antifreeze in a cross flow tube and shell heat exchanger construction. The antifreeze was stored in a tank which holds 0.606 $m^3$ (160 gallons) of coolant.The coolant was pumped at a rate of 0.00315 $m^3/s$ (50 gpm) from the tank through three compressors, each rated for 4 kW of cooling capacity at 0°C. After leaving the compressors, the coolant entered the shell of the heat exchanger and flowed across the 20 parallel tubes which comprise the HPSTM condenser and subcooler (see Figure 2-8). After exiting the shell, the fluid was pumped back to the storage tank, completing the loop.

## 3.4 Safety System

Several safety features were added to the test system in order to protect the porous polyethylene wicking material from excessive temperatures if a pump failure were to occur. In the electrical system, 60 amp ground fault breakers protected each circuit. In addition, two thermostats on each capillary pump were installed so that if a temperature in excess of 70°C was sensed, the relay on that particular circuit would open. Also, a master "Panic" button was installed so that at the operator's discretion, all heater relays would be opened at once.

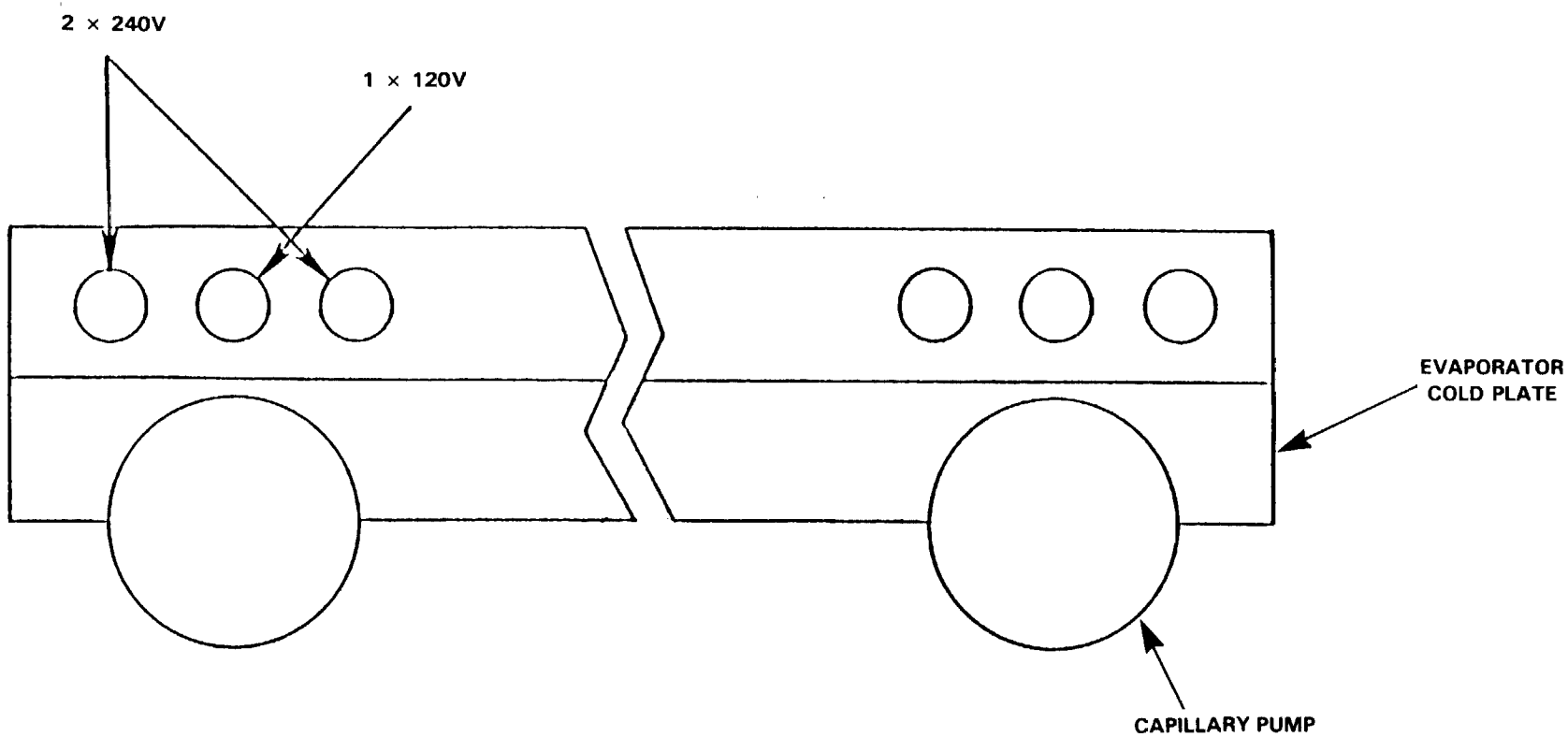


NOTE:

1. THE SAME CONFIGURATION OF HEATERS IS REPEATED FOR EACH CAPILLARY PUMP.
2. ALL CARTRIDGE HEATERS ARE 12 INCHES LONG, THEREFORE THERE ARE TWO HEATER PLATES FOR EACH OF THE THREE CAPILLARY COLD PLATES.

Figure 3-2. HPSTM Header Configuration

Bolted to the bottom of each evaporator plate were four finned copper tubes, joined by a header. Each tube was dedicated to one capillary pump. Plumbed to each header was a bottle of liquid nitrogen, which was valved to the tubing by a solenoid. At the test operators discretion, the valves could be opened by pushing a button, one for each plate, which would then allow liquid nitrogen to flow through the copper tubing. This was an additional safety measure to ensure that the capillary wicks were protected against high temperatures.

# 4 HPSTM TESTING OBJECTIVES

Several objectives were defined for the HPSTM test program. The first goal was to determine the operational performance characteristics of the system in both the capillary and hybrid-modes. The first half of the test program was dedicated to the capillary-mode testing, while the second half of the program was devoted to the study of the HPSTM performance in the hybrid mode. The second goal for testing of the HPSTM was to demonstrate a 10 kW steady-state heat load handling capacity in the capillary-mode, and a 50 kW transient operation in the hybrid configuration. The final major objective of the overall test program was to evaluate in both operating modes several new design features which were unique to this system. These new features included the use of capillary pumps which are 0.609 m (2 ft) long, modular parallel evaporator cold plates with individual isolator headers, and a reservoir feed line which is plumbed directly into the liquid return line, with no connection to the isolator header (as in past CPL designs).

## 4.1 Capillary-Mode Test Plan

Four tests were chosen to characterize the performance of the HPSTM in the capillary-mode of operation: system start-up, heat transport limit, low power limit, and pressure priming recovery. A brief description of each test planned follows.

### 4.1.1 Start-up Test

In a real application, the heat loads which will be dissipated from mounted equipment or payloads to the cold plates will be variable. In a capillary system, flow of the working fluid will not be initialized until heat is applied to the evaporator plates.

System start-up testing was meant to investigate the start-up characteristics of the system under various schemes of power inputs to the cold plates. Uniform and nonuniform heat loads were applied to the plates. A uniform heat load was one in which all three plates had the same heat input. This heat input was evenly applied across the cold plates, so that each capillary pump in the system was heated by the same amount of power. Nonuniform heat loads were those in which the power applied to each plate was different. For each plate, the applied heat load was still evenly dispersed among the four capillary pumps.

A start-up power scheme was also sought which could be used as a regular means of reliably starting the HPSTM during this test program. This was one in which all three cold plates were warmed with the same heat load, and which was presumed to work every time it was attempted. Variable start-ups were attempted only once , whereas the basic start-up procedure was verified many times.

### 4.1.2 Transport Limit Test

Capillary systems are limited by a maximum heat load transport capability. This is because the wick inside each capillary evaporator has its own potential in developing the capillary pressure rise. The pressure to be sustained by an evaporator depends on the power input to that evaporator as well as the total power input to the system. If the pressure to be sustained by an evaporator pump exceeds its capillary pumping capability, the evaporator will deprime. When a deprime occurs, pumping by the deprimed evaporator ceases. If heat is still applied to the deprimed pump, the temperature of the pump will increase until the heat load is removed.

The goal of the transport limit test was to determine the maximum uniform heat load which can be managed by the HPSTM system at three different saturation temperatures before the capillary pumping capability of the weakest evaporator was exceeded.

### 4.1.3 Low Power Limit Test

In a capillary pumped system, the mass flow rate of the working fluid through an evaporator is proportional to the evaporator heat load. Reducing the heat load will reduce the mass flow rate. At a very low heat load, the liquid flow is nearly stagnant. As the ammonia flows from the condenser section back to the pumps, it will become warmer due to heat transfer with the environment. When the liquid approaches the pump , while in the inlet line, it will be heated further due to conduction from the evaporator cold plates along the inlet tube wall. This process can cause the working fluid to reach the

saturation temperature before it enters the pump, resulting in vapor blockage of the wicks. When this occurs, capillary pumping ceases.

Another failure which can be attributed to the low power limit of a given system occurs if the ammonia vapor condenses in the vapor line, before ever reaching the condenser. If the system is not charged with enough ammonia inventory to fully flood the system, the reservoir may become completely depleted of liquid. With a single-phase (vapor only) accumulator, control of the system saturation temperature by the reservoir becomes impossible.

Determining the low power limit of the HPSTM and identifying the failure mode was the goal of this part of the testing.

### 4.1.4 Pressure Priming Test

The two-phase accumulator is the key system component when attempting a pressure priming recovery of a deprimed evaporator. When capillary pumping ceases because the pump has become vapor-locked, one method of rewetting the wick inside the failed pump is to force liquid into its isolator and inlet by creating a pressure differential between the cold plates and the reservoir. The pressure difference can be achieved with a heat load still applied to the working evaporators by increasing the internal temperature (hence pressure) of the reservoir rapidly. Pressure priming under heat load is possible as long as the rate of temperature rise in the reservoir is faster than in the evaporators. The higher pressure in the reservoir forces the liquid to flow to the condenser section, where the pressure is lower, until the condensers are completely blocked by the liquid. At that instant, the evaporators are temporarily under a no load condition, and no capillary pumping is required. Liquid is then injected into the evaporators, and the deprimed pump is now reprimed. The goal of this test was to verify this method and to characterize the conditions under which it could be accomplished.

## 4.2 Hybrid-Mode Test Plan

The second half of the test program was dedicated to determining the operating and performance characteristics of a CPL with a mechanical pump plumbed into the liquid return line operating as the main source of pressure head. Five tests were defined: ammonia inventory requirements, maximum heat input augmentation, flow distribution control by capillary action, steady state capillary-mode and transient hybrid operations, and heat load sharing among evaporators.

### 4.2.1 Ammonia Inventory Requirements Test

In any type of thermal control system, a minimum and maximum system fluid charge is required for the loop to perform effectively. Too small of a charge, and the reservoir could be occupied by vapor only, making it impossible for the reservoir to control the saturation temperature in the loop. During hybrid testing, an insufficiently-charged system could also result in mechanical pump cavitation. If the system is charged with too much ammonia, other problems can occur. The reservoir may be filled with just liquid, making it impossible to control the system saturation temperature. Too large of a charge can also present evaporator flooding problems which would reduce the heat transfer performance in the system. The purpose of this test was to define the minimum amount of system fluid inventory required to satisfy various heat inputs and flow rates so that tests in the hybrid configuration could be performed.

### 4.2.2 Heat Transport Augmentation Test

As was described earlier, the capillary pumps are the only source of pressure head when the HPSTM is operated in the capillary-mode. The maximum pressure rise is directly proportional to the heat transport limit of the system. The goal of this test was to determine if the capillary pressure rise in the evaporator pumps could be utilized to increase the pressure head and to enhance the heat transport capability of the loop when the mechanical pump is operating. Another goal was to determine how much augmentation would be provided at different mechanical pump speeds.

### 4.2.3 Capillary Pump Flow Distribution Test

One benefit of using a pure capillary thermal control system is that the porous wicks will naturally adjust themselves to meet the flow condition required by the heat load, provided that the heat input is within the range of the pumps capabilities. In a hybrid system, liquid ammonia is delivered to the evaporator section at a rate in accordance with the mechanical pump characteristics and the system pressure drop. The mass flow rate to any of the evaporators may exceed that required for total evaporation of the liquid ammonia. Capillary pumping action will be initiated only when the heat input to the evaporator reaches a level such that the flow exit quality is 100%. For any further increase in evaporator heat load for the same mechanical pump speed, the capillary force will help to regulate the flow until the capillary pumping limit is reached. The advantage of this flow regulation function is that during nonuniform heating tests, evaporator plates will not become liquid-starved prematurely.

The goal of the flow control tests was to demonstrate the ability of the capillary pumps to regulate the flow among the three evaporator plates when a mechanical pump is used to provide pressure head in the loop. These tests were performed with uniform and nonuniform heat loads applied to each of the evaporator plates.

### 4.2.4 Steady-State And Transient Test

This series of tests studied the transition from a pure capillary- mode of operation to the hybrid configuration at a steady-state heat load of 10 kW. The tests also evaluated the thermal control capability of the system when heat loads of between 10 and 50 kW were input to the evaporator cold plates. The transient test determined the performance characteristics when the applied evaporator heat load was suddenly increased from 10 kW to 50 kW. At each power level the mechanical pump speed was adjusted to deliver a mass flow rate no less than that required for evaporation before the power change was made.

### 4.2.5 Heat Load Sharing Test

One benefit of the capillary systems tested to date is that they have all successfully demonstrated heat load sharing: the ability of a capillary pump which has a heat load applied to it to share some of the exiting vapor with a capillary pump which is unheated. This allows both pumps to remain at the same temperature, even though only one is actually heated. The purpose of this test was to verify that with a mechanical pump operating in the loop, heat load sharing between evaporators could still be demonstrated under certain operating conditions.

## 5 TEST RESULTS

### 5.1 Summary Of Capillary-Mode Test Results

Results of the capillary-mode testing of the HPSTM were encouraging, with all of the objectives defined in the test plan completed. Transport limits between 21.5 and 24 kW were reached at three different system saturation temperatures with a one-inch adverse tilt (evaporator section higher than the condenser section so that liquid flowing to the pumps was against gravity). These heat loads represented a heat flux density of 3.85 to 4.3 $W/cm^2$. In addition, a low power limit was determined as a system heat load of 600 W (50 W per pump) at a saturation temperature of 25°C. This heat load was maintained for seven hours without any

pumps depriming. Individual pumps could be operated with as little as 25 W on each provided that the total system heat load was 600 W or higher. The system was also operated for 5 hours with 10 kW applied to the evaporator plates without any anomalies. All capillary-mode tests confirmed that the new features in the HPSTM design had no adverse effects on initializing or maintaining heat acquisition and transport. A baseline start-up technique was defined and proven successful on all 10 of the attempts, while 8 other start-up scenarios were run without failure. Finally, the pressure priming evaporator recovery technique was performed successfully three times.

### 5.1.1 System Start-Up Techniques

A baseline procedure for starting the HPSTM system was defined and verified. The technique was started by first controlling the reservoir temperature, hence system saturation temperature, at 25°C. A sensor compared the temperature between a thermocouple on the outer surface of the two-phase reservoir with the selected set point temperature. The reservoir heater would stay on at 100 W, warming the reservoir until the surface temperature reached the set point, when it would then turn off automatically. The reservoir heater would then cycle on and off for the remainder of the test to keep the reservoir at the desired set point. The condenser, meanwhile, was cooled to 0°C by three compressors, each of which was rated for a 4 kW cooling capacity. Once the reservoir and condenser temperatures stabilized, a 125 W heat load was applied to each of the capillary evaporator pumps (500 W per plate) for 30 minutes. The start-up was successful if no pump deprimed at the 125 W level for 30 minutes.

The results were identical for each attempt: liquid inside the capillary pumps was warmed to the saturation temperature and vaporized. The dry vapor flowed out of the pumps and into the vapor transport section. After traversing the 10-meter vapor line, the vapor displaced liquid from the vapor transport line and condenser with a piston-like effect. Excessive liquid was collected by the reservoir until an equilibrium was established for the given power input and operating conditions. The liquid formed in the condensers when the vapor condensed. The ammonia liquid then ran the length of the liquid line back to the capillary evaporator pumps, completing the cycle.

Figure 5-1 displays a typical start-up profile for plate 2, evaporator 2 (E22). The first effect seen by applying power to the plate at 11:22 was an increase in temperature to the pump, inlet, and isolators. This was a conduction effect, as the heat warmed the plate and conducted along the inlet line before the cold liquid flow from the condenser had reached the evaporator. The reservoir temperature, which indicated the system saturation temperature, was at 23°C when power was first applied, while the inlet, isolator, and pump temperatures were uniformly at 19°C.

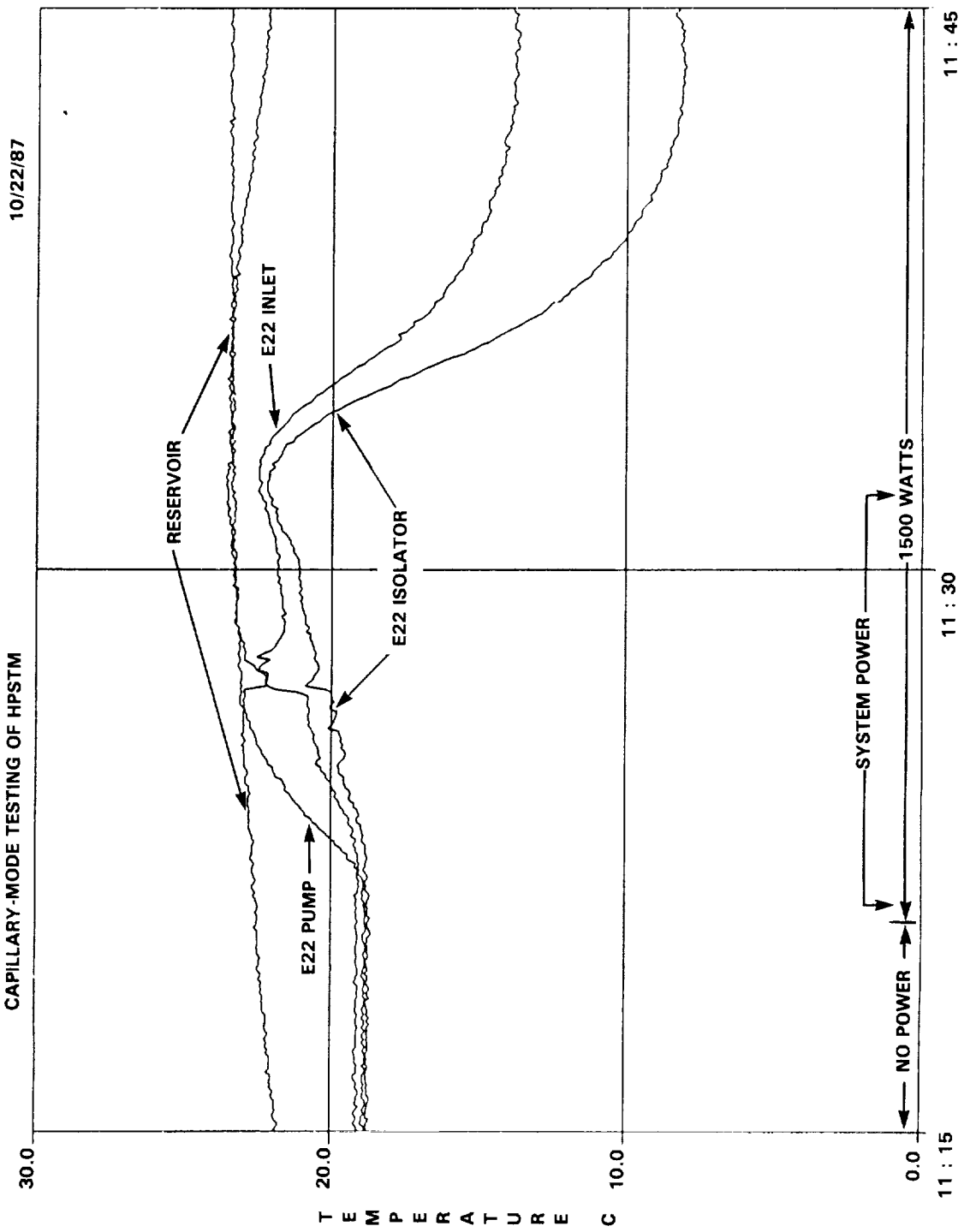


Figure 5-1. Start-up Test E22 Profile

About 10 minutes after the initial application of heat, cold liquid from the condenser reached the isolator and inlet section, dropping these temperatures over the next five minutes, until they stabilized. The inlet remained warmer than the isolator, and the pumps warmer than the inlet, as a result of conduction from the plate. The same effect was seen on all other capillary pumps in the system.

One objective of this testing was to determine the effects of using parallel cold plates with separate isolators on the operation of the system. Would flow be equally distributed to each plate, or would one plate be flooded with liquid while another starved?

While the flow from the liquid return line was equally distributed between the plates, one effect of the parallel arrangement on the system response was a time lag between when cold fluid was injected into each of the plates. During the baseline start-up runs, the normal time difference between when heat was first applied to the evaporators to when cold liquid was felt by the capillary pumps of the evaporator cold plate nearest the condenser (plate 3) was 10 minutes. Fluid injection into the next two cold plates was not detected for several more minutes as the liquid travelled one meter to reach each of the next two cold plates. The temperature distribution of the isolators between plate 3 and plate 1 was linear, with about a 0.1°C warming trend going from E34 to E11 (from the nearest to the furthest pumps from the condenser). This warming trend was due to the parasitic heat gain from the environment as the liquid ammonia travelled a slightly greater distance to reach each subsequent plate in the system, allowing for more time to gain heat from the surroundings. In no way were the capillary pumps adversely affected by this small parasitic heat gain.

Table 5-1
HPSTM System Start-Up Power Profiles

| Plate 1 Power (Watts) | Plate 2 Power (Watts) | Plate 3 Power (Watts) | Total Power (Watts) | Plate 3 Fluid Injection (mins.) | No. of Times Perfor |
|---|---|---|---|---|---|
| 500 | 500 | 500 | 1500 | 10 | 10 |
| 400 | 400 | 400 | 1200 | 13 | 4 |
| 500 | 0 | 0 | 500 | 24 | 1 |
| 200 | 200 | 200 | 600 | 21 | 1 |
| 0 | 500 | 0 | 500 | 20 | 1 |
| 500 | 500 | 0 | 1000 | 16 | 1 |
| 2000 | 200 | 200 | 2400 | 8 | 1 |
| 0 | 500 | 500 | 1000 | 10 | 1 |
| 2000 | 2000 | 2000 | 6000 | 6 | 2 |

Though this baseline start-up procedure was proven effective, it by no means represented the only way in which flow in the HPSTM could be reliably started. Variations were made on the heat load magnitude and uniformity among the three cold plates. Table 5-1 shows the different start-up scenarios which were attempted during the capillary- mode of testing. The data indicated, not surprisingly, that the higher the initial evaporator heat load, the faster the cold condenser liquid reached that evaporator. None of the start-ups attempted failed during the capillary-mode testing.

### 5.1.2 Heat Transport Limit Test

Capillary transport limits were observed at heat loads between 21.5 and 24 kW at three different saturation temperatures: 25, 35, and 45°C. These transport limits were the maximum uniform heat load that could successfully be maintained without a capillary pump deprime.

In past tests of capillary systems, two modes of evaporator failures have been observed: inlet deprimes and evaporator dryouts. In an inlet deprime, the capillary pumping ceases in the deprimed evaporator, and liquid in the inlet and isolator vaporizes. The pump temperature then rapidly increases. The entire heat load applied to the failed pump must be removed before that pump can be reprimed. In a pump dryout, liquid is still present in the inlet and isolator section, and only part of the wick in the evaporator is liquid-starved. This type of failure is indicated by a more gradual increase in the pump temperature. Another characteristic of a dryout is that the pump will be fully recovered by lowering the evaporator heat load by about 30% of the dryout-inducing power level.

Each of the eleven attempts of the transport limit tests ended with an inlet deprime of evaporator E11, followed by an inlet deprime of the remaining evaporators in plate 1 (E12-E14). These tests consisted of six runs with a 25°C set point, three tries at 35°C, and two attempts at 45°C. Table 5-2 summarizes the results of the tests performed.

Of particular interest when analyzing the results of a transport limit test is the temperature difference between the top of the capillary cold plates and the system saturation temperature. As the heat load is increased, the surface temperature of the capillary plate also increases. This is a result of thermal conduction as well as, to a lesser extent, the evaporation process. One observation from the data generated in Table 5-2 is that while the " delta T " measured at each power level was roughly the same for plates 1 and 2, the third plate always operated 10-15% warmer.

The reason for this offset is most likely due to differences in the contact pressure and contact area between the plates and the pumps. Heat is conducted through the plates to the evaporator pumps surface. A difference in pressure between the plates and the pumps will result in a difference in resistance to heat flow which will change the amount of heat which is transferred from the heaters to the capillary pumps.

The temperature difference could also be related to the fact that each capillary pump in the system has its own capacity to provide a pressure head for the fluid. The capillary wicks have an average pore diameter of 10 microns. Some pores are larger, while others are smaller. Before testing in the system, each pump was individually tested for its permeability, static wicking height, and dynamic wicking height. Each pump had slightly different values for these parameters. Taken as a group, then, the pumps in plate 3 may provide a slightly different pressure head than the pumps in plates 1 and 2. However, an analysis of the individual pump data shows no reason to establish this premise as the cause of the temperature differences observed. Regardless of the cause, the differences seen in the temperature distribution between the plates caused no difficulties in all of the tests.

Another parameter given in Table 5-2 is the subcooling availability when the evaporator deprime occurred. The available subcooling is defined as the temperature difference between the system saturation temperature in the reservoir and the ammonia liquid temperature as it exits the subcooler.

Table 5-2
Summary of Transport Limit Testing

| Saturation Temp. (C) | Heat Load @ Deprime (kW) | Temp. Difference @ Deprime(C) PL 1 | PL 2 | PL 3 | Subcooling @ Deprime (C) |
|---|---|---|---|---|---|
| 25 | 16.5* | 11 | 11 | 12 | 5 |
| 25 | 19.5* | 12 | 12 | 13 | 5 |
| 25 | 24.0 | 14 | 14 | 16 | 10 |
| 25 | 24.0 | 14 | 14 | 16 | 12 |
| 25 | 24.0 | 15 | 15 | 17 | 12 |
| 25 | 24.0 | 14 | 14 | 15 | 15 |
| 35 | 25.5 | 15 | 15 | 17 | 17 |
| 35 | 25.5 | 15 | 15 | 16 | 23 |
| 35 | 25.5 | 15 | 15 | 16 | 18 |
| 45 | 24.0 | 15 | 15 | 17 | 22 |
| 45 | 24.0 | 15 | 15 | 17 | 22 |

* = Deprime caused by a subcooling limitation

The first two attempts at the transport limit test ended prematurely. The lack of subcooling available caused evaporators to deprime before the maximum heat transport limit could be attained. The reason for this is related to the limited cooling capability of the compressors in the HPSTM system. The three compressors were rated for a total cooling capacity of 12 kW; however, the actual cooling provided was only 9 kW. As discussed in the system description, heat was transferred from the HPSTM condenser section by flowing across a mixture of high-velocity antifreeze, which was stored in a 0.606 $m^3$ (160 gallon) tank.

At heat loads above 9 kW, more heat was applied to the evaporator than could be removed by the heat exchanger. The result was steadily warming ammonia being returned from the HPSTM condenser section to the capillary pumps. If a heat load in excess of 9 kW was applied long enough, regardless of the theoretical capacity of the capillary pumps, the system would run out of condensing area, and ammonia vapor would be returned to the capillary pumps rather than liquid. During the first two transport limit tests, the liquid ammonia was warmed to a point that vaporization occurred before the liquid ever reached the annulus of the capillary pump.

In Figure 5-2, the transient nature of the condenser is illustrated. Over the two hour period that the first test was run, the temperature of the subcooler outlet increased by 18°C. Two distinct trends are seen in the isolator that are typical of the CPL systems. At the lower power levels, when the heat load was raised at 10:50 from 6 kW to 9 kW, the isolator temperature decreased. This indicates that a higher mass flow was entering that pump. However, when subcooling became limited, as seen by the transient in the subcooler temperature, a further increase in the evaporator heat load did nothing to lower the isolator temperature. This would also suggest that the cooling capacity of the compressors was probably lower than the 4 kW rating which each received, since the isolator temperatures began warming at a system heat load of 9 kW.

To work around the cooling limitation , the thermal mass of the antifreeze in the 0.606 $m^3$ cooling storage tank was used. The idea was that if power levels on the evaporators were raised fast enough, the capillary system would have ample subcooling and condenser area to continue operating at the higher powers for a short period of time. To reduce the cooling limitations, fewer power steps were taken in bringing the system from the start-up power condition to the deprime power condition. All nine transport limit tests which were performed until a capillary pump deprimed were characterized by the same failure: after a period of time at either the 24 or 25.5 kW system power level, the first evaporator on the first cold plate (E11) deprimed. Once this pump deprimed, within twenty seconds, all other pumps on plate 1 deprimed in order, from pumps 2-4.

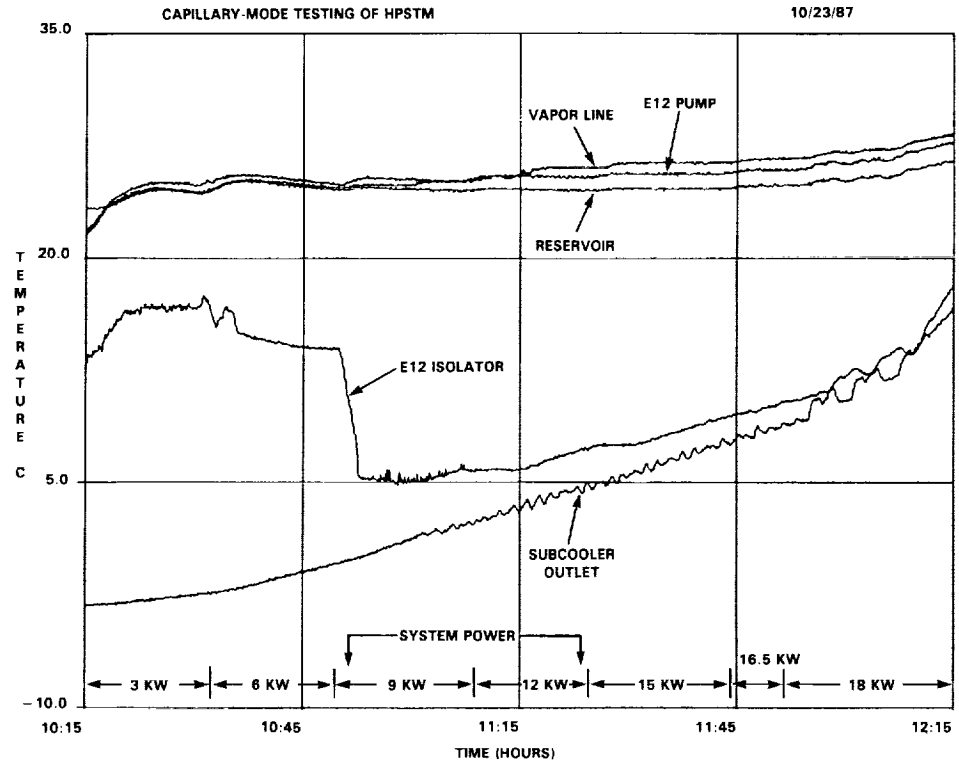


Figure 5-2. Transport Limit Test Condenser Transient

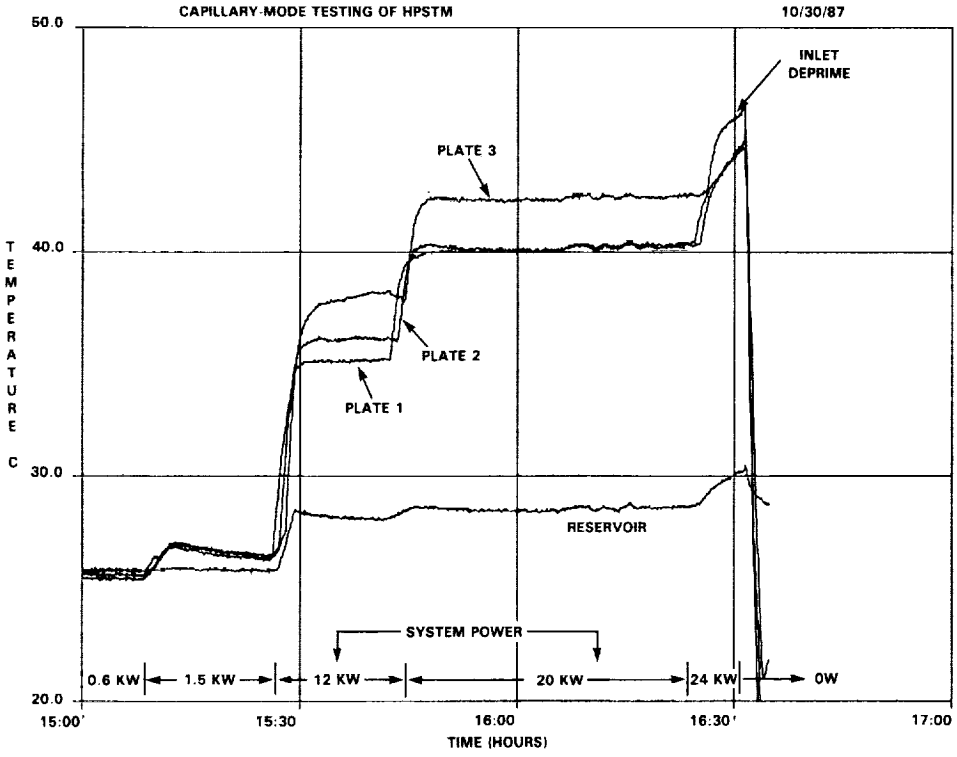


Figure 5-3. 25°C Transport Limit Test

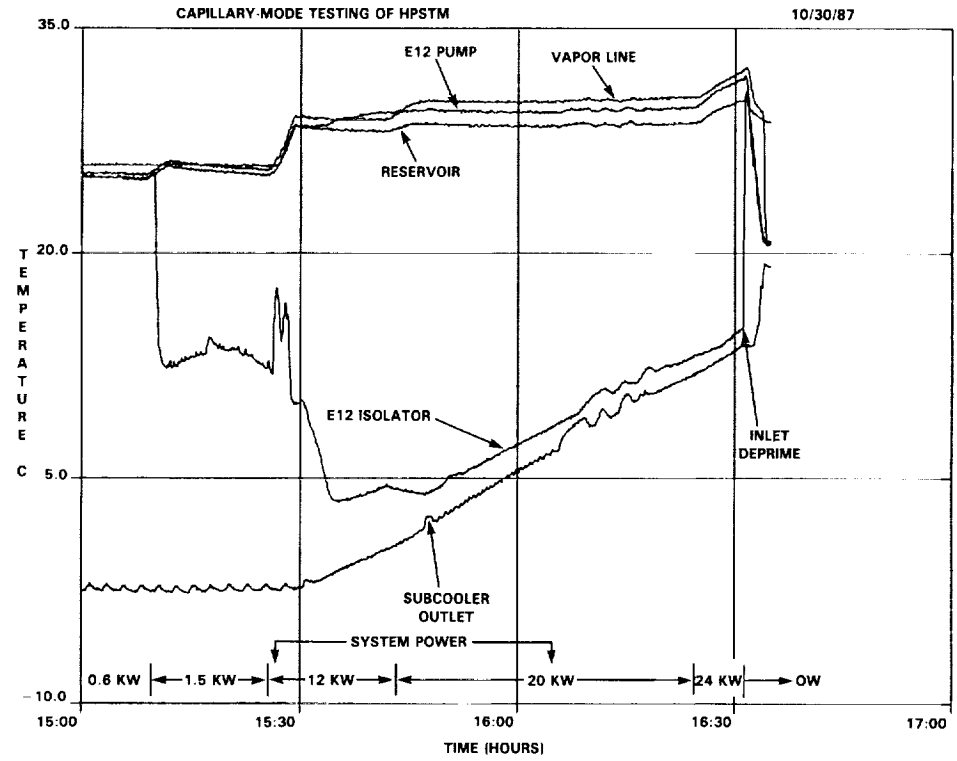


Figure 5-4. 25 °C Transport Limit Test

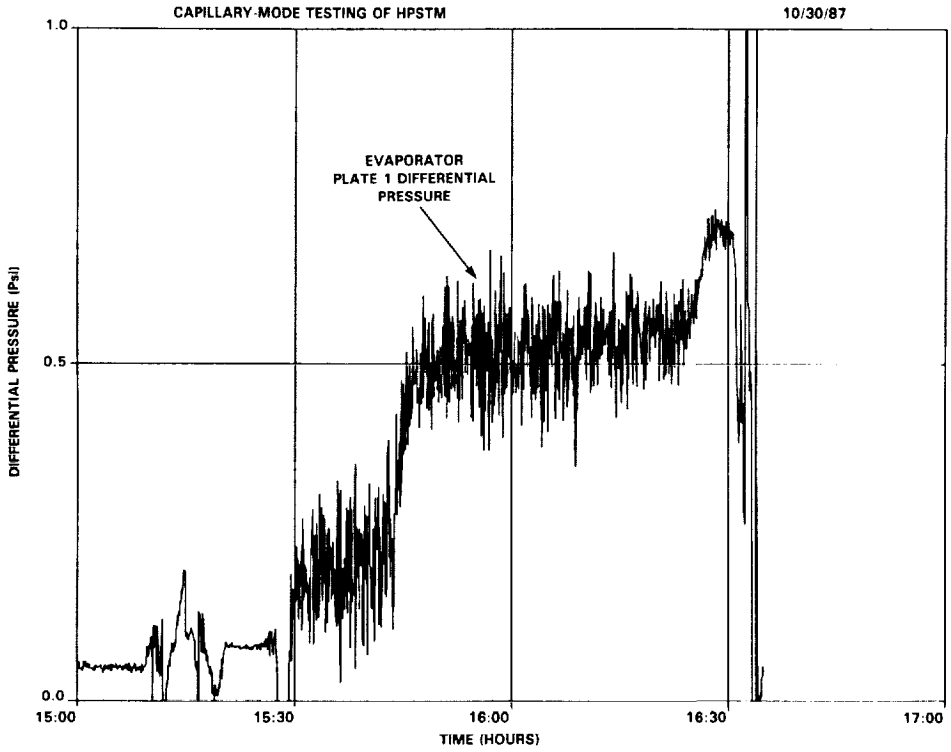


Figure 5-5. 25 °C Transport Limit Test

The reservoir control temperature in Figure 5-2 shows that the saturation temperature in the loop was fairly stable at 25°C. Notice however that at the 16.5 kW power level and above, this temperature began to drift upward. The gradual rise in saturation temperature was most likely an effect of vapor compression work which occurred in the vertically-mounted reservoir tank. As more vapor filled the condenser region in order to dissipate the higher heat loads, some of the liquid in the condenser was forced into the reservoir tank. When liquid entered the reservoir, vapor, which was at the top of the accumulator bottle, was compressed. This work was seen thermally as an increase in the temperature at the top of the reservoir tank. The E12 pump and the vapor header temperatures followed the same trend, indicating that the reservoir was still the saturation temperature- control device.

In Figure 5-3, which shows representative data from the first successful transport limit test at 25°C, the same temperature pattern resulted as was seen in the previous figure. This time, however, higher power levels were attained because more subcooling was available. At the 20 kW system level, the capillary pumps were receiving liquid which was 25°C subcooled. At 24 kW, the condenser was nearly filled with vapor, and the temperature rise on both the liquid side of the system and the reservoir was sharper than in the test illustrated in Figure 5-2. The deprime occurred at 16:32, when the isolator temperature shot up to the system saturation temperature, indicating the presence of vapor in this region. The reservoir was still in control of the saturation temperature, as the reservoir, vapor line and pump temperatures all followed the same trend.

Figure 5-4 shows the thermal response of the top of the evaporator cold plates and the reservoir temperature at the various power levels during this test. As was seen throughout the tests, plates 1 and 2 were nearly identical at the higher powers, while plate 3 operated 10% warmer. At 20 kW, the temperature difference between the plates and the reservoir was 12°C for the first two plates and 15°C for plate 3.

A differential pressure transducer was installed to measure the pressure rise across the evaporator plate 1. In Figure 5-5, it is seen that as the heat load was increased, the pressure rise across the pumps were also increased. The fluctuations in the pressure measurements taken for most of the test have not been explained yet. It is important to note that the phenomenon observed here is not unusual for systems where boiling occurs. Pressure and thermal oscillations are one common observation noted by other researchers working with two- phase systems. The complexities involved in analyzing pressure oscillations are beyond the scope of this report. The reader is referred to several sources for further information (5-7).

At both the low powers and the highest powers, the pressure differential was much more stable. When the deprime in E11 occurred, the pressure rise across E11 was greater than the

theoretical pumping limit of the capillary pumps: 0.7 psi versus 0.5 psi. The theoretical pumping limit, derived from capillary pump bench-test data taken for each pump prior to integration in the system, was based on the largest pore in the wick. The larger the pore size is, the smaller the capillary pressure rise in the wick. It appears, however that this weakest pore is not the limiting factor in the pump. The theoretical limit is therefore a conservative estimate of the pressure head potential of the pumps in plate 1 of HPSTM.

The failure of the other pumps in the same order, from E11 to E14, every time was most likely a result of thermal cross-talk along the isolator section. Once evaporator 1 stopped pumping, vapor immediately filled the inlet 1 tube. Heat was then conducted back to the isolator wall from the inlet tube of pump one. Although the isolators are designed such that the vapor from a failed pump does not flow back to the other isolators, heat can still flow along the tube wall, from isolator 1 to the adjacent isolators. Only a few watts of power are required to heat the isolator wall enough to cause an inlet deprime in that particular pump. Thus, when one pump failed due to a transport limit having been reached, the entire plate failed because of subsequent heat flow back to the isolator header, depriming the other pumps.

This mode of parallel pump failure had never been seen in other systems of similar design. It may be due to the very large heat flux densities which were input to the evaporators. No other pumps in the system failed, which suggests that no vapor flowed back into the liquid header. Thus, while the isolators did the job of preventing vapor back flow, the type of failure observed indicated that isolator conduction was a separate issue that must be addressed.

In the analysis of the previous transport limit tests, it was seen that although the temperature of saturation in the system did increase from vapor compression, the loop operating temperature was nevertheless controlled by the reservoir. This implied that vapor and liquid were present in the accumulator tank. One test showed what happens if only the liquid phase were present in the reservoir. In Figure 5-6, what appears to be the same thermal patterns shown previously is viewed again until 11:34, when plate 1 deprimed. Instead of removing power from the entire system, or performing a pressure priming evaporator recovery, the other two plates were allowed to operate with the same 8 kW heat load on each. As shown in the figure, the subcooler and isolator temperatures continued to increase since the capacity of the cooling system had been exceeded. The vapor header and pump temperatures increased along with the reservoir temperature until the deprime occurred. Thereafter, the reservoir control temperature began to deviate from the others, actually cooling while the saturation temperature indicated by the vapor line and pump temperatures continued to increase. It was here that the reservoir was totally filled with liquid that had been displaced from the condenser. The other two plate's

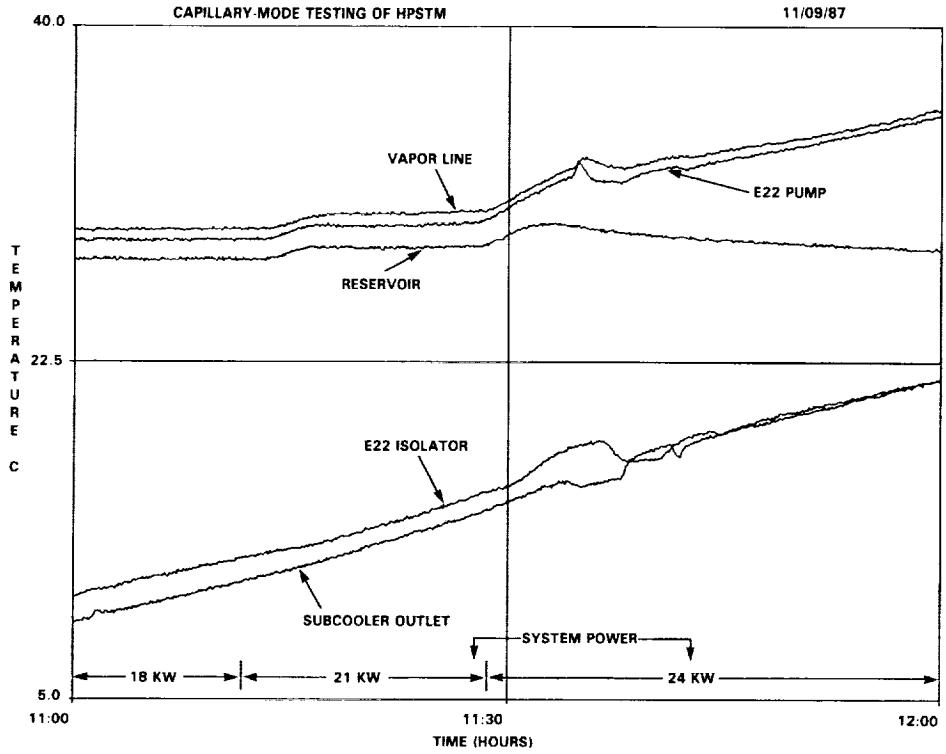


Figure 5-6. 25 °C Transport Limit Test

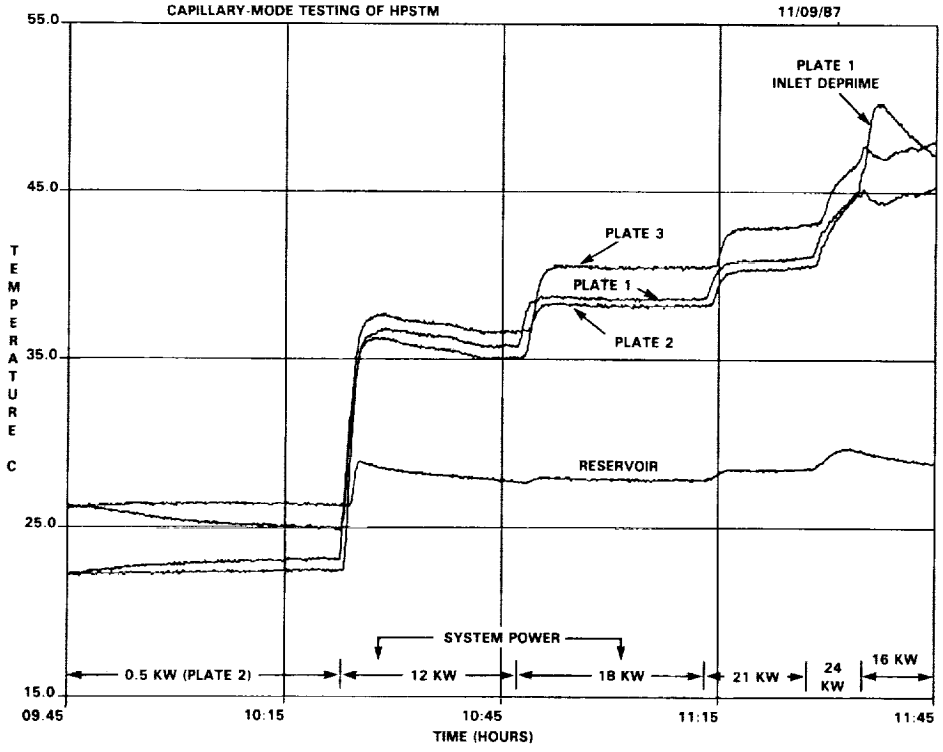


Figure 5-7. 25 °C Transport Limit Test

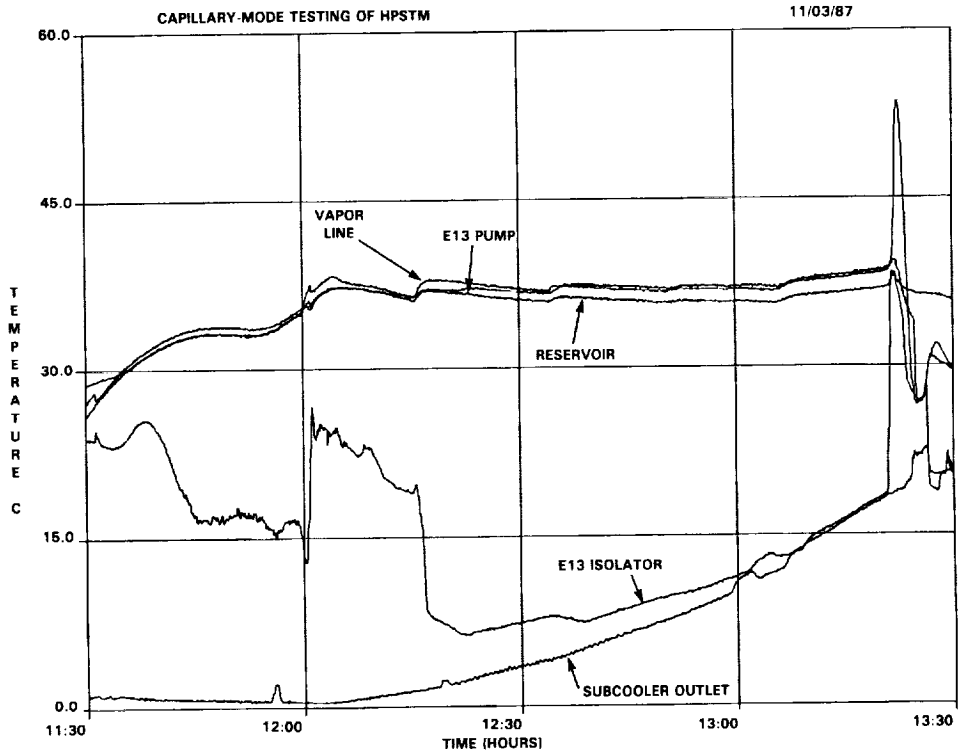


Figure 5-8. 35 °C Transport Limit Test

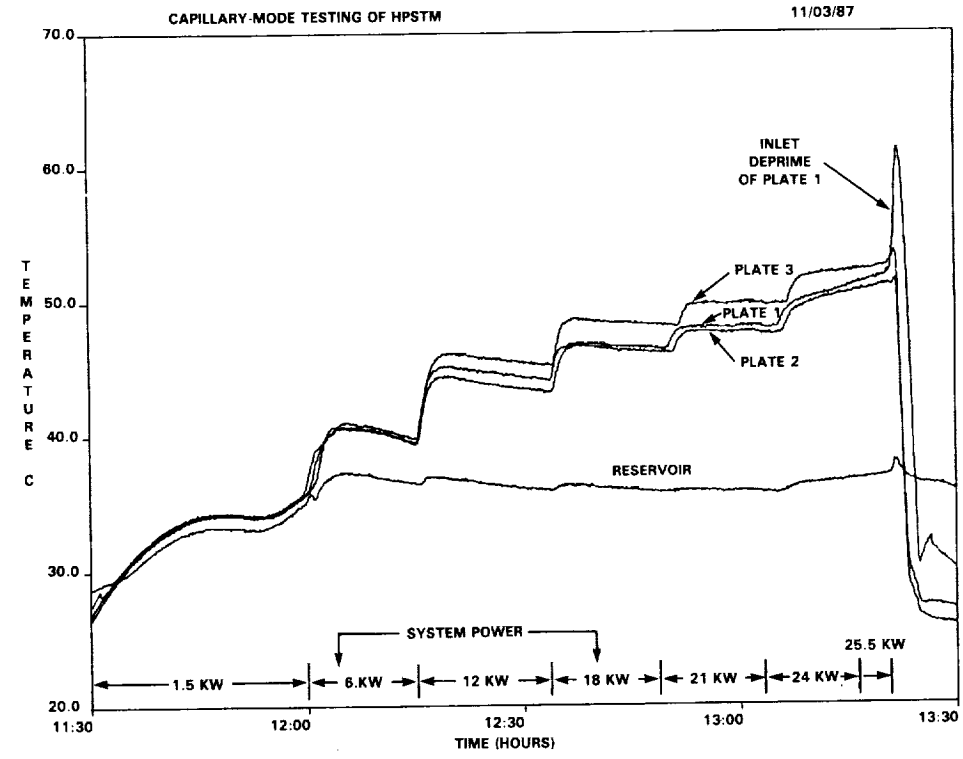


Figure 5-9. 35 °C Transport Limit Test

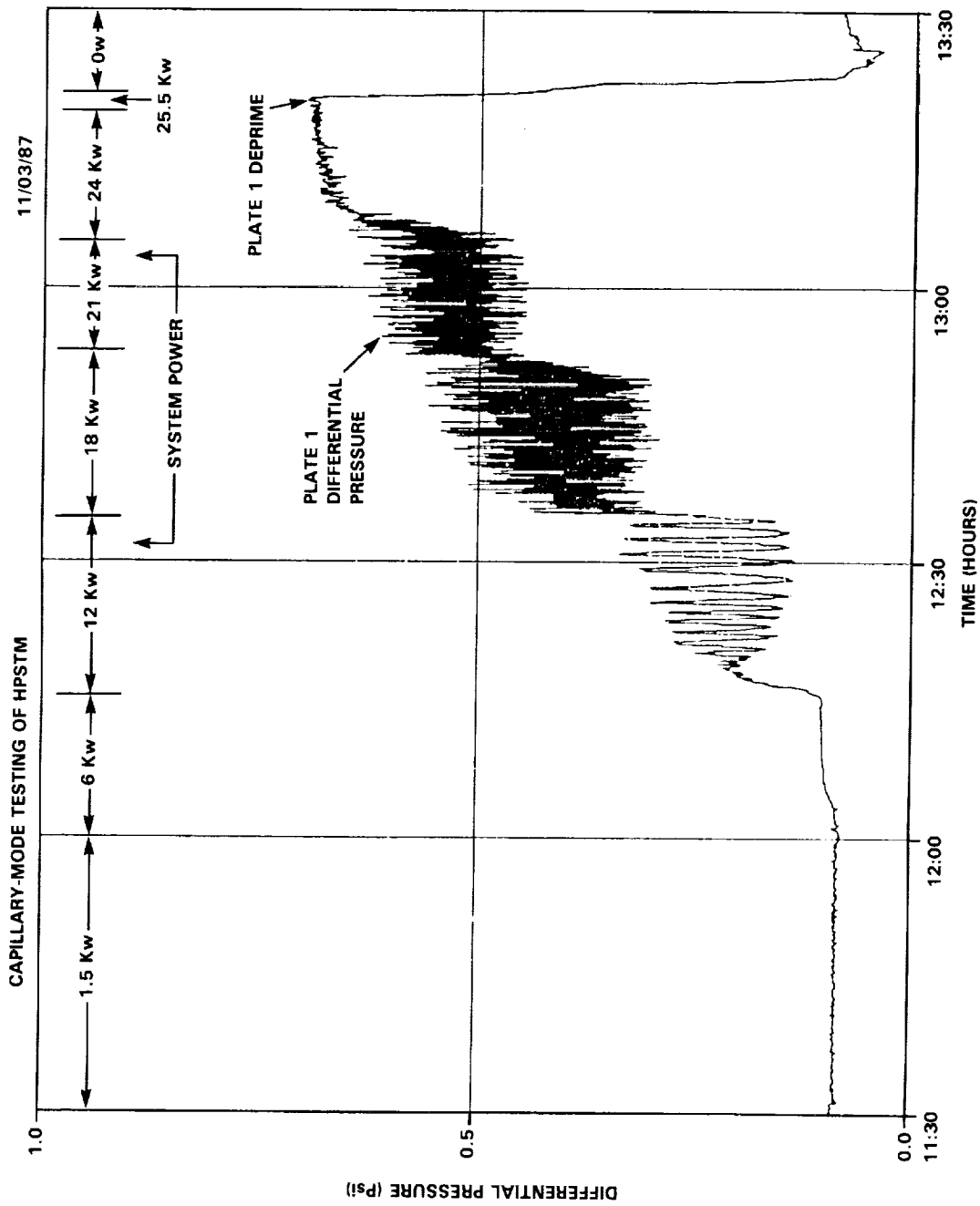


Figure 5-10. 35 °C Transport Limit Test

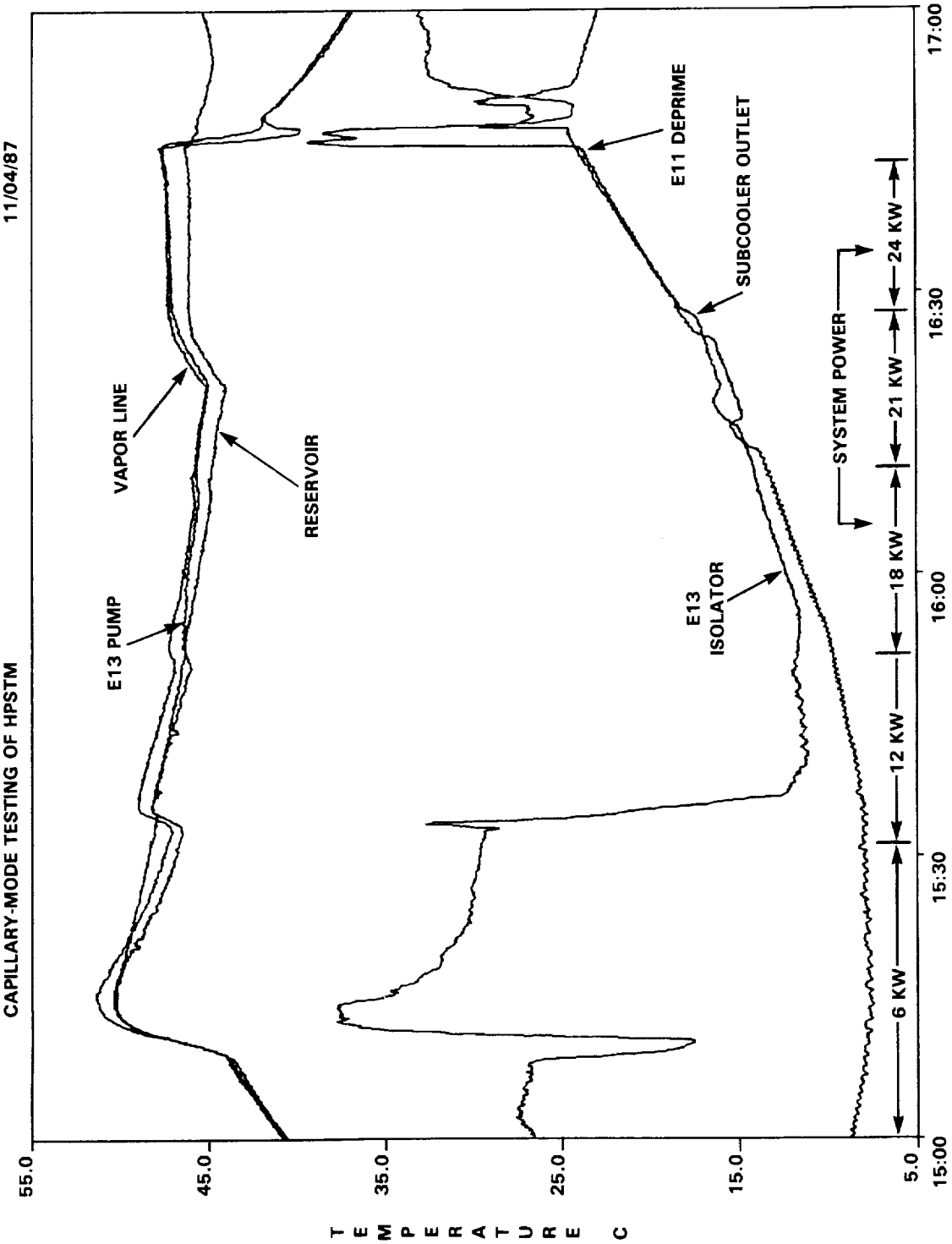


Figure 5-11. 45°C Transport Limit Test

continued to warm, though gradually, as they were heated.

Figure 5-7 shows the plate temperatures and the reservoir temperature during this same test. Plate 1, which was deprimed, reached a peak and cooled when the heaters were shut, while the other two plates continued to warm, uncontrolled by the reservoir, though still primed.

Transport limit tests were also run at saturation temperatures of 35 and 45°C. Results of these two tests were similar to what was seen in the 25°C transport limit tests. In Figures 5-8 through 5-10, the response of part of the system during the 35°C test is presented. Figure 5-8 shows the familiar warming in isolator and subcooler temperatures with time, while the reservoir controlled the saturation temperature indicated by the E13 pump and vapor line temperatures. A very slight warming trend in the saturation temperature can be seen in that figure and in Figure 5-9. In the latter figure, the tops of the three cold plates follow the same pattern as in the 25°C transport limit test: plate 3 runs warmer than the other two, while plate 1 deprimes first.

One interesting point to note is that during this transport limit test, no evaporator deprimed at the 24 kW level after 20 minutes. The next power increase to a system level of 25.5 kW resulted in a plate 1 deprime. Figure 5-8 shows the isolator increased by 15°C almost instantaneously. In Figure 5-10 the differential pressure curve follows the same pattern seen in the other tests, with oscillations on the order of +/- .15 psi.

Results of the transport limit test at 45°C were similar. Plate temperature differences were the same order and followed the same pattern as in the other tests. E11 was always the first pump to deprime after about 20 minutes at the 24 kW level, with 20°C of subcooling available. Figure 5-11 shows all the familiar trends in liquid and saturation temperature during most of the test. The plate 1 deprime is seen at 16:45 when the isolator temperature rises rapidly.

### 5.1.3 Pressure Priming Recovery Technique

When the plate 1 failed, the evaporators in the plate could be reprimed using the pressure priming recovery technique. The procedure went as follows: power to the 8 other working evaporators was reduced to 100 W each while the power level on the reservoir was raised from 100 W to 300 W. To ensure that the heater stayed on long enough to raise the internal reservoir pressure, the temperature controller on the reservoir was raised by 10°C. Four minutes after this was done, a cold surge of liquid entered the isolators and inlets of all the pumps. Any vapor in the isolators, inlets, or pumps on the first plate was forced out into the vapor line. The reservoir power level and temperature controller were then returned to their initial

conditions, and power was reapplied to the failed plate at 100 W per pump. All capillary evaporators remained primed each of the three times this method was used.

### 5.1.4 Low Power Limit Test

Several tests were performed to investigate the HPSTM systems performance at the low power levels, and to determine the mode of failure. All tests were conducted at a saturation temperature of 25°C. Results of the tests performed showed that capillary pumping is still accomplished at heat loads of as little as 25 W per evaporator (300 W on system) without any pumps depriming resulting from a lack of subcooled liquid in the inlets.

However, at this low power level, a loss of reservoir temperature control was observed. While the reservoir was set to control the saturation temperature at 25°C, the actual saturation temperature in the system as measured by the pump and vapor header temperatures drifted below this point at the 600 W system level. These observations, the opposite of what was seen during the transport limit test (cooling saturation temperature rather than warming), were caused by ammonia condensation in the vapor line. Subsequently, only the vapor phase existed in the reservoir, and the condenser remained completely filled with liquid (See Section 2.2.5 for discussion of reservoir control requirements).

The next set of figures, from Figure 5-12 to 5-16, clearly show how the system temperature control varied depending on the conditions inside the two-phase reservoir. Figure 5-12 shows the thermal profiles of the isolator, inlet, and pump for E22 and the reservoir temperature which should govern the temperature where evaporation is taking place. After a baseline start-up routine was performed, with each pump at 125 W, the capillary pump's power levels were lowered to 75 W each (900 W system) at 14:34. The reservoir was in control of the saturation temperature at this point. However, when the power levels were lowered to 50 W each (600 W system), the reservoir temperature stayed constant, while the evaporator pump temperature began drifting downward. A further drop in power to 25 W per capillary pump showed a further deviation from the reservoir setting. Figure 5-13 shows that the vapor header temperature tracked the pump temperature, but that these temperatures again were not controlled by the reservoir set point. Another indication of the absence of liquid in the reservoir was observed at 15:48, when the set point on the reservoir was raised to 30°C to see if the pump and vapor temperatures would respond to the change. Obviously, this was not successful. The reservoir increased in temperature, while the vapor and pump temperatures continued to float downward.

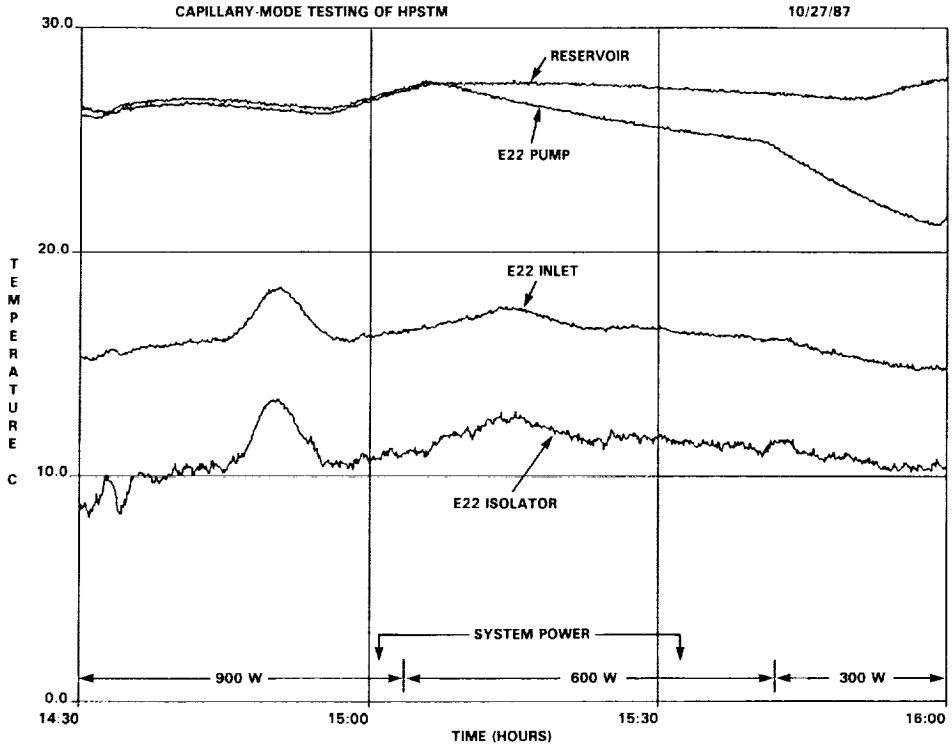


Figure 5-12. Low Power Limit Test

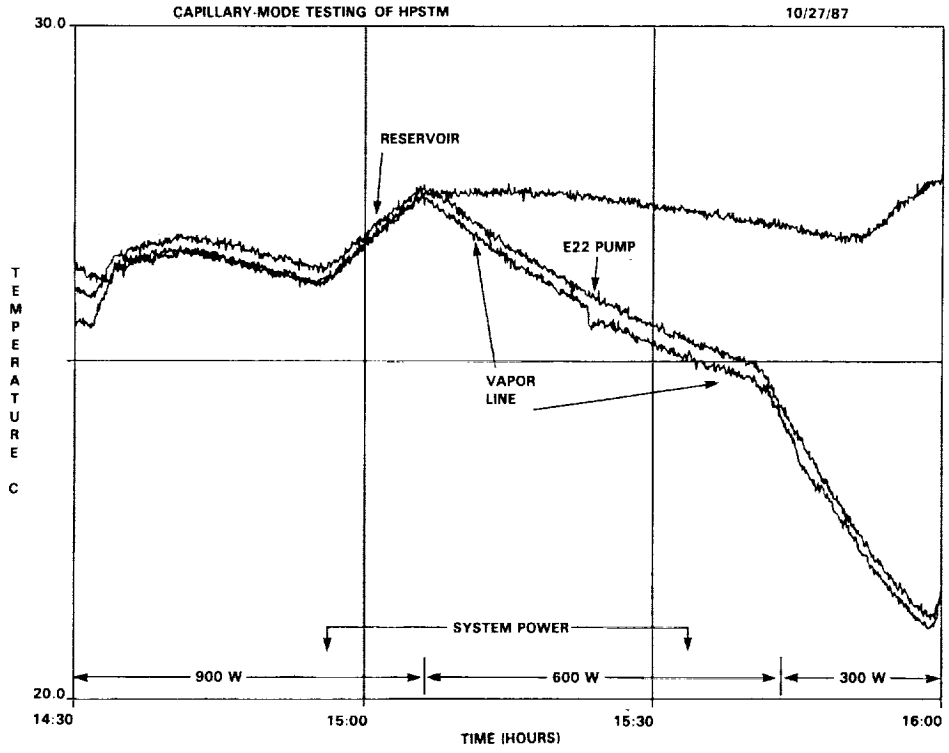


Figure 5-13. Low Power Limit Test

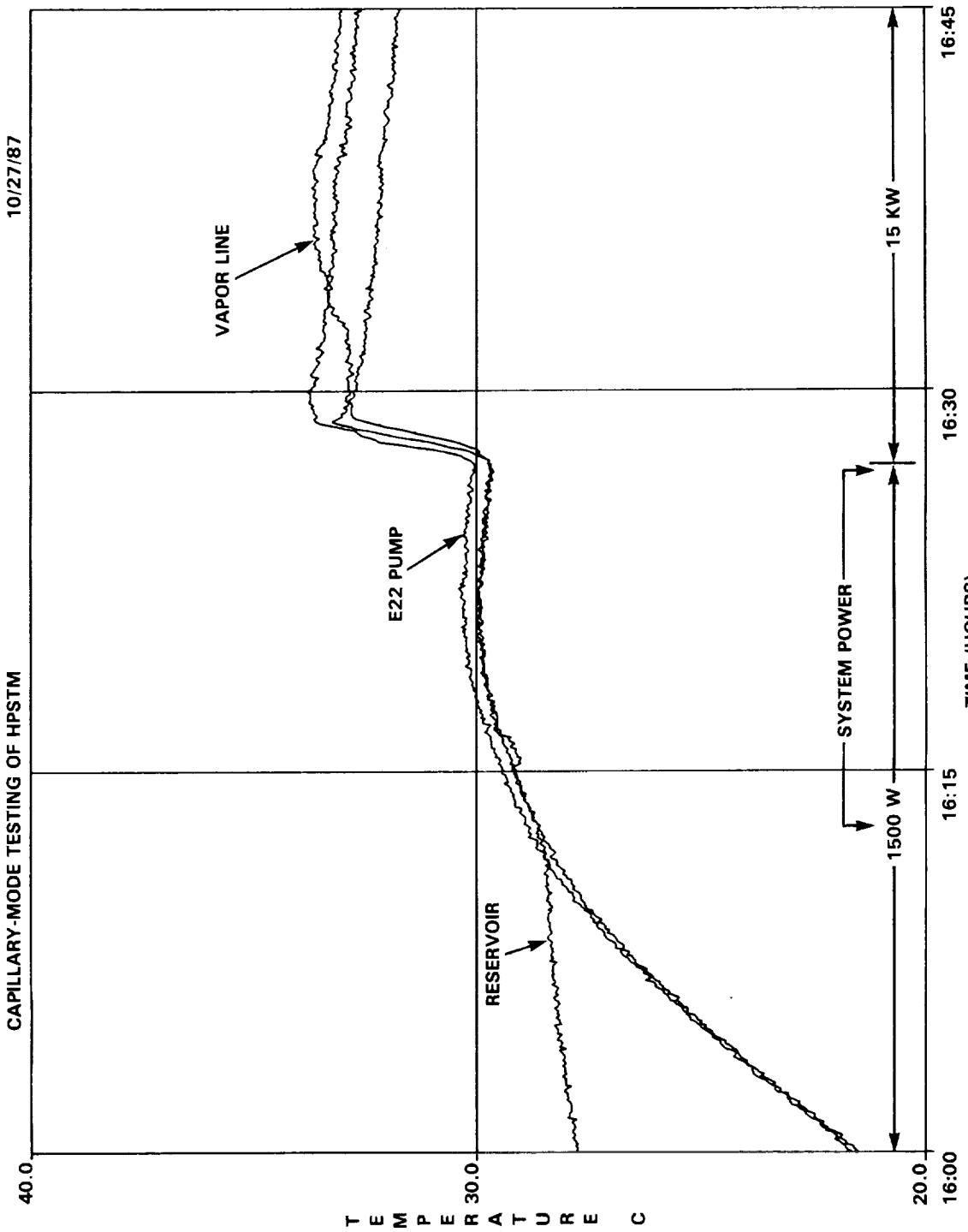


Figure 5-14. Low Power Limit Test

In Figure 5-14, it is seen that the pump and vapor header temperatures began increasing and eventually reached the saturation temperature of the reservoir at 16:12. This was in response to a change in evaporator power at 16:00 from 25 W to 125 W per evaporator. By increasing the heat load on the evaporators, some liquid was displaced from the condenser section to the reservoir. The reservoir was then the system temperature control device.

An excellent display of the reservoir vapor-compression effect can be seen in the Figure 5-14 at 16:27, when the system heat load was raised from 1500 W to 15 kW. As was described earlier, the change in heat load forced liquid out of the condenser into the reservoir. This caused the vapor in the accumulator to become compressed, increasing the system saturation temperature by 4°C in less than 1 minute.

Another low power limit test was performed which showed that all capillary pumps remained primed and the reservoir maintained control of the system saturation temperature with a 600 W heat load on the evaporator section (50 W per pump) for seven hours. While this would seem to contradict the results of the previous tests, there were two differences in the testing conditions that may help explain the performances.

In the test which was run on 10/27/87, shown in Figures 5-12 through 5-14, the condenser was cooled to 0°C. Also, the system was started with 1500 W, and was subsequently lowered to 900, 600, and 300 W. In the seven-hour test, the system was started and maintained at the 600 W level, and the condenser was warmer than before, at 10°C rather than 0°C. The effect of operating with a warmer condenser was that vapor displaced more fluid from the condenser, since a larger condenser area was required to dissipate the same heat load with a smaller temperature difference. The displaced liquid entered the reservoir, and the result was that the reservoir controlled the saturation temperature.

Figure 5-15 shows that the saturation temperature followed the reservoir temperature for the duration of the test. Note in the figure the effect of the reservoir heater on the saturation temperature. As was described earlier, the reservoir temperature was controlled by a heater which turned on when the sensor temperature on the surface of the bottle fell below the set point temperature. One problem which was noted during the testing was that the heater often stayed on for several minutes after the sensor temperature had reached the set point, causing the saturation temperature in the loop to overshoot the desired set point by 2-3°C. The overshoot caused by the reservoir heater is reflected in the figure by the change in the slope of the reservoir temperature.

All of the low power limit tests discussed so far deal with uniformly- applied heat loads to each of the evaporator plates. However, one test showed that heat loads of as little as 25 W per

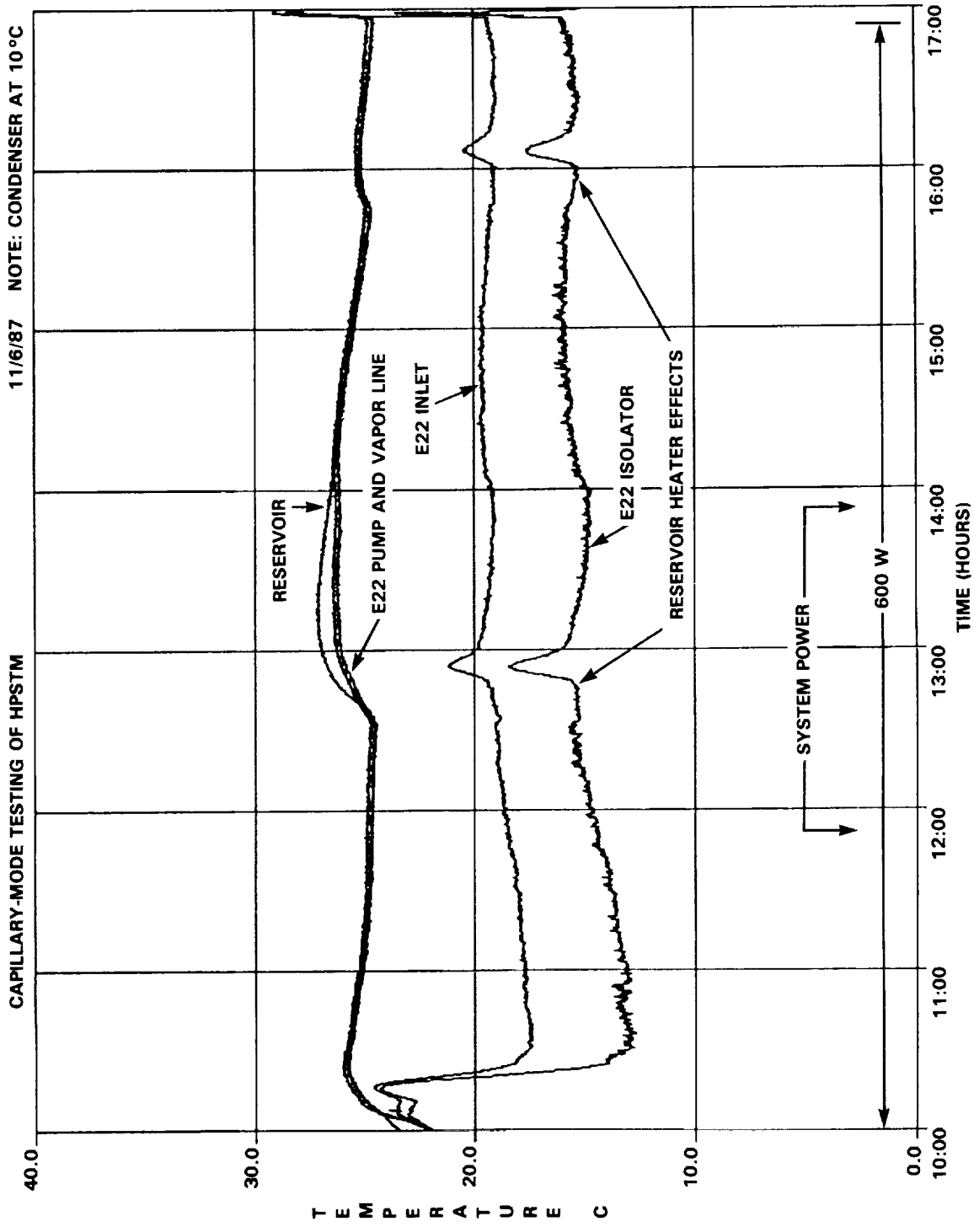


Figure 5-15. Low Power Limit Test

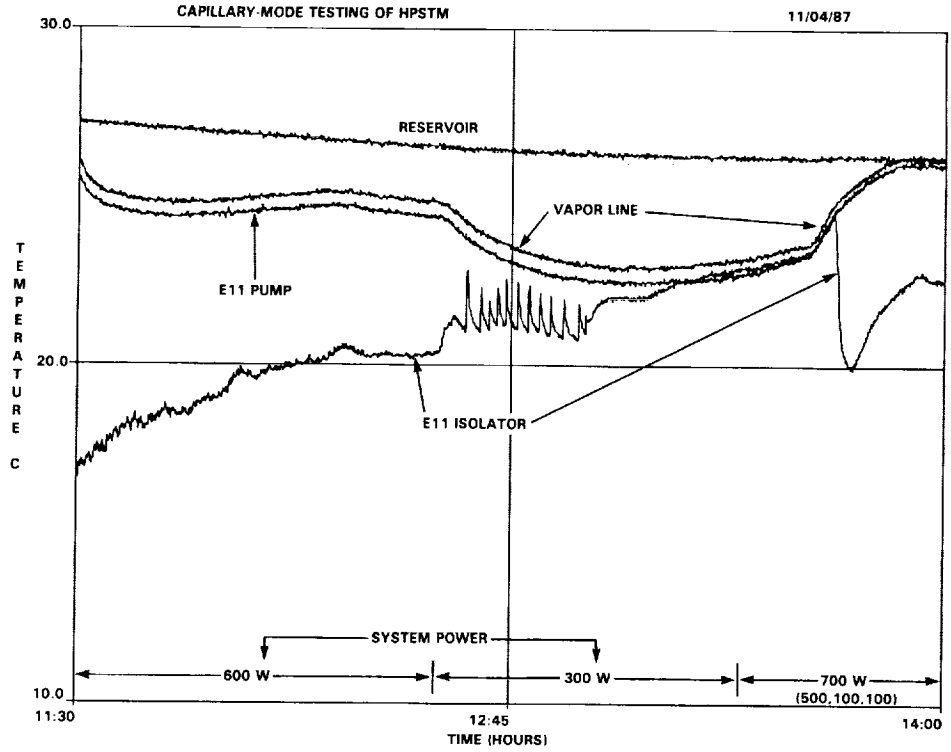


Figure 5-16. Low Power Limit Test (Nonuniform)

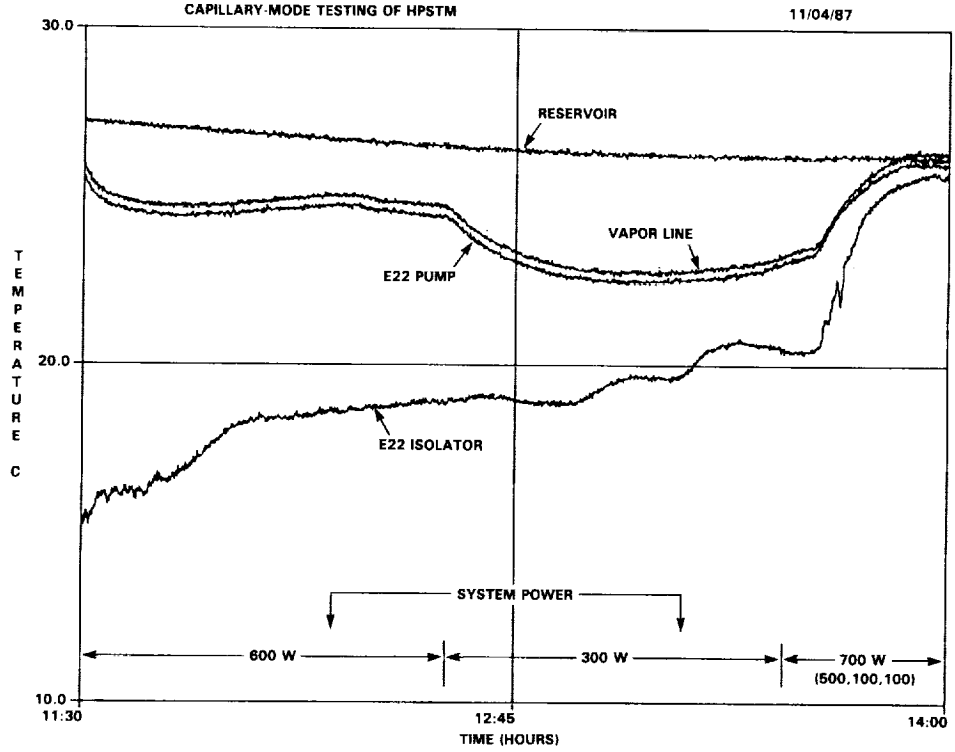


Figure 5-17. Low Power Limit Test

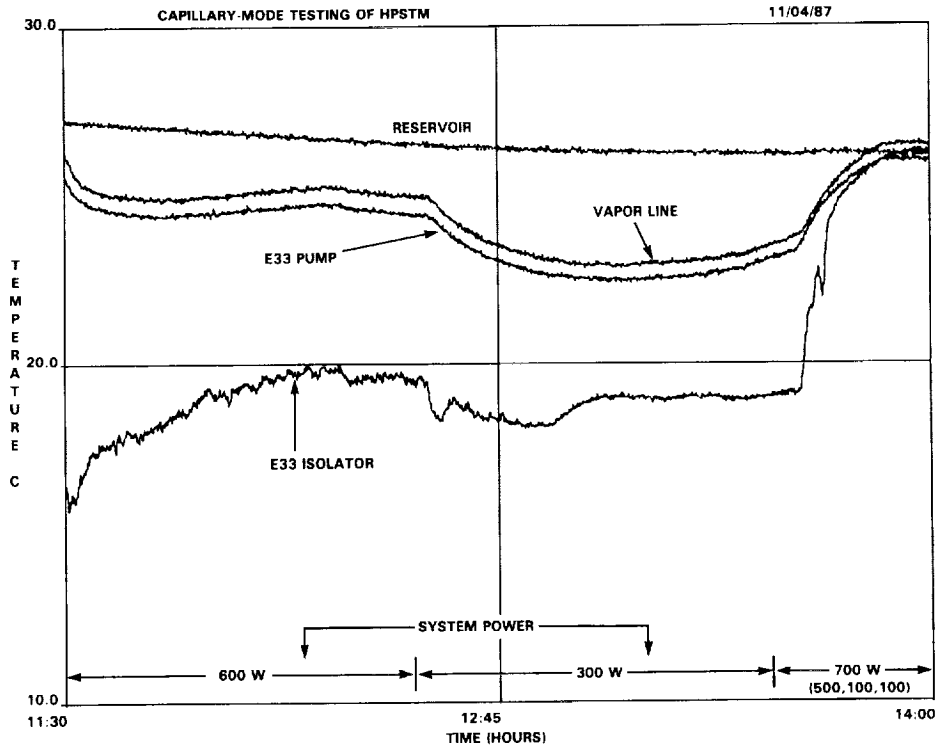


Figure 5-18. Low Power Limit Test

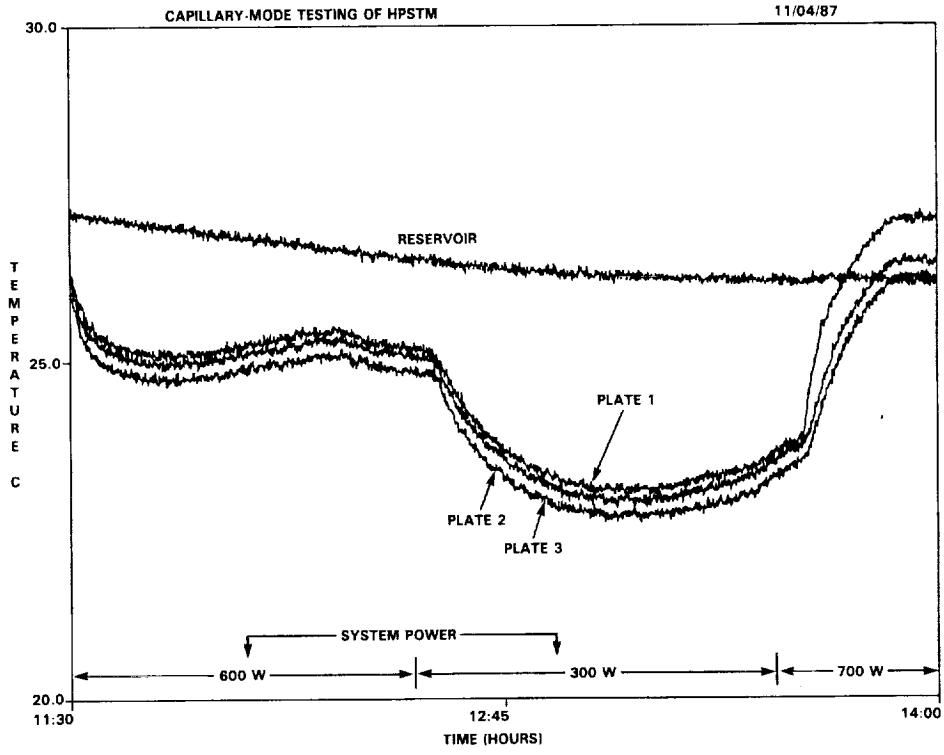


Figure 5-19. Low Power Limit Test

evaporator could be maintained on the pumps to two of the plates when the power level on the third plate is held at the 500 W level. The next set of four figures shows this behavior. Figures 5-16 to 5-18 display the isolator, pump, vapor line and reservoir temperatures for evaporators E11, E22, and E33 respectively. At 11:25, all of the evaporators were lowered from 125 W each to 50 W each. As seen in the figures, the saturation temperatures declined even though the reservoir temperature was constant. At 12:30, all pumps were lowered to 25 W each (300 W on the system), resulting in an even lower saturation temperature. Then at 13:37, plate 1 was raised to 125 W per evaporator, while the other plates remained at 25 W per evaporator (system total power of 700 W). When the power to plate 1 was increased, the other pumps on plates 2 and 3 also increased to the reservoir control temperature. Figure 5-19 shows the response of the tops of the evaporator plates to the change in power. The results clearly indicate that individual pumps can handle a power input as low as 25 W each if there is enough fluid displaced from the condenser to ensure that liquid and vapor are maintained in the accumulator.

### 5.1.5 10 KW Verification Test -

One of the primary objectives for the HPSTM was to show that the system could manage 10 kW steady-state in the capillary-mode. To verify this, the system was run for five hours with a load of 833 W per evaporator at a saturation temperature of 25oC. No deprimes or anomalies occurred during this time; however, the cooling capacity of the condensers was exceeded at this level. The result was that the liquid returning from the subcooler to the evaporators warmed at a rate of 2oC per hour. The test could not be called a steady-state verification due to the transient nature of the condensers. But operating for five hours at this heat load, while maintaining a constant temperature on the cold plates and operating temperature control by the reservoir, was as good a result that could be expected.

## 5.2 Summary Of Hybrid-Mode Test Results

Results of the hybrid-mode testing demonstrated the feasibility of a hybrid concept. The maximum heat transport capability of the system increased with the increase in the mechanical pump speed. Capillary pumping action was initiated when the evaporator exit quality reached 100%, and before any evaporator deprimed in the heat transport augmentation test. Differential pressure measurements confirmed that capillary evaporators regulated the fluid flow under certain nonuniform heat loads. Flow regulation was demonstrated for heat inputs to various evaporator plates with a ratio of 20:1. The heat load

sharing function of the capillary plates in the hybrid-mode was verified with a mechanical pump speed at 10% full scale. A transient heat input of 52 kW was applied to the cold plates for 15 minutes without any evaporator deprimes. Test results also indicated that a fully-flooded system was not required for proper operation if certain procedures were followed.

### 5.2.1 Liquid Inventory Requirement Test -

Under the normal capillary-mode of operation, the vapor header and evaporator grooves are occupied by ammonia vapor. The condensers contain ammonia liquid and/or vapor. The liquid return line and the rest of the loop are occupied by liquid ammonia. For the two-phase reservoir to control the system operating temperature under all possible heat load conditions, the reservoir volume must be at least as large as the condenser volume.

Under hybrid-mode operations, the system does not need a liquid ammonia inventory that is able to completely flood the loop in order for the system to operate properly if the evaporator exit quality is regulated. When the exit quality is uncontrolled, allowing the output from the plates to vary from 100% liquid (no evaporation) to 100% vapor, a fully flooded system is required. A fully-flooded loop needs not only a large ammonia inventory which must be managed, but also a larger reservoir with a minimum volume which is greater than the sum of the condenser,vapor line, and evaporator groove's volumes, since some or all of this liquid could potentially be displaced into the reservoir. This test was designed to evaluate the system performance characteristics with both a fully flooded and partially flooded loop with various heat inputs and mechanical pump speeds.

Theoretical calculations of the volumes of CPL components and the reservoir are presented in Table 5-3. Note that the reservoir volume is less than the sum of the volumes of the vapor line, the evaporator grooves, and the condenser section (.0059 versus .0076$m^3$) Based on the theoretical calculation of the loop volume and the ammonia density at 25°C, 7.5 kg of ammonia was required to completely flood the loop (excluding the reservoir). The system was charged with 8.15 kg of liquid ammonia to ensure that liquid was always present in the reservoir, and that the mechanical pump would never be in danger of cavitating.

Table 5-3
Theoretical Calculations of CPL Component Volumes

| Component | Volume ($m^3$x100) |
|---|---|
| Vapor Header | 5.270 |
| Evaporator Grooves | 0.698 |
| Condensers | 1.654 |
| Liquid Header and Balance | 4.898 |
| Total Loop Volume | 12.52 |
| Hybrid-Mode Reservoir | 5.900 |

The total loop and the reservoir volumes were first verified experimentally. During the volume verification test, no power was applied to the evaporators, while power was applied to the reservoir to raise its temperature above ambient. Ammonia liquid was forced to flow from the reservoir to the loop, due to the pressure difference, until the loop was completely filled. A scale was used to measure the reservoir weight, which was used to calculate the amount of liquid ammonia in the loop under a completely flooded condition.

The experimental data are shown in Table 5-4. The amount of liquid ammonia in the loop under a completely flooded condition was about 7.5 kg. Based on the density of liquid ammonia at 25°C, the loop volume was calculated to be .00125 $m^3$. This is very close to the theoretical value of .001252 $m^3$.

Table 5-4
Experimental Data for Loop Volume Verification

| Date | Reservoir Wt with flooded loop (kg) | Ammonia left in reservoir* (kg) | Ammonia in the loop (kg) |
|---|---|---|---|
| 12/2/87 | 10.32 | 0.62 | 7.53 |
| 12/3/87 | 10.34 | 0.64 | 7.51 |
| 12/4/87 | 10.33 | 0.63 | 7.52 |

* Reservoir tare weight = 9.7 kg

To verify the volume of the reservoir, a test was conducted under the capillary-mode of operation. The reservoir temperature was kept at 25°C, and power was applied to the evaporators. Liquid was forced to flow into the reservoir as vapor that had formed in the evaporators began to displace liquid in the loop. As the power input increased, more condenser area was utilized in order to dissipate the increasing power, forcing more fluid to

flow into the reservoir. When the reservoir was completely filled with ammonia liquid, the reservoir scale showed a constant weight. At the same time, the reservoir lost the control of the system operating temperature, and the condenser had a fixed conductance. The system operating temperature drifted higher and higher in order to dissipate the input power. The total weight of the reservoir under this condition was 13.3 kg. The net weight of liquid ammonia in the reservoir was 3.6 kg, and the reservoir volume was calculated to be 0.006 $m^3$, as compared to the theoretical volume of 0.0059 $m^3$.

Testing confirmed that although a loop completely filled with liquid will guarantee a successful startup, the reservoir will be filled with liquid and lose its temperature control function at high exit quality conditions because the reservoir volume is smaller than those of the vapor header, evaporator grooves and condensers combined (see Table 5-3). To determine the appropriate inventory for the system, a series of tests were performed with various mechanical pump speeds and system powers. The results are shown in Table 5-5. Note that at 25°C the reservoir capacity is 3.6 kg, and the system capacity is 7.5 kg for liquid ammonia. At the 10% pump speed and a 6000 W power input, the reservoir was almost filled with liquid , indicating that a completely filled loop is inappropriate. However, at a 20% pump speed and 1500 W power input, the loop excluding the reservoir was almost filled with liquid ammonia, which means a completely flooded system is needed. Otherwise, the liquid flow would not be continual and a cavitation in the mechanical pump would occur. In this latter case, either the power input must be increased or the pump speed must be reduced if the loop is not completely filled with ammonia liquid to ensure that the reservoir is always partially filled with liquid.

Since the system could be started with a power input of 1500 W and a pump speed of 10% of full scale in the hybrid-mode tests, two kilograms of ammonia were removed from the loop and stored in the capillary-mode reservoir. With the system charge at 6.146 kg, the loop could not be completely filled, but the reservoir could still control the operating temperature at higher evaporator exit quality conditions. To prevent the cavitation of the mechanical pump, the pump speed was not increased to more than 15% full scale for system powers less than 6000 W.

Table 5-5
Liquid Inventory Test

| Pump Speed (%) | System Power (W) | Total Reservoir Weight (kg) | Fluid in Reservoir (kg) | Fluid in Loop (kg) |
|---|---|---|---|---|
| 10 | 1500 | 12.615 | 2.915 | 5.231 |
| 10 | 6000 | 13.695 | 3.595 | 4.551 |
| 15 | 1500 | 11.855 | 2.155 | 5.991 |
| 15 | 6000 | 13.155 | 3.455 | 4.691 |
| 20 | 1500 | 10.443 | 0.740 | 7.403 |
| 20 | 12000 | 12.640 | 2.940 | 5.206 |

### 5.2.2 Hybrid-Mode Start-Up

The start-up procedure for hybrid-mode testing is outlined as follows:

1. Set the condenser to 0°C by starting the chiller and waiting until the chiller reaches an equilibrium (about two hours). Set the reservoir controller to 25°C. Apply 100 W to the reservoir. Wait until the reservoir reaches its set point temperature.
2. Apply 125 W to each evaporator (total 1500 W). When the vapor header is clear of liquid ammonia and the vapor front reaches the condenser section, as indicated by an increase in condenser inlet temperature, start the mechanical pump with its speed at 10% full scale.
3. Wait for 15 to 30 minutes before proceeding to the scheduled test. If the desired mechanical pump speed is more than 15% full scale, increase the system power to 6000 W (500 W/evaporator), then set the desired pump speed.

This start-up procedure was the most convenient procedure for the hybrid-mode program, and was used throughout these tests. Since most of the hybrid-mode tests required high powers and/or prolonged periods under given conditions, and the heat dissipating capability of the chiller was limited to about 9000 W, setting the chiller to 0°C provided enough subcooling and heat capacity to allow all of the desired testing.If the mechanical pump was started before any power was applied to the evaporators, as was done in one test, cold liquid was injected into the evaporators, and there was a considerable time delay before the evaporators were warmed to the reservoir set point and started the evaporation process.

### 5.2.3 Heat Transport Augmentation Test

For a given mechanical pump speed, a relationship exists between the pressure head developed and the mass flow rate delivered by the pump: the higher the pressure head is, the lower the mass flow rate. In the hybrid-mode testing of the HPSTM, the majority of the pressure drop occurred in the thermal flowmeter that was installed in the bypass to the liquid return line. Any variation of pressure drop in the vapor line due to a change in evaporator exit quality was insignificant compared to the large pressure drop in the liquid return line. Consequently, the loop pressure drop was nearly constant, and the mechanical pump delivered a nearly constant mass flow rate even though the evaporator heat load increased.

This characteristic was true until the vapor exit quality reached near 100%. Any further increase in the evaporator power level would require a higher mass flow rate than was being delivered by the mechanical pump at a fixed speed. The capillary pumping function of the wicks in the evaporator were then activated to develop enough capillary pressure rise so that the total mass flow rate in the loop met the demand of the evaporators and the pressure heads developed by the mechanical pump and the capillary evaporators balanced the total pressure drop in the loop. When the capillary pumping requirement exceeded the wicks potential, the evaporators deprimed.

Figure 5-20 illustrates the heat transport augmentation function of the capillary evaporators in the hybrid-mode with a mechanical pump speed at 10% of the full scale. Three parameters are plotted as a function of the total power input to the evaporators: the mass flow rate, the pressure head developed by the mechanical pump, and the pressure difference across the evaporators (the vapor header relative to the liquid header). As previously explained, all three variables were at constant values for powers up to 6 kW: the mass flow rate at 4.8x10-3 kg/sec, the pressure head of the mechanical pump at 0.5 psi, and the pressure differential across the evaporators at a slightly negative value, indicating that the capillary pumps were actually a pressure drop. As the power input increased to 6.6 kW, capillary pumping of the evaporator wicks was activated, as seen by a pressure rise across the evaporator pumps on plate 1. Consequently, the pressure head of the mechanical pump dropped, and a higher mass flow rate was delivered. For each power increase thereafter, the capillary pressure rise and mass flow rate increased, and the pressure head across the mechanical pump decreased. Note that at the incipience of capillary pumping action, the total system power input of 6 kW was close to the power required to evaporate liquid ammonia circulated at a rate of 4.8x10-3 kg/sec (100% vapor quality). At any subsequently higher power level, the flow rate corresponded to a vapor quality of 100%.

The heat transport augmentation tests were also conducted at other mechanical pump speeds. Test results are shown in Table 5-6. Notice that the pump speed was adjusted with a dial-type controller, which had a very poor resolution. The actual pump speed and flow rate was very sensitive to the dial setting. The speed setting shown is therefore a poor parameter for comparing data. The mass flow rate is a better basis of comparison. The maximum heat input prior to the capillary deprime in the table refers to the highest heat load maintained without a deprime. No intermediate power levels between this power and the deprime power was used during this test. At high pump speeds, the frictional pressure drop was already high. The contribution of capillary pressure rise to the total pressure head, and hence the heat transport augmentation, became less significant. Nevertheless, the capillary pumping in the evaporators was activated prior to the evaporator deprime, since the pressure difference across the evaporators changed from a negative value

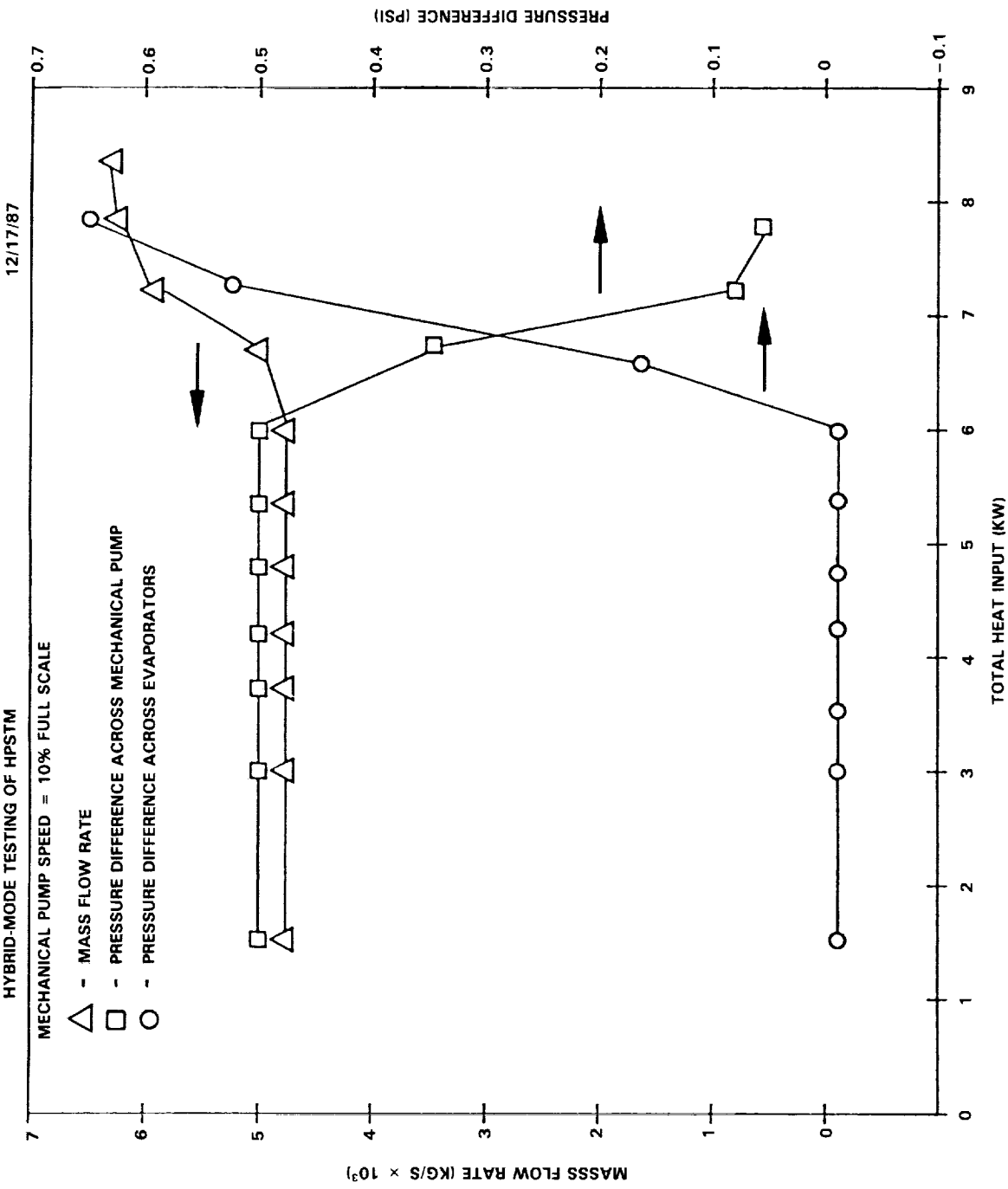


Figure 5-20. Heat Input Augmentation by Capillary Pumping

to a positive one in all of the tests. Once a capillary deprime occurred, the system could not be primed again unless the system power was lowered to a level below that of the incipience of the capillary pumping action.

Table 5-6
Capillary Heat Transport Augmentation
at Various Pump Speeds

| Pump Speed (% full) | Max. Q Without Cap. Pumping (kW) | Mass Flow Without Capillary Pumping (kg/s) | Max. Q at Cap. Deprime (kW) | Max. Q Before Capillary Deprime (kW) | Mass Flow Before Capillary Deprime (kW) |
|---|---|---|---|---|---|
| 9 | 4.2 | 0.0032 | 7.2 | 5.4 | 0.0044 |
| 10 | 6.0 | 0.0048 | 8.4 | 7.2 | 0.0055 |
| 10 | 6.0 | 0.0048 | 8.4 | 7.8 | 0.0062 |
| 11 | 7.3 | 0.0053 | 9.0 | 8.5 | 0.0062 |
| 15 | 18.0 | 0.0155 | 19.2 | 18.0 | 0.0150 |
| 15 | 18.0 | 0.0156 | 19.2 | 18.0 | 0.0156 |
| 20 | 33.0 | 0.0310 | 36.1 | 33.0 | 0.0310 |

Some basic characteristics of the capillary heat transport augmentation test are summarized as follows. First, the capillary pumping action of the evaporators was initiated when the mechanical pump could no longer provide a higher mass flow rate required by the evaporators at the higher power levels. This occurred when the vapor exit quality was about 100%. Second, the incipience of the capillary pumping action was indicated by a pressure rise across the evaporators and an increase in the total mass flow rate of ammonia in the loop. Third, the system transport limit for a given mechanical pump speed was reached when the required pressure rise across an evaporator reached its capillary pumping capability. Fourth, transport limits for mechanical pump speeds at 10, 15, and 20 percent full scale were 8, 19, and 36 kW, respectively. While the first two transport limits seem low when compared to the transport limit achieved in the capillary-mode of testing, the cause of this was related to the excessive pressure drop in the bypass line caused by the thermal flowmeter. Finally, when the system experienced a capillary deprime, the deprimed evaporators could not be reprimed unless the total power input was reduced below the power corresponding to the incipience of capillary pumping.

### 5.2.4 Flow Distribution Control Test

One of the advantages of using a hybrid system is that the parallel capillary evaporators can distribute the flow amongst each other according to the mechanical pump speed and the heat load applied to the evaporators. The importance of such a flow control function can be explained by first considering a parallel, pumped two-phase loop without capillary evaporators,as seen in Figure 5-21. This loop consists of all the basic elements seen in the CPL systems, without the capillary pumps.

With low power inputs to the evaporators, the system pressure drop characteristics can be shown schematically in Figure 5-22. From this pressure distribution, one can conclude that evaporator 3 will get the highest flow rate, while evaporator 1 will get the least. If the power applied to evaporator 1 increases while the power to the other plates remain the same, evaporator 1 will soon burnout due to insufficient flow even though evaporators 2 and 3 may be flooded with liquid. Similar results will be obtained if evaporator 2 or 3 is getting the majority of the total system power input. The mechanical pump may be providing enough flow so far as the total system power is concerned. The problem is that a lack of flow distribution control exists among the evaporators. A regulated valving system is required for flow control that would add an element of complexity and unreliability to the system.

If capillary evaporators are used, much of the flow distribution problems can be resolved in the system shown in Figure 5-21. For example, assume a constant power input is applied to evaporators 2 and 3, while the power to evaporator 1 is increasing. The flow quality at the exit of evaporator 1 will increase. When the flow quality reaches about 100%, the capillary pumping action will begin in evaporator 1, and a higher flow rate will be seen through the evaporator to prevent liquid starvation. Much of this excess liquid will be drawn from the other two evaporators; therefore, the flow exit qualities through evaporators 2 and 3 will also increase. The result is that a more isothermal evaporator section is seen.

One possible pressure distribution for the system is shown in Figure 5-23a. Evaporator 2 or 3 will start the capillary pumping action when the flow quality in the individual evaporator reaches 100%. Whenever any evaporator starts capillary pumping, the mass flow rate in that evaporator is determined by the power input such that the flow exit quality is 100%. Each evaporator will continue its capillary function until the required pressure rise exceeds its capillary pumping capability.

Slightly different results will be seen if power inputs to evaporator 1 and 2 are constant, while the heat input to evaporator 3 is increased. As the power in evaporator 3 rises, the mass flow to that evaporator will also increase at the expense of the flows to the other two evaporators. When evaporator 3 reaches a 100% exit quality condition, the other two pumps must also start capillary pumping as long as all the pumps are receiving power. This situation, shown in Figure 5-23b,

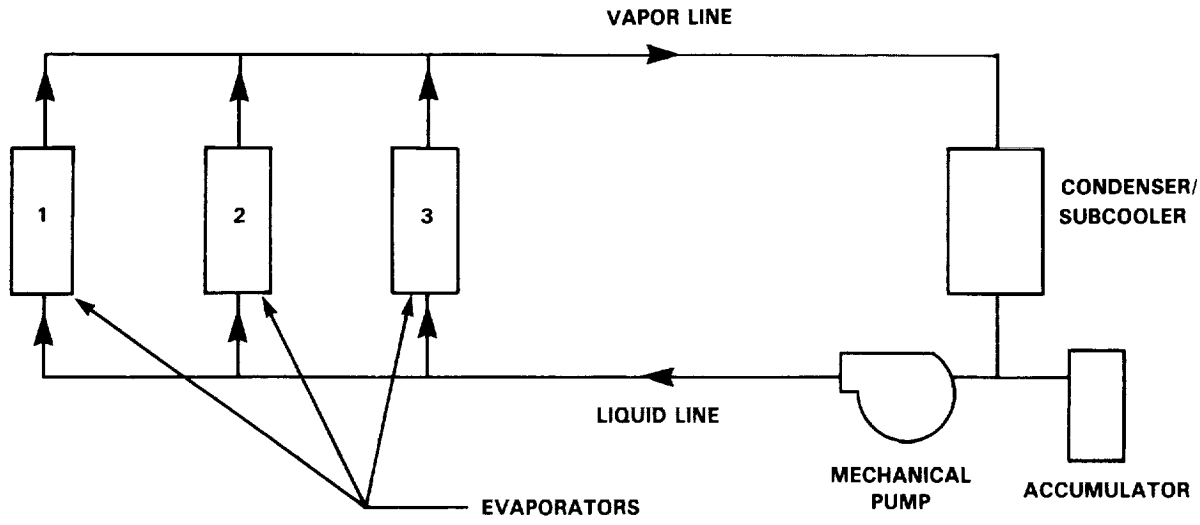


Figure 5-21. Pumped Two-Phase Heat Transport System, Non-Capillary Evaporators

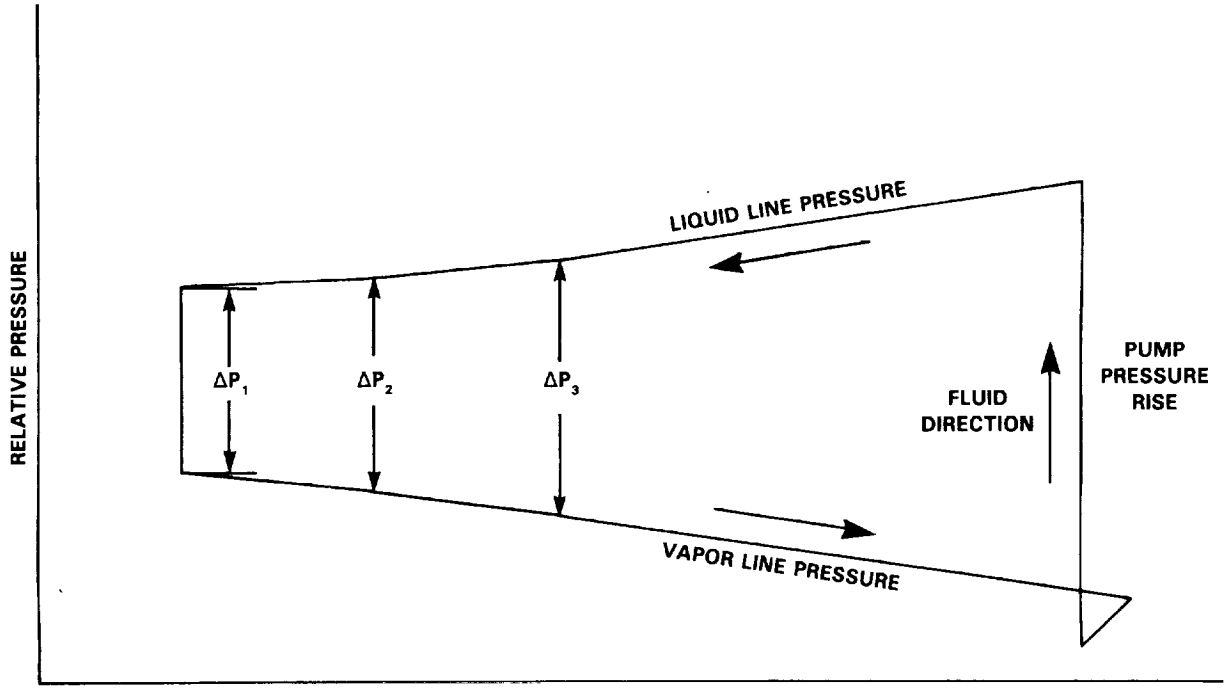


Figure 5-22. Relative Pressure Drop vs. Location in a Non-Capillary Two-Phase System

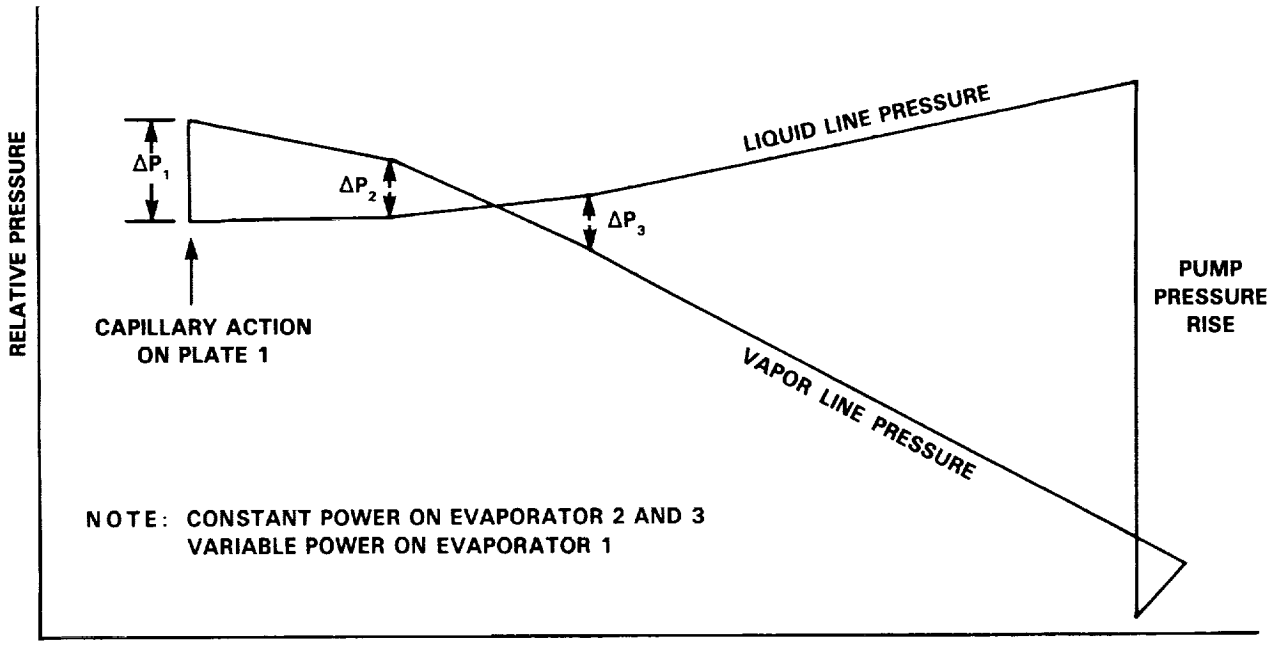


Figure 5-23a. Possible Pressure Distribution in a Capillary System

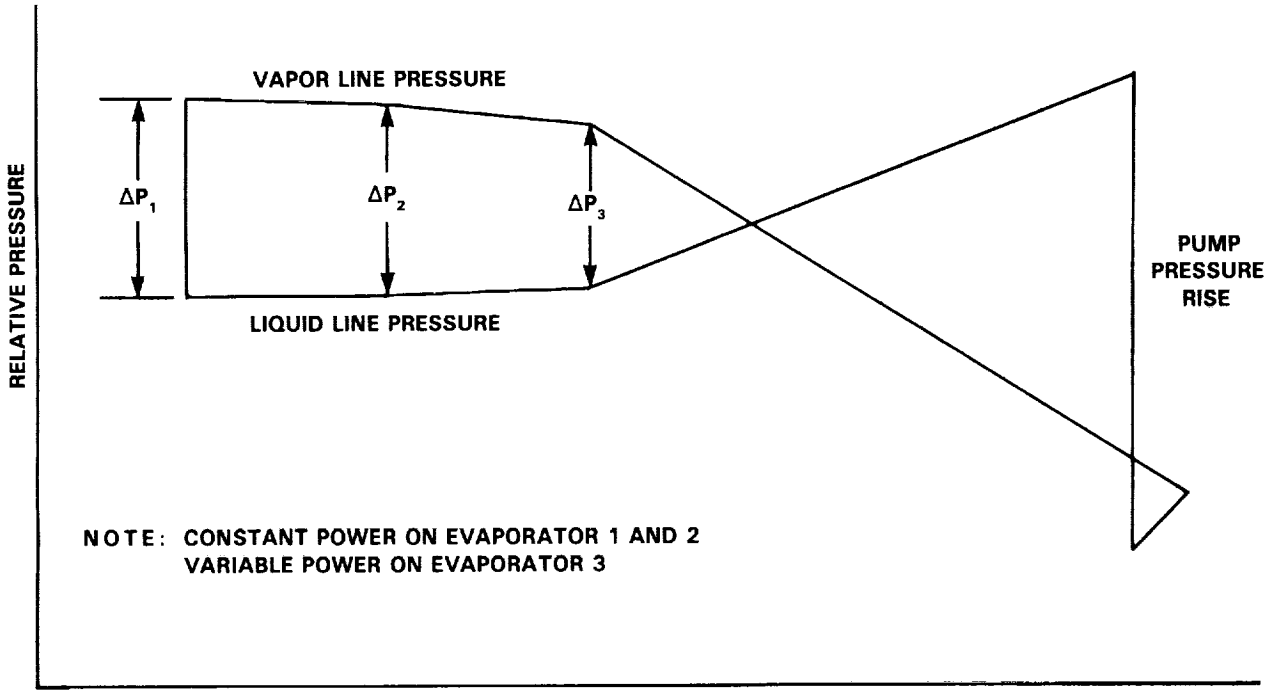


Figure 5-23b. Possible Pressure Distribution in a Capillary System

differs from the case illustrated in Figure 5-23a. However, the overall effects on flow control and evaporator isothermality are the same.

Several tests were conducted to demonstrate the flow control function of the capillary evaporators in the HPSTM hybrid-mode of operation. The first test was performed with various pump speeds and power ratios to the evaporator plates. Figure 5-24 through 5-26 show the evaporator temperatures, pressure difference across plate 1, and the power input to each evaporator on the three plates.

At low powers, where the capillary pumping action had not started, the pressure difference across the evaporator plate 1 became increasingly negative each time the mechanical pump speed was increased (see Figure 5-25). This occurred because the mass flow rate in the loop, and hence the pressure drop across plate 1 increased with the increasing pump speed. As power inputs to plates 1,2 and 3 reached 8,4, and 1 kW respectively, the capillary pumping action was initiated in plate 1, as evidenced by an increase in the pressure difference across plate 1. Also, the evaporator temperature exceeded the reservoir temperature, as seen in Figure 5-24. The pressure difference across plate 1 was still negative because this pressure difference was measured between the isolators and the vapor header, which included not only the capillary pressure rise, but also the pressure drops in isolator and evaporator wicks. Only when the capillary pressure rise exceeded the pressure drops would this measured pressure difference become positive. Capillary pumping started in evaporators on plate 2 at power inputs of 16,4, and 1 kW to the three evaporator plates. Capillary pumping began in plate 3 when the power levels were raised to 20,4, and 4 kW.

The reservoir temperature changed with the increase in system power. As the evaporator heat loads increased, more condenser area was required to dissipate the heat load, forcing liquid to flow into the vertical reservoir. Compression work was done to the vapor at the top of the reservoir, causing temperatures in the reservoir and the system saturation temperature to increase. Conversely, when liquid was forced out of the reservoir, the vapor expanded in the reservoir, and the saturation temperature dropped.

Another flow control test consisted of varying the power input to one of the evaporator plates while maintaining a constant load on the other two plates, with the mechanical pump operating at 10% of its potential speed. Figures 5-27 and 5-28 show the isolator temperatures on the three plates and the pressure difference across plate 1. Power inputs to plates 1 and 3 were held at 500 W each. Note from Figure 5-27 that the plate 1 and 3 isolator temperatures increased when more heat was applied to plate 2, indicating a reduced flow to plates 1 and 3. Capillary pumping did not start until the power applied to plate 2 increased to 5 kW. The differential pressure measurement did not show the initiation of capillary pumping until 20 minutes

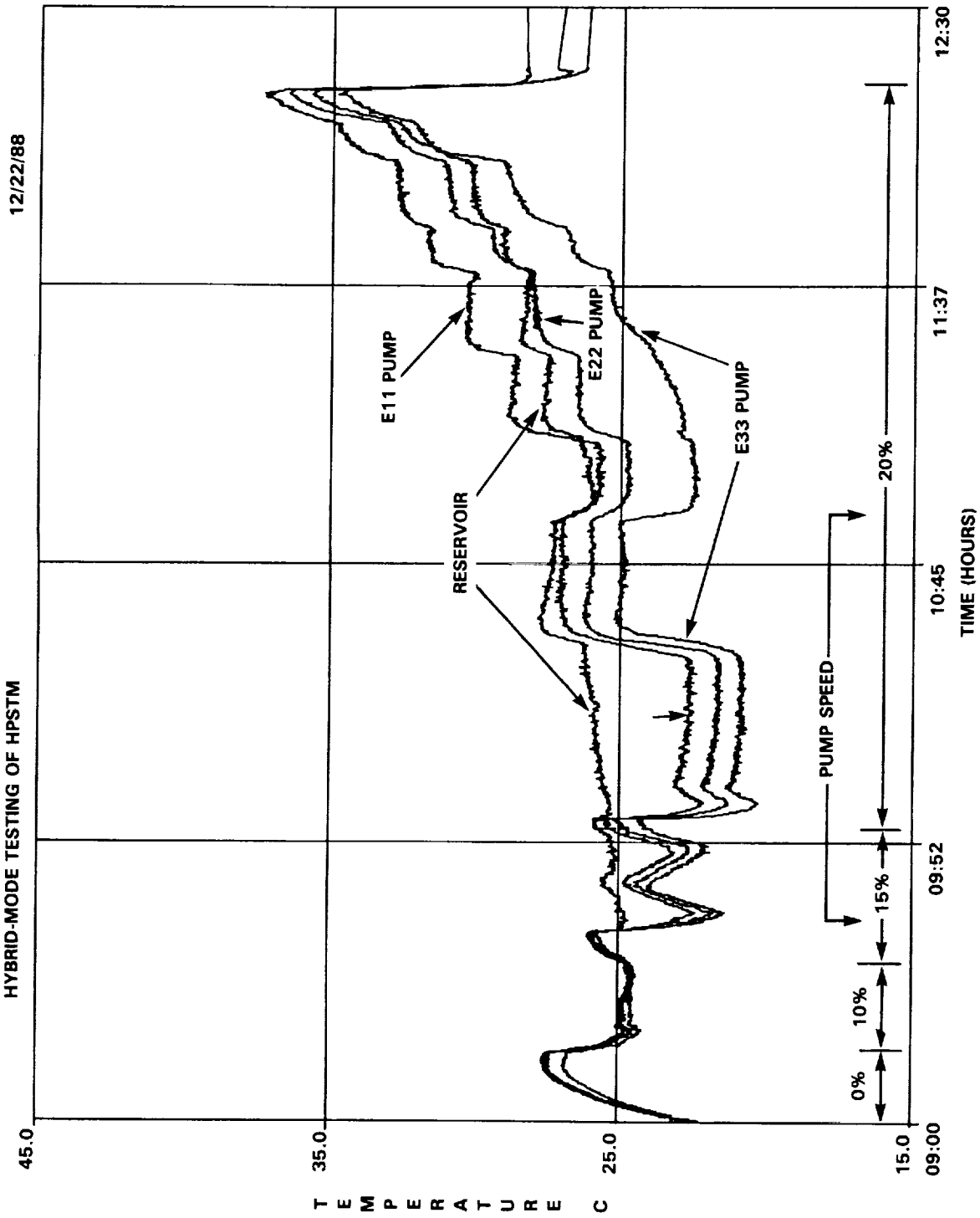


Figure 5-24. Capillary Pump Temperatures in a Flow Control Test

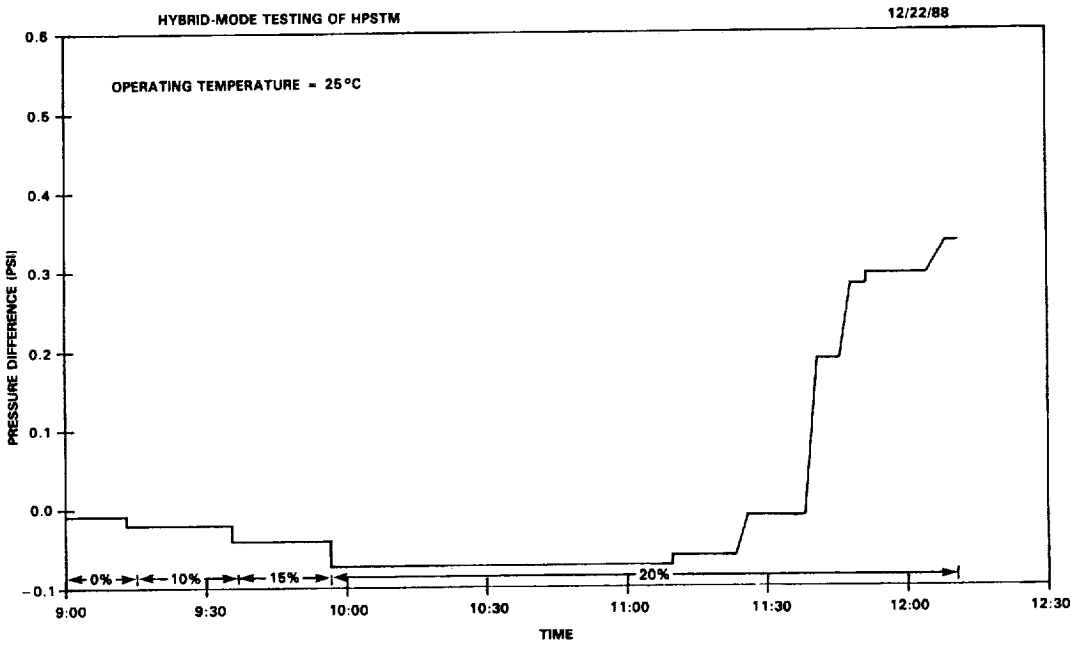


Figure 5-25. Plate 1 Pressure Differential, Flow Control Hybrid Test

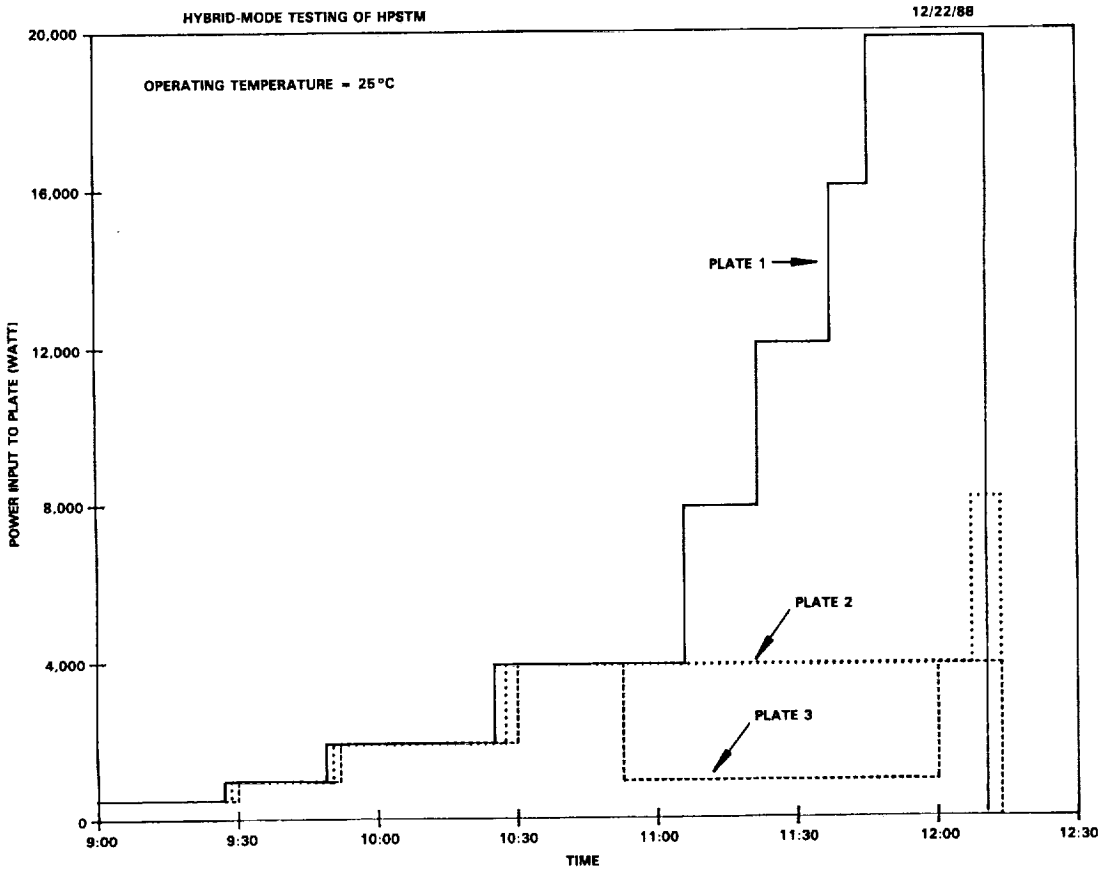


Figure 5-26. Plate Powers During Hybrid Flow Control Test

after the plate 2 power input was raised to 5 kW. This delay represented the transient from mechanical pumping to capillary pumping. Figure 5-29 shows the evaporator temperatures. Although there was a large difference in the power applied to the three plates, the evaporators were fairly isothermal. This is because the capillary evaporators adjusted the flow distribution according to the power input.

Figures 5-30 and 5-31 show the pressure differential across plate 1 and the evaporator temperatures for the case when the plate 3 power input was varied. The capillary pumping action started when plate 3 power level increased to 5 kW; twenty minutes later, the pressure differential switched from a negative to a positive value. Again, the evaporators displayed nearly isothermal conditions.

The capillary pumping action will start in an evaporator when the flow quality in that evaporator reaches 100%. Since the mass flow rate in the loop and the flow distribution among the evaporators are functions of the total system power, it is expected that the onset of capillary pumping action in an evaporator will depend on the power inputs to that evaporator as well as the power input to the other evaporators. To investigate the relationship between the onset of capillary pumping and the system power profiles, three tests were conducted: a) Plates 2 and 3 were kept at a constant heat load of 500 W each, while plate 1 power was increased, b) plates 2 and 3 were held constant at 1500 W each, while plate 1 power was increased, and c) uniform powers were applied to all three plates and were increased. All tests were conducted with a mechanical pump setting of 10% full scale.

Table 5-7
Summary of Flow Control Test

| Power Input (W) | | | | Events |
|---|---|---|---|---|
| Plate 1 | Plate 2 | Plate 3 | Total | |
| 6500 | 500 | 500 | 7500 | Capillary action started |
| 8000 | 500 | 500 | 9000 | E11 deprime |
| 4500 | 1500 | 1500 | 7500 | Capillary action started |
| 5800 | 1500 | 1500 | 8800 | E11 deprime |
| 2400 | 2400 | 2400 | 7200 | Capillary action started |
| 3000 | 3000 | 3000 | 9000 | E11 deprime |

Note: Mechanical pump speed at 10% full scale for all tests

A summary of the test results is shown in Table 5-7. With 500 W on plates 2 and 3, the capillary action started with plate

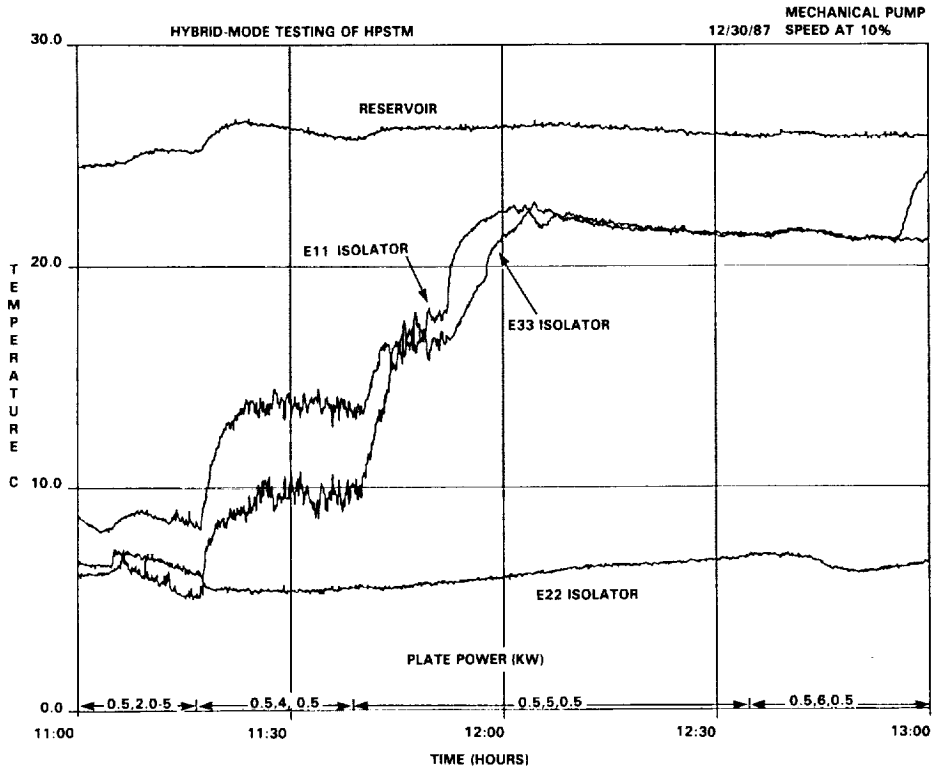


Figure 5-27. Hybrid Flow Distribution Control Test

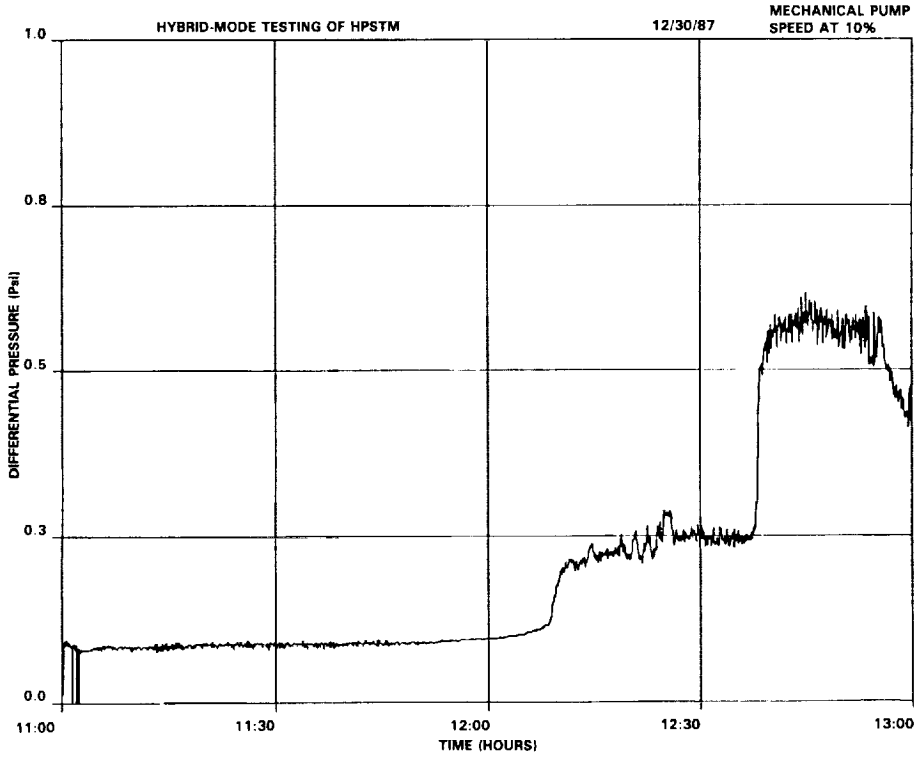


Figure 5-28. Hybrid Flow Distribution Control Test

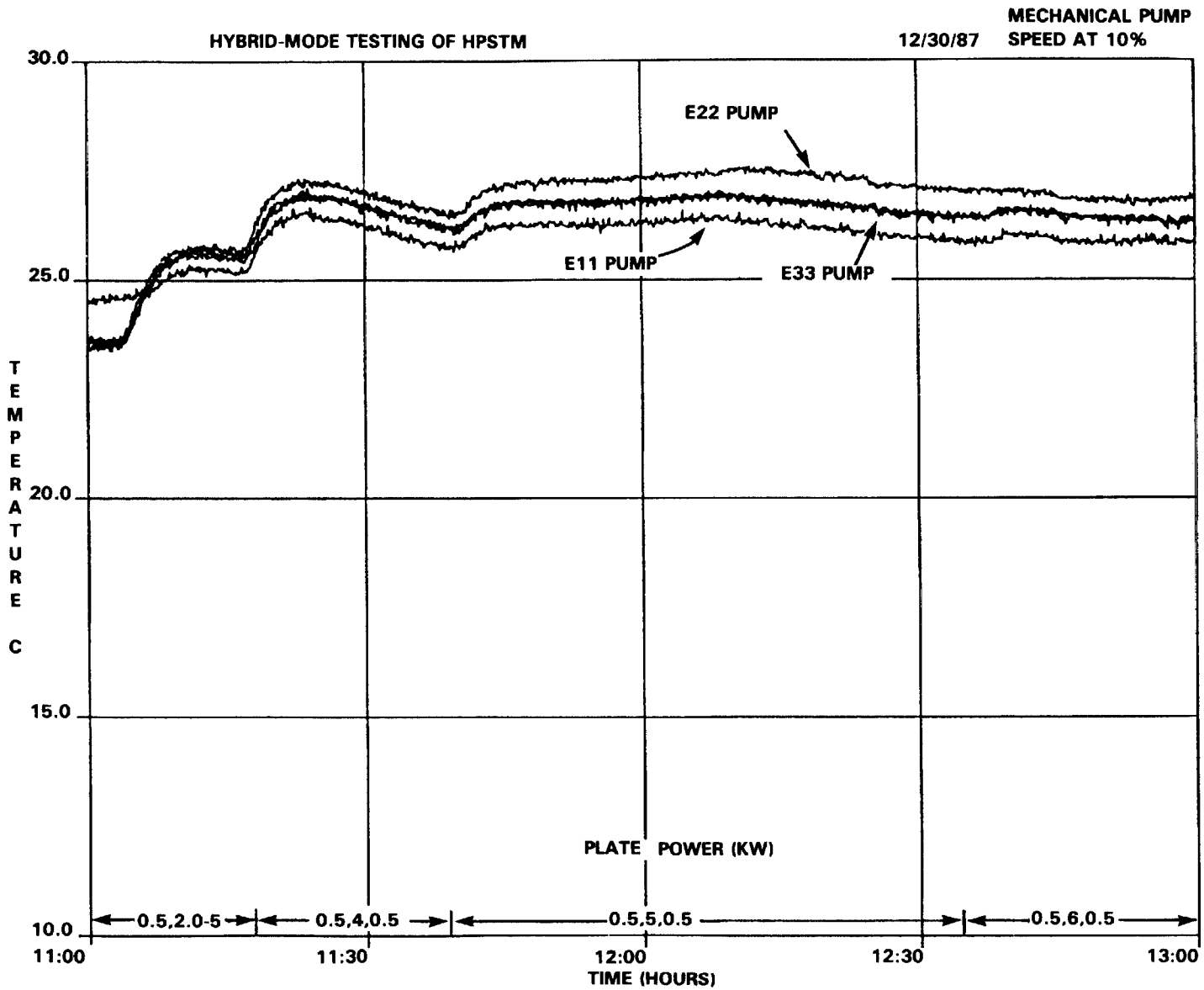


Figure 5-29. Hybrid Flow Distribution Control Test

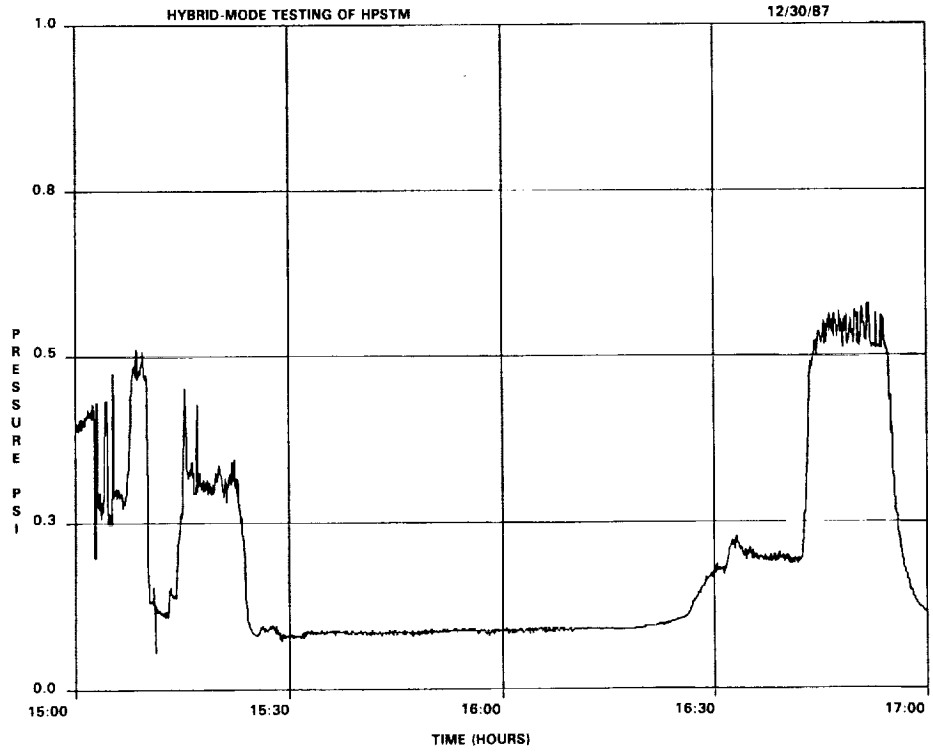


Figure 5-30. Hybrid Flow Distribution Control Test

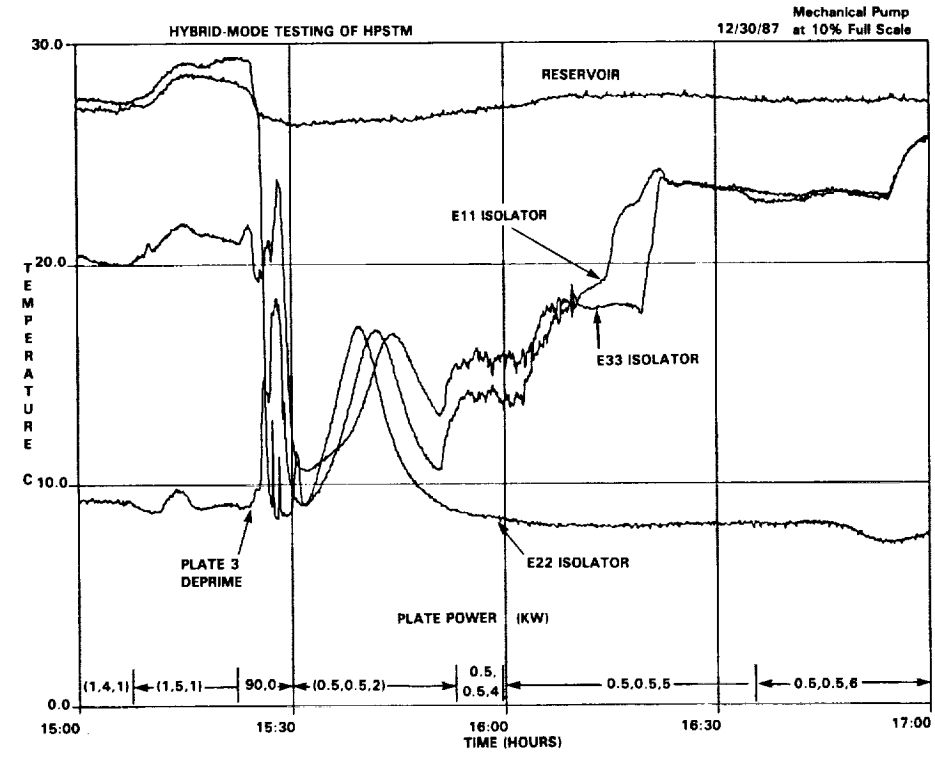


Figure 5-31. Hybrid Flow Distribution Control Test

1 power at 6500 W ( total system power of 7500 W), and E11 deprimed when the plate 1 power was increased to 8000 W (total system power of 9000 W). With 1500 W on plates 2 and 3, the capillary action started with the plate 1 power at 4500 W (total system power of 7500 W), and E11 deprimed when the plate 1 power level reached 5800 W (total system power of 8800 W). For the uniform heat input test, the capillary action began at 2400 W per plate (7200 W system power), and E11 deprimed at 3000 W per plate (9000 W on the system).

The incipience of capillary pumping of the evaporators on plate 1 and the capillary limit of the system depended mainly on the total system power and much less on the individual plate power. This is because the pressure drop in the hybrid-mode was dominated by the impedance of the thermal flow meter in the liquid return line. Any variations in the mass flow rates and associated pressure drops in the evaporator section were insignificant when compared to the high pressure loss in the liquid return line.

### 5.2.5 Steady-State And Transient Operations

The objectives of the steady-state and transient operations tests were: a) to evaluate system performance during capillary-mode, hybrid- mode, and the transition from one mode to the other; and b) to verify that the hybrid system could handle 50 kW of power input. Tests were conducted with a power input of 10 kW in the steady-state, capillary-mode operation, and 50 kW during the transient hybrid-mode. The mechanical pump speed was set to 30% full scale in the hybrid-mode. The bypass valve in the pump-assist package was used to control the fluid flow; the valve was shut in the capillary-mode test and opened in the hybrid- mode.

Three successful tests were performed. Cycles consisted of capillary steady-state operation at 10 kW, followed by hybrid operation at 52 kW for 15 minutes, and a return to capillary steady-state operation at 10 kW for 45 minutes. The transition between the capillary-mode and the hybrid-mode was made by a simple manual operation of a bypass valve. The evaporator pump and isolator temperatures during a typical test are shown in Figure 5-32. The reservoir set point increased rapidly when power was increased from 1.5 to 10 kW and from 10 to 52 kW due to compression work done to the vapor in the reservoir. When the power input decreased from 52 to 10 kW, vapor ammonia in the reservoir expanded, and the reservoir temperature decreased immediately. Both the pump and the isolator temperatures decreased sharply during that part of the transition after the mechanical pump was started but before 50 kW were applied.

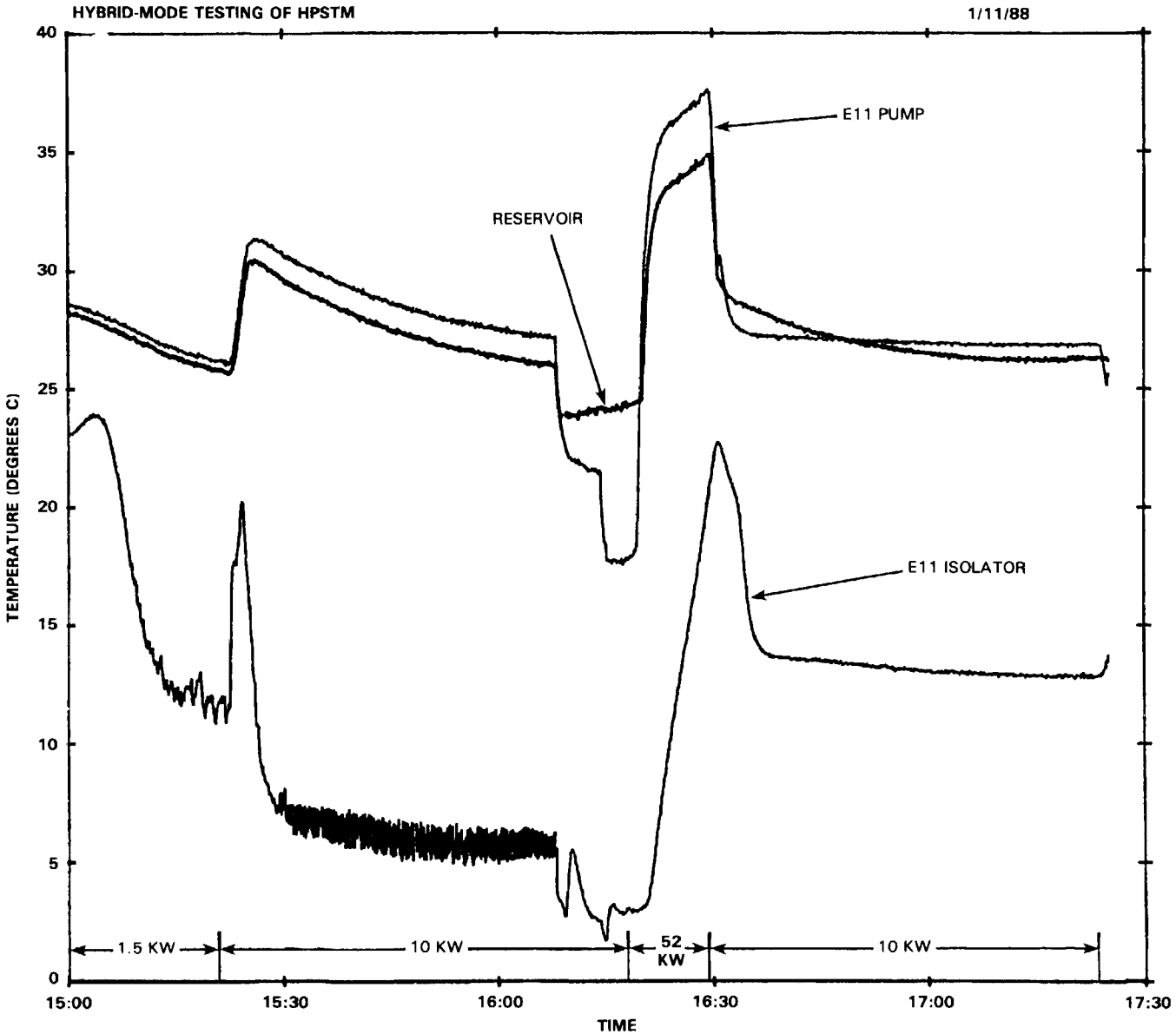


Figure 5-32. Steady-State and Transient Operations

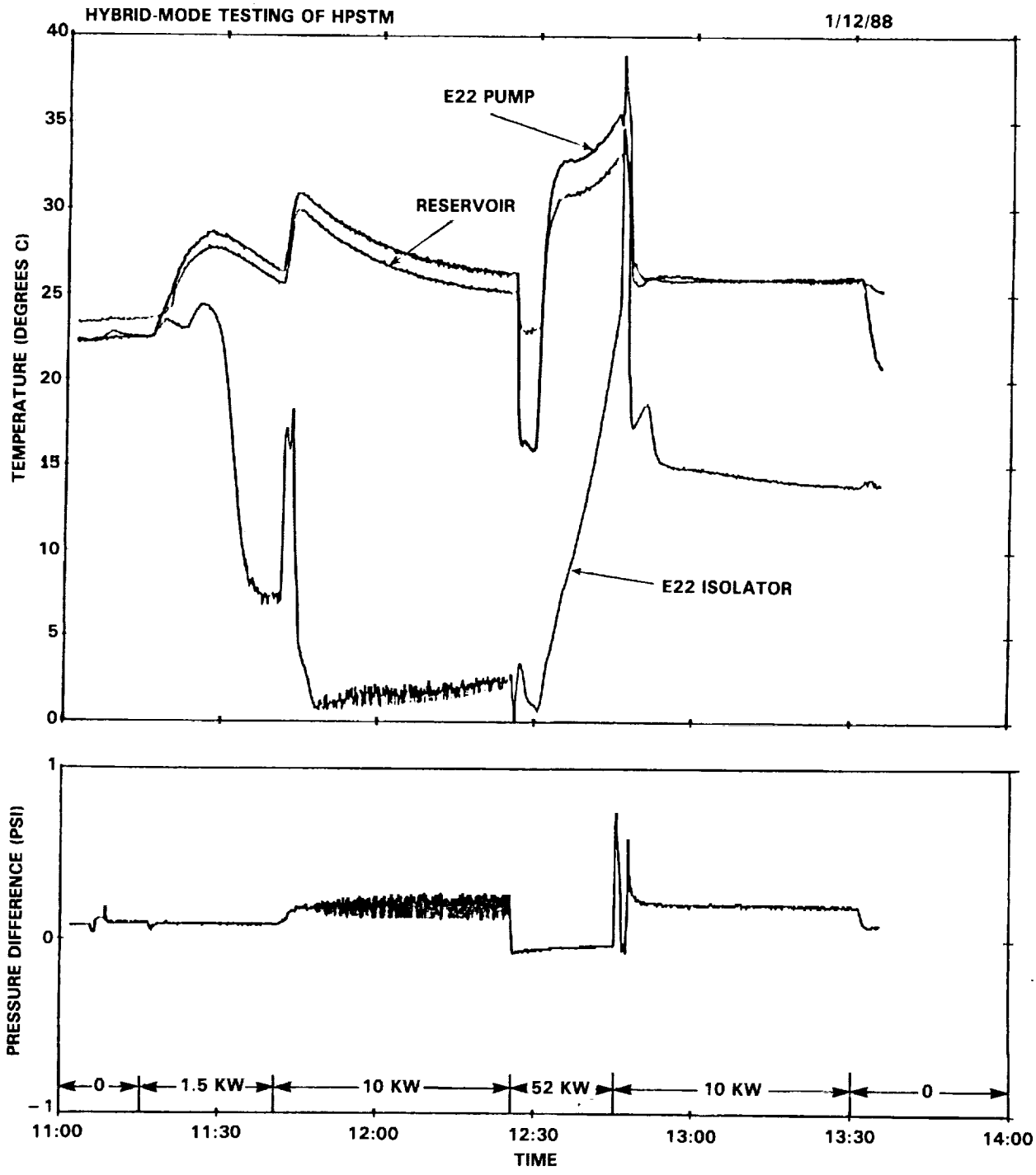


Figure 5-33. Steady-State and Burst Power Operations

In another cycle, the mechanical pump was stopped prematurely in going from the hybrid-mode to the capillary-mode of operation. As a result, some evaporators deprimed because the residual heat in the evaporator plate demanded a capillary pressure rise in excess of the capability of the evaporator pumps. The deprimed evaporators were reprimed immediately after the mechanical pump was restarted. The test continue until the cycle of steady-state and transient power test was completed. Temperature profiles of the reservoir, the evaporator pump, and the isolators, along with the differential pressure across plate 1 for this test are shown in Figure 5-33.

In both Figures 5-32 and 5-33, pressure and temperature oscillations were seen during the 10 kW capillary-mode of operation. These oscillations disappeared when the power level was raised to 50 kW in the hybrid-mode. When the evaporator heat load was lowered back to 10 kW in the capillary-mode, the oscillations did not reappear during the 45 minutes that the system was operated in these conditions. These phenomena were similar to those seen in Figure 5-5, and will require further study to determine their causes.

### 5.2.6 Heat Load Sharing Test

The purpose of the heat load sharing test was to demonstrate that heat load sharing under the hybrid-mode is still possible, depending on the pressure distribution in the evaporator section. As was stated in the flow distribution control test results, the pressure distribution is a function of evaporator section configuration, heat input, and mechanical pump speed.

Heat load sharing in the hybrid-mode was verified by applying power to one of the evaporator plates and varying the mechanical pump speed. Initially, the mechanical pump was set to a high speed to deliver sufficient liquid to the evaporators so that no capillary pumping and hence no heat load sharing appeared. The mechanical pump speed was then gradually decreased. The flow quality in the evaporator with heat input reached 100 percent at a certain pump speed. At the same time, capillary pumping was initiated in that evaporator. The higher pressure on the vapor side forced vapor to flow through the unheated evaporators if the pressure distribution in the evaporator section allowed that to happen. Heat load sharing function was verified from the temperature distribution in the evaporator section. Note that heat load sharing under the hybrid-mode was possible only when the pressure distribution in the evaporator section allowed reverse flow in some of the evaporators.

Heat load sharing verification tests were conducted as follows: The mechanical pump was started with a speed at 12.5% full scale. A heat power of 1.5 kW was applied to plate 2 and

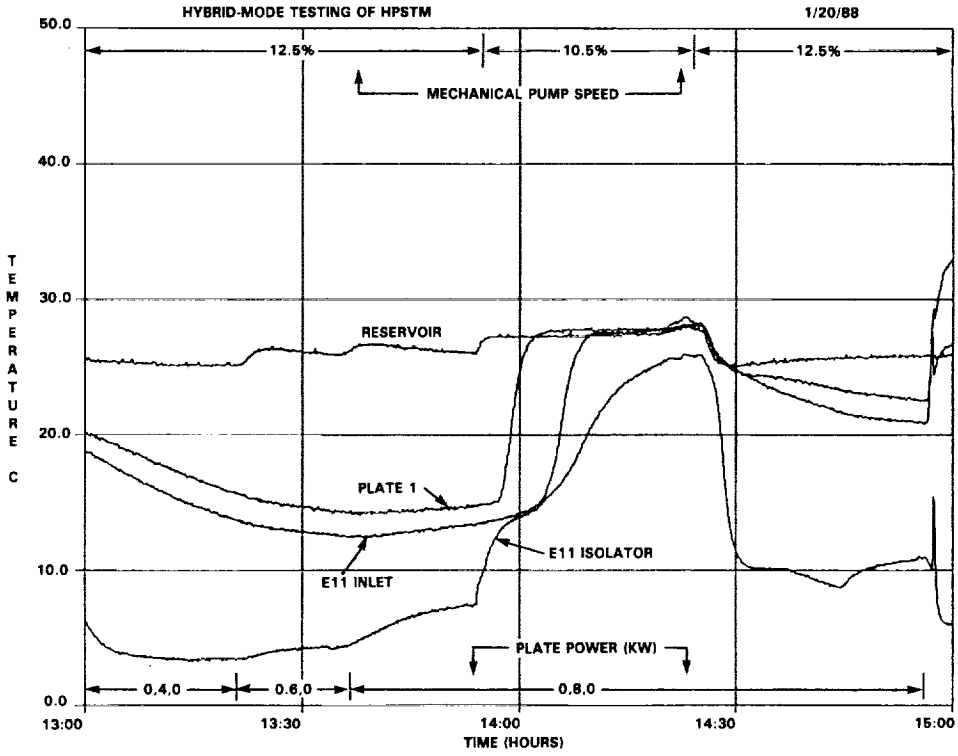


Figure 5-34. Heat Load Sharing Test, Plate 1

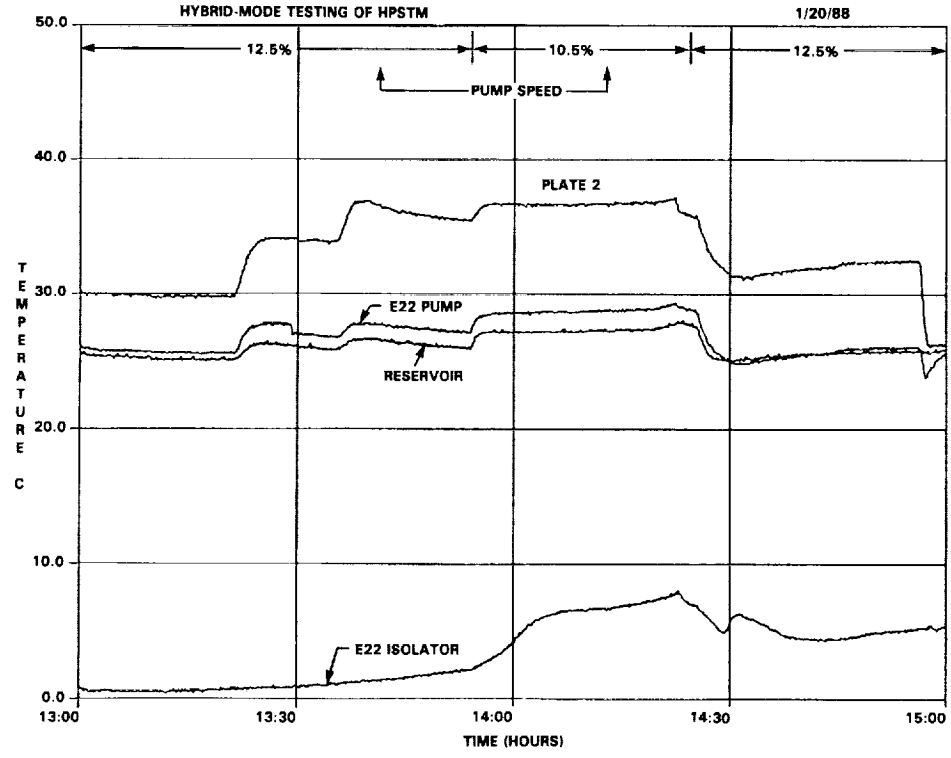


Figure 5-35. Heat Load Sharing Test, Plate 2

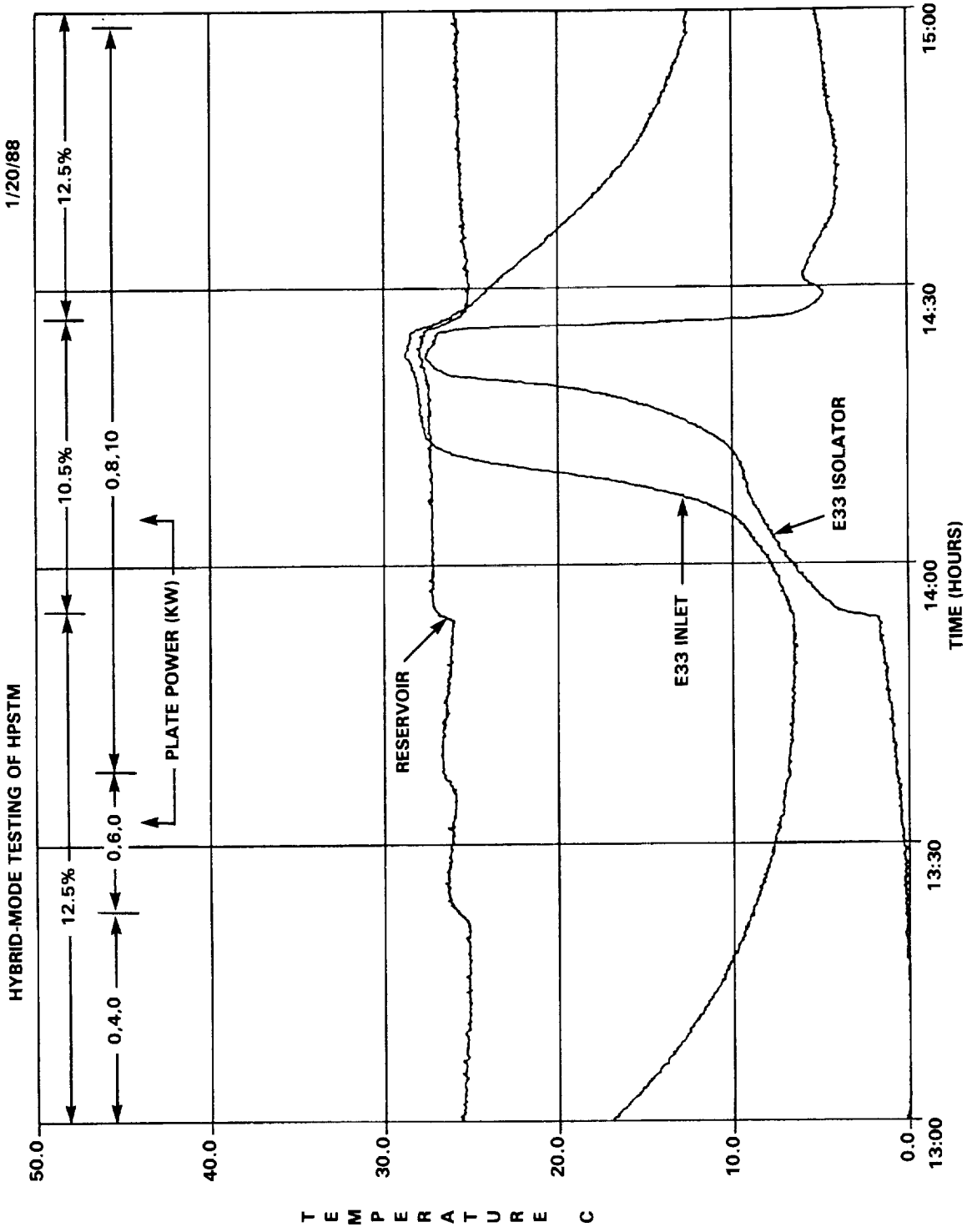


Figure 5-36. Heat Load Sharing Test, Plate 3

gradually increased to 8 kW. Then the mechanical pump speed was reduced to 10.5% to verify the heat load sharing function. The pump speed was then returned to 12.5% full scale. The test was repeated twice, with power applied to plate 1 and plate 3 only.

When the mechanical pump was running at a speed of 12.5% full scale with a power input of 8 kW, test data indicated no capillary action or heat load sharing. A negative differential pressure was shown across the evaporator plate 1, and all evaporators were at subcooled temperatures. Figures 5-34 to 5-36 show the temperature profiles of evaporators on plates 1, 2, and 3, respectively. As the mechanical pump speed was decreased to 10.5%, capillary pumping started in plate 2 as evidenced by a pressure rise across the evaporator plate 1. Temperatures of evaporator pumps, inlets, and isolators on plates 1 and 3 rose to the reservoir temperature, indicating a reverse flow and heat load sharing condition on these plates. Heat load sharing occurred first in plate 1, then in plate 3. When the mechanical pump was increased back to 12.5%, the capillary action of evaporators on plate 2 stopped. Heat load sharing on plates 1 and 3 also disappeared and all temperatures of evaporator pumps, inlets, and isolators became subcooled again. Similar results were obtained when power input was applied to plate 1 or 3 only.

In another test, heat load sharing was demonstrated by changing power input to an evaporator plate while keeping the mechanical pump at a constant speed. The cycle started with an initial condition where the mechanical pump was running at a speed of 10% full scale and power inputs to plates 1, 2, and 3 were 0.5, 6, and 0.5 kW, respectively. Typical isolator temperatures from each plate are shown in Figures 5-37, and the pressure difference across the evaporator plate 1 is shown in Figure 5-38. When the power input to plate 1 was removed, isolator temperatures of plate 1 immediately increased to almost that of the reservoir saturation temperature, which was an indication that heat sharing had started in plate 1. The differential pressure across plate 1 decreased somewhat due to a reverse flow on the vapor header from plate 2 to plate 1. When the power input to plate 1 was increased to 1 kW, isolator temperatures of plate 1 decreased immediately, indicating that cold liquid from the liquid return line was flowing from the isolator to the evaporator pump, and that heat load sharing had stopped on plate 1. There was further evidence of this from the increase of pressure rise across plate 1. Similarly, plate 3 started heat load sharing when the power input to plate 3 decreased from 0.5 to 0 kW.

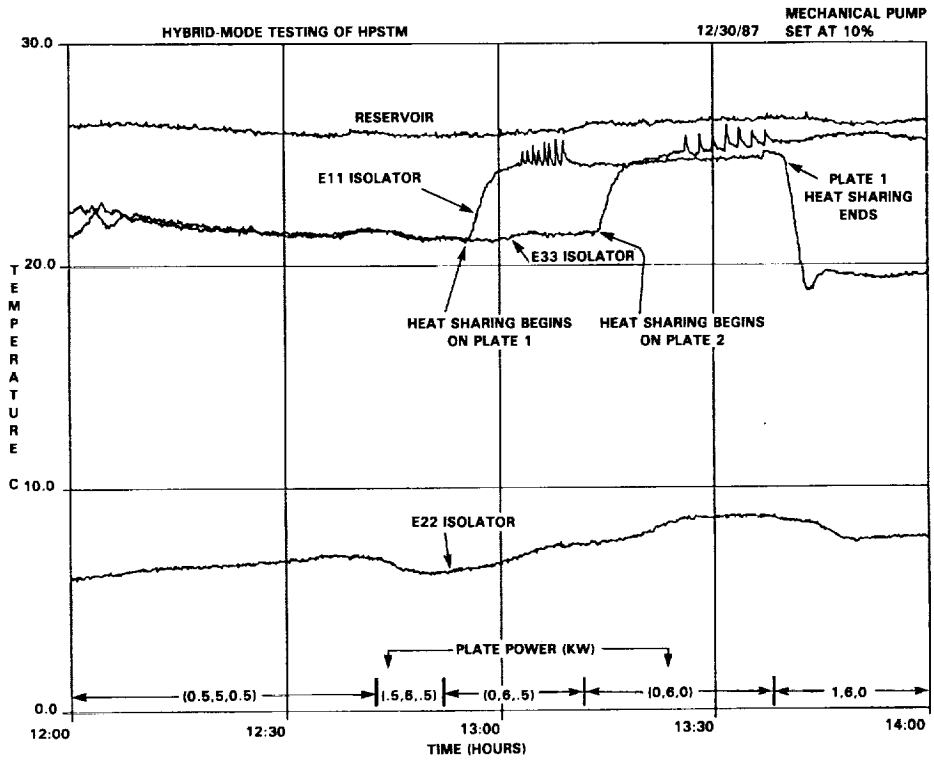


Figure 5-37. Heat Load Sharing Test

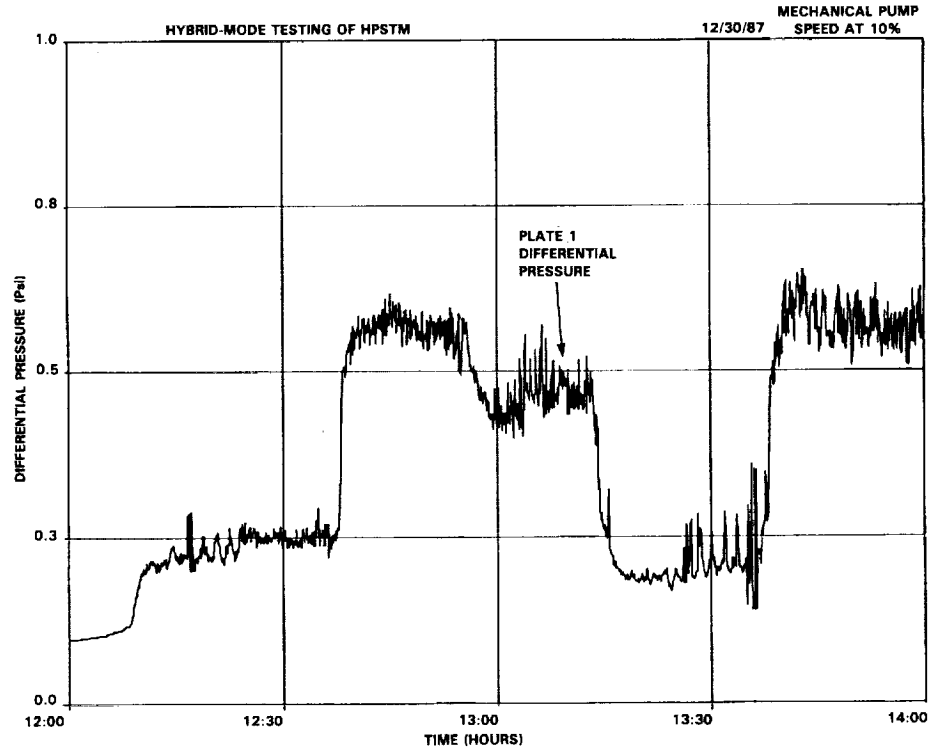


Figure 5-38. Heat Load Sharing Test

# 6 SINFAC SIMULATION OF THE HPSTM

## 6.1 Introduction And Description

In conjunction with the data analysis, a model of the HPSTM system was developed using the Systems Improved Numerical Fluids Analysis Code (SINFAC, Reference 8). The model was to serve four main purposes: 1) to determine the accuracy and flexibility of the SINFAC program and where modifications to the program can be made to improve these qualities, 2) to show relationships between various flow and thermal characteristics of the system that were not measured during the testing, 3) to help in determining future tasks for the system, and 4) to use for predicting the response of the system to conditions that can not be tested in the laboratory.

As described in detail earlier, the HPSTM hybrid system consists of a mechanical pump in series with three mounting plates each with four capillary pumps (or capillary-pump evaporators, CPE's). Instead of using twelve capillary pumps in parallel, the model uses only three, so the four capillary pumps on each plate are represented by only one pump in the model. This reduces the complexity of the program while still maintaining the same thermal and flow relationships between the evaporators. The main differences this created when comparing the model results to the actual system data were that the flow rate and total heat for the model were one-fourth that of the data. With regard to the heat, this was no problem since the results could be correlated on a heat-per-pump basis (all capillary pumps on a plate were kept at the same heat load). As mentioned, reducing the flow rate of the model did not affect the relative flow characteristics of the evaporators. But, it did mean that the dimensions used for the piping had to be smaller than those found in the actual experiment in order to obtain the same system pressure drop. In the model, most of the system pressure drop occurred in the vapor line (RPIPE 108); whereas, in the experiment, the liquid return line was responsible for the majority of the system pressure drop. Since the relationship between flow rate and pressure drop was essentially the same in both cases, the results were still consistent.

In addition to the three capillary pumps and their isolators, the SINFAC model consists of a mechanical pump, a RPIPE representing the liquid return line, a RPIPE for the vapor line, a condenser, and a mechanically-actuated accumulator. This type of accumulator is single- phase and uses a mechanical piston to control the system pressure. The HPSTM system uses a two-phase accumulator which is controlled by a heater. The mechanically-actuated accumulator allows for faster convergence of the program without affecting the comparison between the model and real HPSTM systems. The flow diagram for the model is shown in Figure 6-1. The individual parameters for each component will not be discussed here, but the input file listing all this information is included in Appendix A.

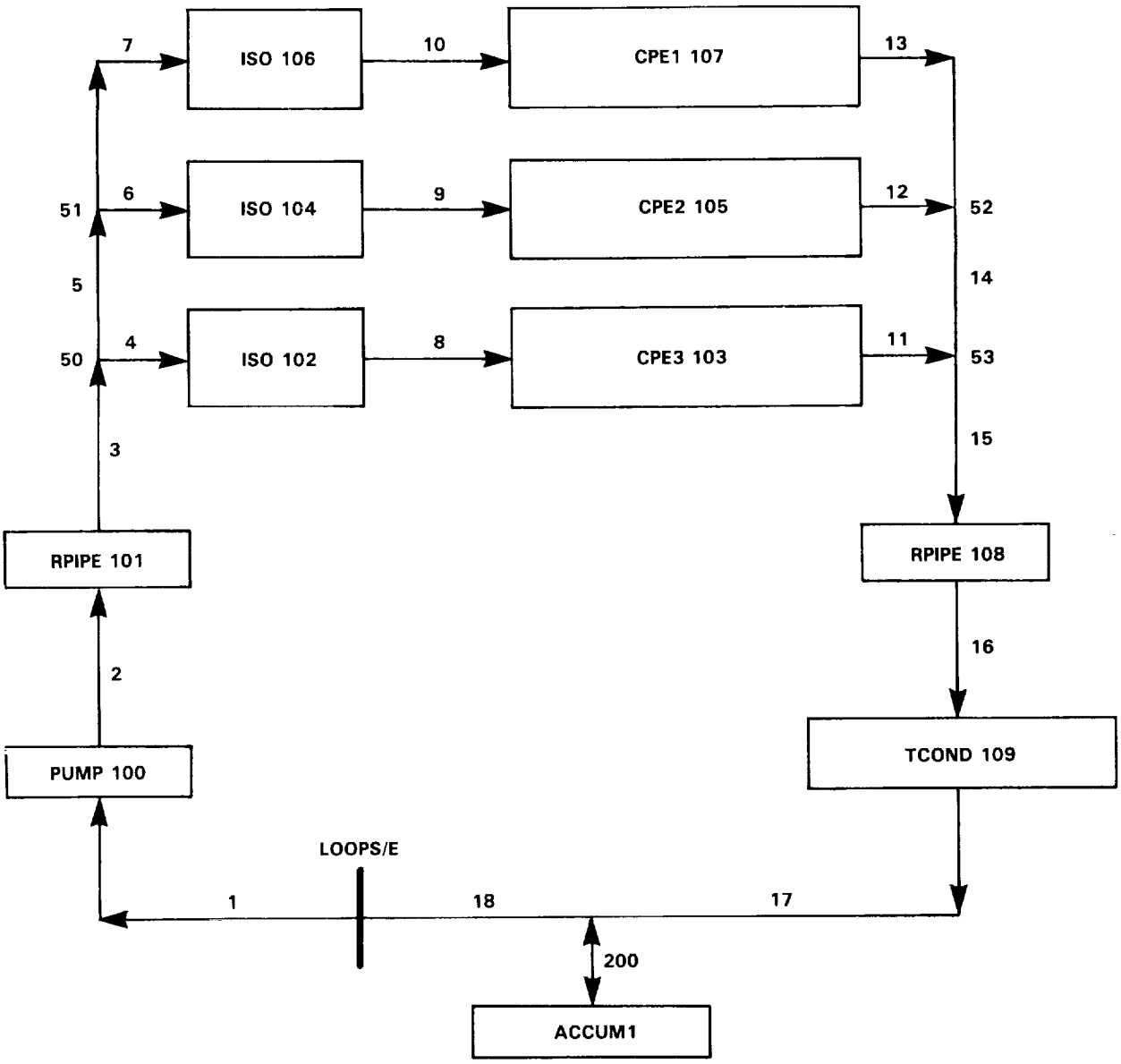


Figure 6-1. Flow Diagram for HPSTM SINFAC Model

In order to simulate the HPSTM system, it was necessary to determine which data readout would provide the best aspect of comparison between the model and the experiment. Unlike many of the previous tests with CPL's and hybrids, the HPSTM system used a pressure transducer to measure the pressure drop/rise from the isolator header to the outlet header of the capillary pumps on the first plate. When the total heat load had been increased to a sufficient magnitude, the pressure difference across the evaporator began to increase, changing from a pressure drop or zero pressure difference to a pressure rise. This indicated the incipience of capillary pumping in the system. This proved to be the best data for comparison since the incipience and magnitude of the pressure rise is a function of many factors, including the system pressure drop, heat input and removal, mechanical pump characteristics and speed. As a result, the capillary pressure rise versus heat input was used to characterize the system. How this relationship was affected by certain system parameters was a primary step in developing the SINFAC model.

One special note to make about the pressure rise in the capillary pumps is that the pressure drop across the isolators was so small in the model results it could be ignored. If this was true of the experimental system, then the pressure change measured by the transducer was essentially that of the capillary pumps alone; however, there was no way to determine the isolator pressure drop in the HPSTM system.

## 6.2 SINFAC Modification

It was hoped that, by comparing the results from the SINFAC model with those from an actual experiment, some of the algorithms used in SINFAC could be modified to provide a better representation of actual processes. One aspect which had not been sufficiently investigated was the relationship between the capillary pressure rise in a capillary pump and the quality of the stream exiting the pump. Prior to this study, the SINFAC algorithm for the capillary pump component was written such that most of the capillary pressure rise would occur over the exit quality range of 0.99 to 1.0. With a large pressure change occurring over such a small range, the state variable step sizes and perturbation factor (used for computing the derivatives of the error variables with respect to the state variables) had to be constantly adjusted whenever the exit quality was near one. This greatly increased the amount of computation needed to reach a converged solution. In cooperation with Fred Costello (the SINFAC developer), the algorithm was changed so that the majority of the capillary rise occurred from 0.95 to 1.0. This made convergence much easier and eliminated the need to change the SINFAC parameters. The difference in the results of the two ranges was very small, with the larger range (0.95-1.01) having a slightly higher pressure rise at a given heat rate. Since this did not appreciably change the pressure rise versus quality curve, the correlation between the model and HPSTM results was unaffected.

## 6.3 Condenser Variation

The first of the system parameters to be investigated pertained to the condenser. There were two main condenser conditions that were varied in the model: the condenser heat transfer area and the cooling fluid temperature. The results of this study are shown in Figure 6-2.

By increasing the temperature of the cooling fluid from -18 to -7°C and maintaining the same area of 0.66 $m^2$, the pressure rise in the evaporator was increased. This was to be expected since the enthalpy of the liquid entering the evaporator was now greater, and less heat was needed to remove the subcooling. The net result was a higher flow rate in the system. When the temperature was kept constant and the area was decreased from 0.66 to 0.58 $m^2$, the capillary pressure was increased at the higher heat inputs (600 and 650 W). This was due to the condenser's inability to remove the increased heat load on the system, thus raising the enthalpy of the returning liquid. In both cases, increasing the enthalpy of the inlet stream increased the mass flow rate in the system. A higher mass flow rate resulted in a higher system pressure drop, and yet the pressure head of the mechanical pump actually decreased due to the pumping characteristics. Thus, the capillary pressure of the evaporators had to increase to balance the new system pressure. In addition, though not shown in the simulation data, the heat load, at which capillary pumping is initiated, should also be dependent on the inlet enthalpy.

The importance of the condenser study was to determine how the pressure rise was affected by changes in the condenser and then to relate these results to the HPSTM data. After studying the results of the condenser study and the experimental data, it was decided to use a condenser area of 0.93 $m^2$ and a fluid temperature of 4°C. This gave isolator temperatures in the same range as the experiment and pressure-rise curves very similar to those from the experiment.

## 6.4 Flow Rate Variation

The other system parameter that proved to be of major significance was the flow rate delivered by the mechanical pump. Once the condenser conditions had been selected, a series of simulations were run using various pump flow rates. The flow rate of the model pump was changed by increasing or decreasing the speed of the mechanical pump and is that of the system prior to the incipience of capillary action. Figure 6-3 shows the capillary pressure rises for mechanical pump flow rates of 0.0011 kg/s (1250 RPM), 0.00125 kg/s (1500 RPM), 0.00145 kg/s (1750 RPM), and 0.00169 kg/s (2000 RPM). As indicated by the graph, the greater the mechanical pump flow rate is, the greater the heat load per evaporator needed to initiate capillary pumping and the smaller the pressure rise for a given heat load. Since the capillary pumping function will not be initiated unless the

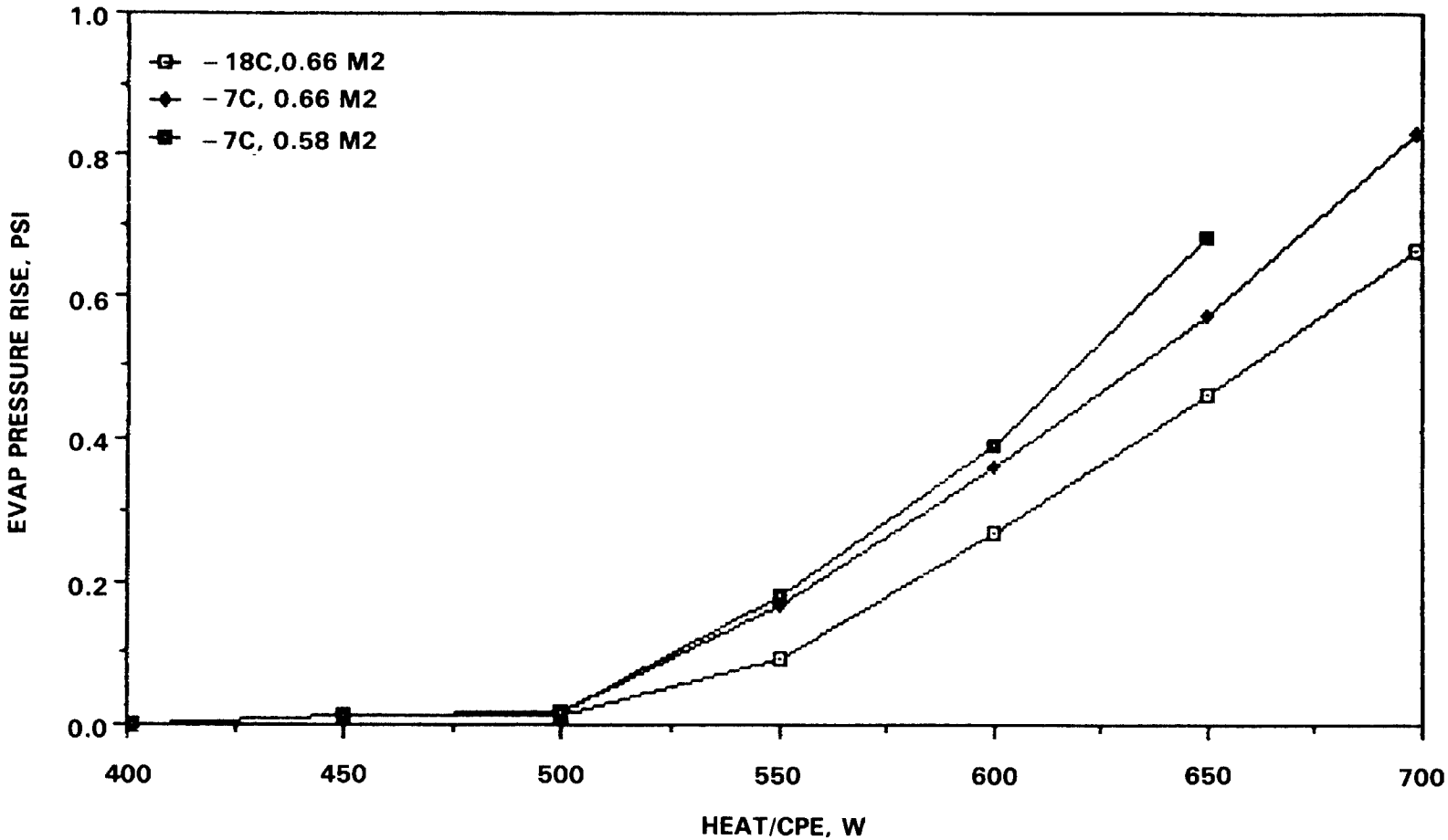


Figure 6-2. Condenser Variation (Simulation)

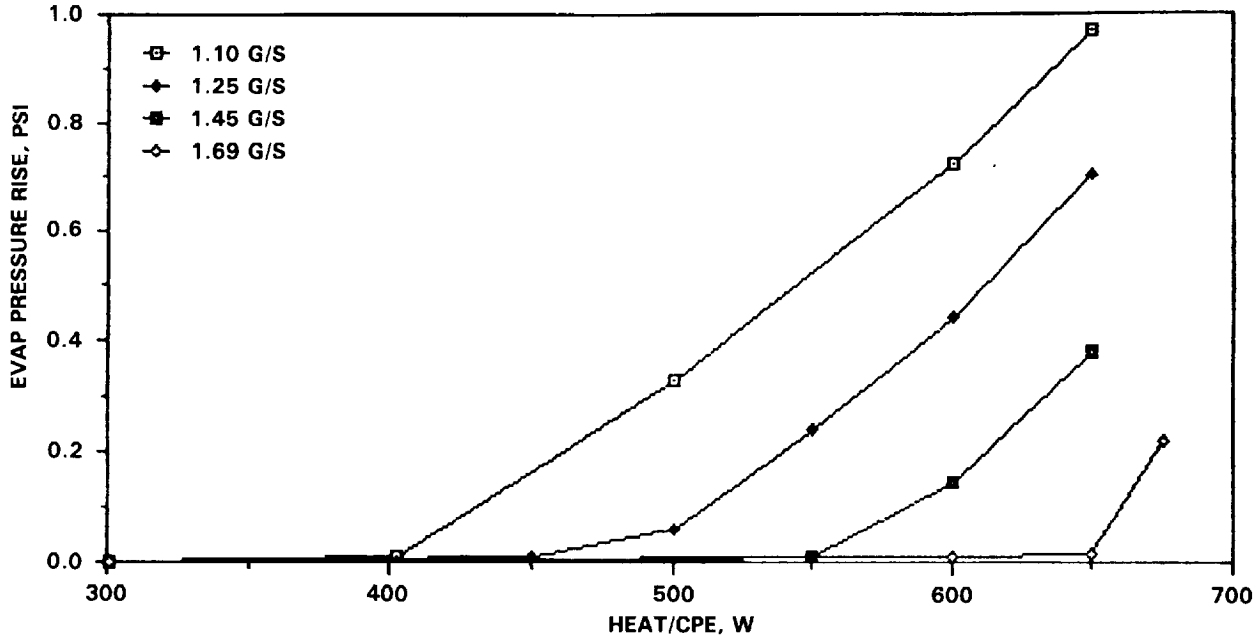


Figure 6-3. Flow Variation (Simulation)

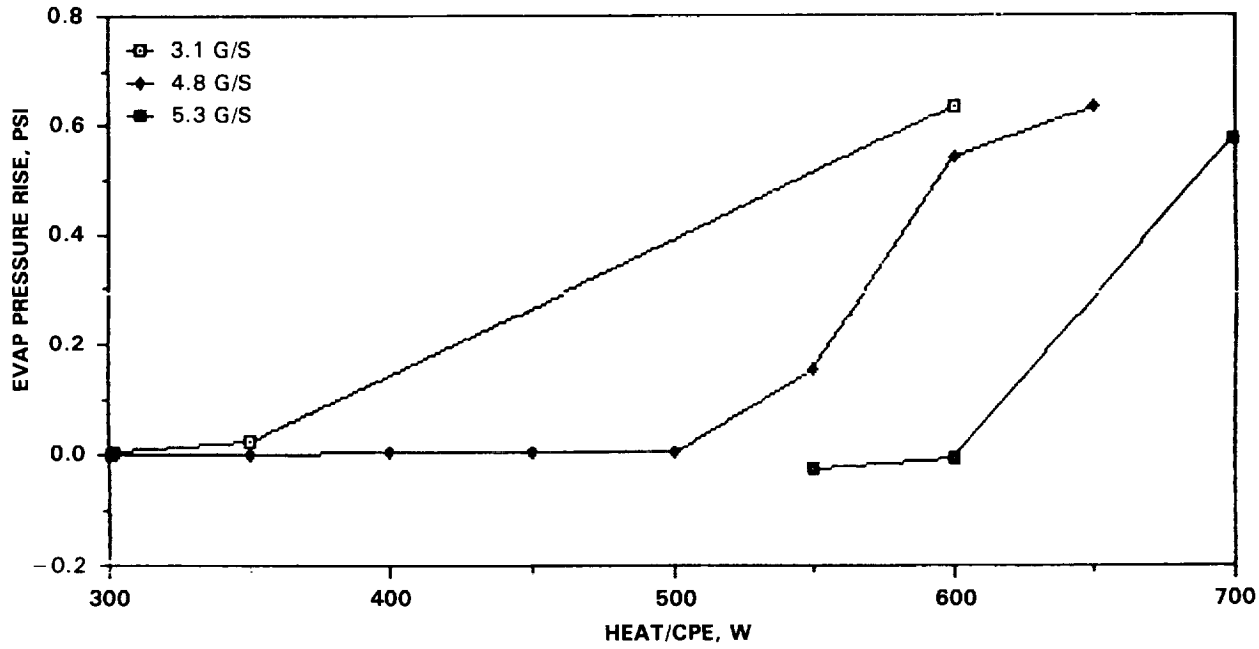


Figure 6-4. Flow Variation (Experimental)

quality reaches 100%, a higher flow rate demands a higher heat input in order to totally vaporize the incoming ammonia. As the heat load is further increased, a greater mass flow rate is needed to remove the heat, and, as described earlier, this results in a decrease in the mechanical pump head and an increase in the capillary pressure head. For the HPSTM system, there is a constant mass flow rate prior to the incipience of capillary pumping due to the high flow impedance in the liquid return line. The other system pressure drops became insignificant when compared to this pressure drop.

In Figure 6-4, the capillary pressure rises from the HPSTM experimental data are shown for three different flow rates: 0.0031 kg/s (12/16/87), 0.0048 kg/s (12/17/87), and 0.0053 kg/s (1/22/88). It is interesting to note that all three of these runs were made with a nominal pump speed setting of 10% of scale. Even though the data are somewhat inconclusive, it is clear that the experimental results follow the same trend demonstrated in the model results: the larger the pump flow rate; the smaller the capillary pressure rise for a given heat load.

## 6.5 Comparison With Uniform Test Data

The next stage of the simulation was to compare the results from an experimental run with those of the model. This comparison is shown in Figures 6-5, 6-6, and 6-7. The experimental data are from a uniform run made on 12/17/87. The term "uniform" refers to having equal heat loads on each plate; the term "nonuniform" refers to having differing heat loads on each plate but with all the pumps on a plate having the same load. This day's data proved to be the most complete data to demonstrate the incipience of capillary pumping since the run was made twice. Where there were more than one value for a given heat load, averages were used. The mechanical-pump flow rate for the experimental run was about 0.0048 kg/s (10% of scale) and for the simulation was 0.0013 kg/s (1550 RPM). The respective flow rates are shown in Figure 6-5 with the flow rate for the experiment divided by a factor of four to compensate for the difference in the number of capillary pumps (see Introduction). At 550 W/CPE, both flow rate curves show an increase, marking the incipience of capillary pumping (albeit small for the experimental data). As expected, the two curves show the same trend of increasing flow rate with increasing heat load with good correlation between the two sets of data. To convert from the experimental flow rate to that of the simulation, a factor of 3.7 instead of 4, gave a better correspondence. The discrepancy is probably due to the difference in the characteristics of the real and model pumps.

The incipience is more clearly demonstrated in the plot of the pressure rise across the capillary pump (Figure 6-6). Starting at 550 W/CPE, the pressure rise increases sharply for both model and experimental data. The two sets of data correspond very well with the exception of that at 600 W/CPE.

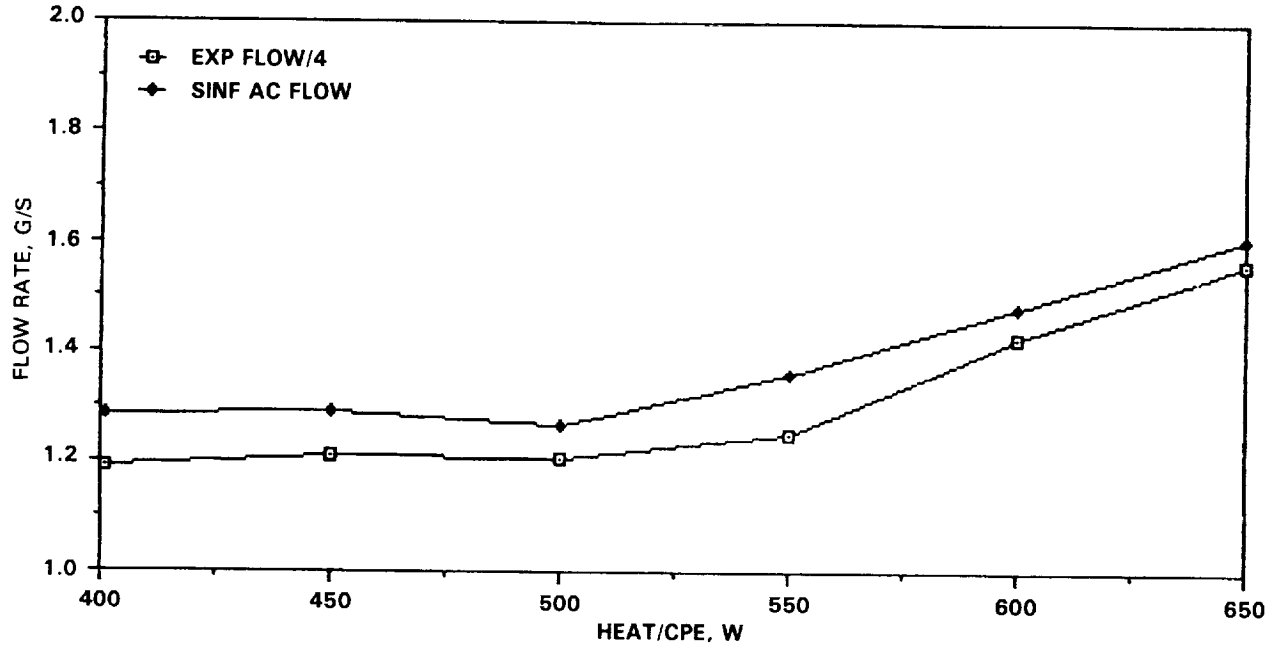


Figure 6-5. Experimental and Simulation Results

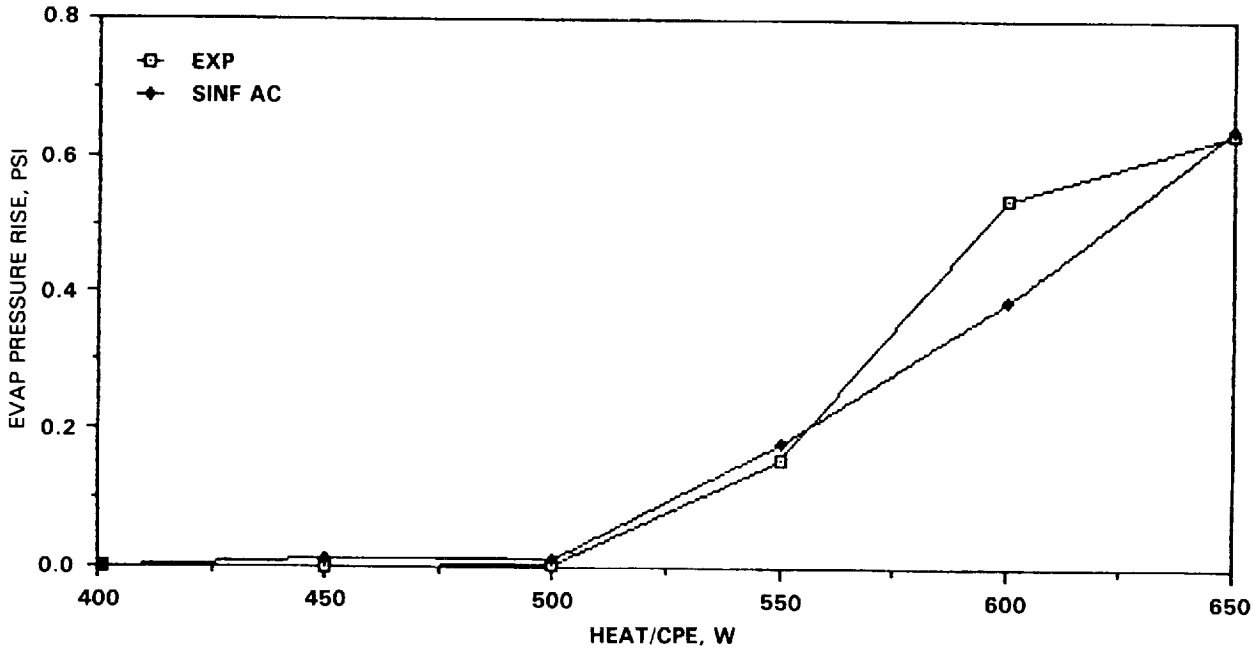


Figure 6-6. Experimental and Simulation Results

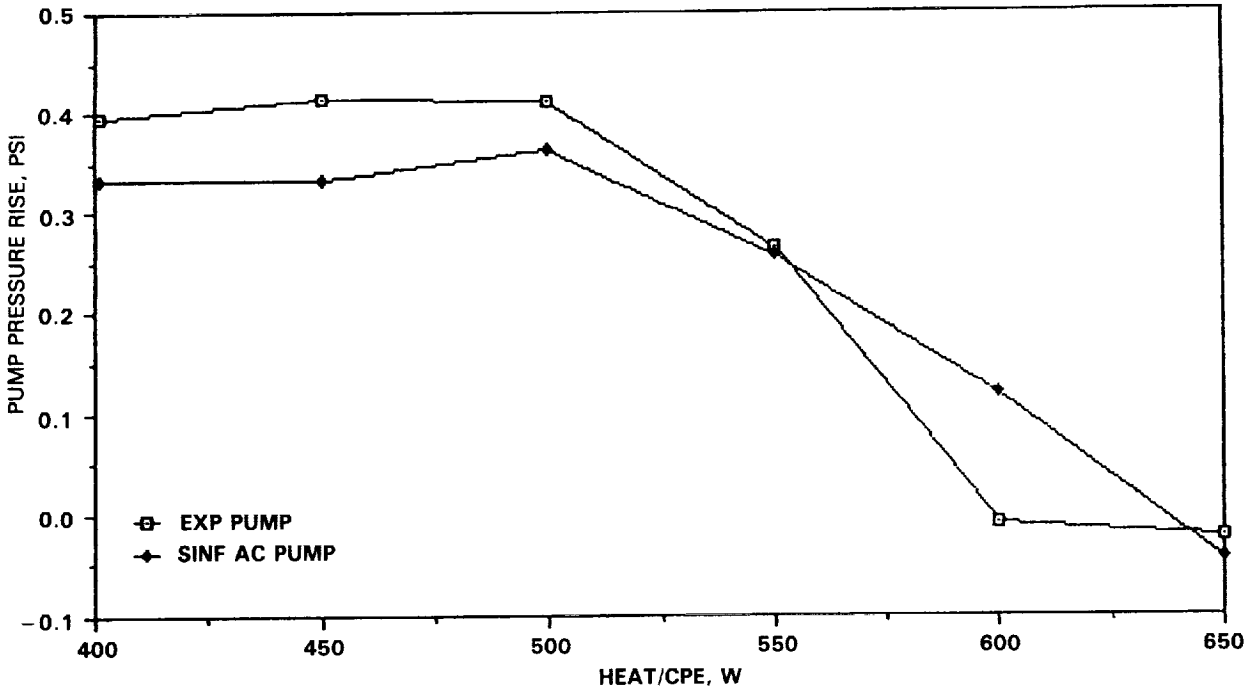


Figure 6-7. Experimental and Simulation Results

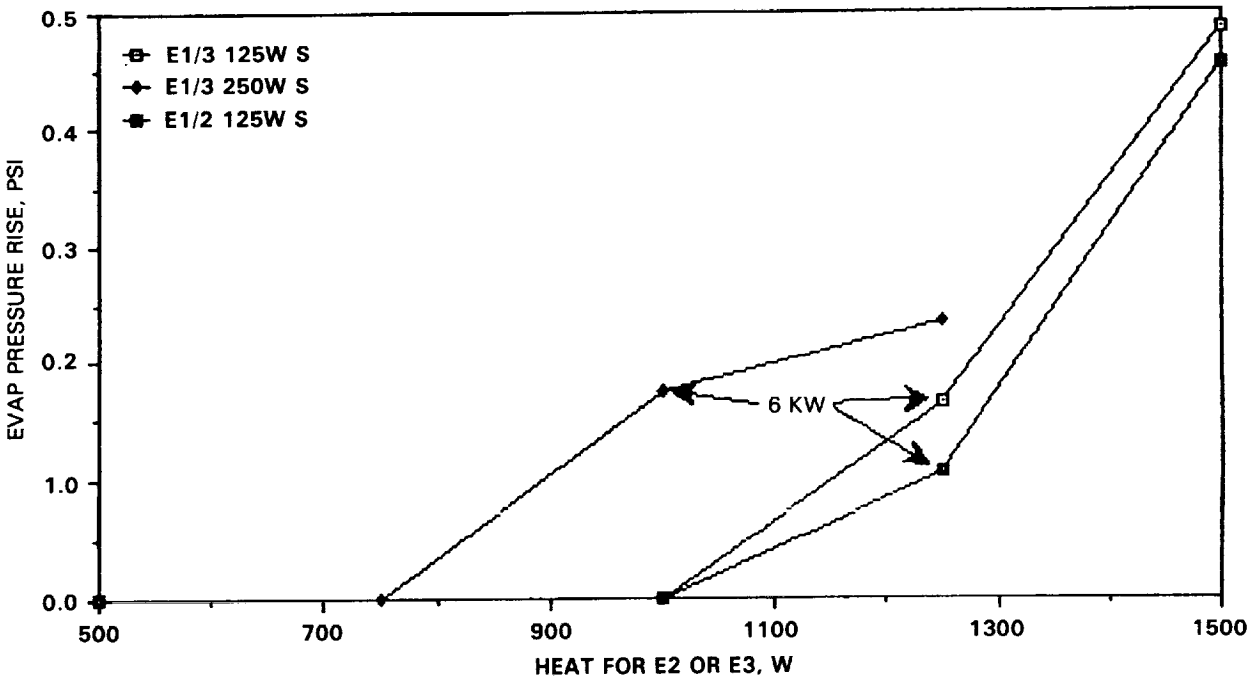


Figure 6-8. Nonuniform Data (Experimental)

This may be significant since the experimental pressure curve is S-shaped with the one for the model being almost linear. The easiest way of rectifying the discrepancy would be to assume the experimental data at this point is incorrect, but the pressure rise at this heat load was almost the same for both runs, indicating repeatability. If the pressure rise at 700 W/CPE had been obtained experimentally, then the S-shape of the curve would have been proven or disproven; but the system experienced deprime at this heat load. The other runs using uniform or nonuniform heating do not help to corroborate this observation since they usually provide only one or two pressure-rise points in the capillary-pumping range. One explanation for the discrepancy could be the nature of the two systems. Since the quality of the capillary-pump exit streams could not be measured experimentally, the exit qualities of the two systems may be sufficiently different so as to make a difference in the system characteristics, notably the system pressure profile. The final answer to this question will have to be determined by further experimentation. This is on the agenda for future testing.

Figure 6-7 shows the pressure change across the mechanical pump. With the incipience of capillary pumping for heat loads above 500 W/CPE, the pressure rise across the pump begins to decrease, eventually becoming a pressure drop above 600 W/CPE. This is a result of the increasing flow rate through the pump. For a low mechanical pump speed (such as in this case), the capillary pressure head may actually exceed that of the mechanical pump, causing the pressure difference across the pump to be negative. The mechanical pump would then become an impedance to the flow and increase the system pressure drop.

Another interesting similarity between the model and the experiment was that deprime was encountered at 700 W/CPE for both systems. This seems to indicate that the model may be used in the prediction of high-power capillary-pump deprime.

## 6.6 Nonuniform Test Data, Experimental

One of the main reasons for developing the SINFAC model was to obtain a better understanding of the flow and pressure relationships that occur during nonuniform heating. Neither the flow rate nor pressure drop of an individual pump was measured, so this information had to be extrapolated from the pressure transducer data of the first plate and temperature data. Obviously, this data was not sufficient to provide more than a knowledgeable estimate of the flow conditions in the pumps. To determine whether these estimates were correct, the SINFAC model was developed, and the results compared to data from nonuniform runs.

The data chosen for the comparison was from the runs made on 12/30/87. There were a total of three runs: 1) the heat loads to the first and third plates were kept at 125 W/CPE and that to the second was increased incrementally from 500 to 1500 W/CPE, 2)

the heat loads to the first and third plates were kept at 250 W/CPE and that to the second was increased incrementally from 500 to 1250 W/CPE, and 3) the heat loads to the first and second plates were kept at 125 W/CPE and that to the third increased incrementally from 500 to 1500 W/CPE. This data was chosen because the flow rate was low enough (0.0043 kg/s) to provide more than one data point in the capillary-pumping range (though for the second run the second data point in this region was found to be incorrect, see below). In addition, the heating sequence demonstrated the effect of increased heating on one plate, as compared to another, and the importance of the total heat load, as compared to individual plate loads, in determining the capillary pressure rise.

The capillary pressure rise data for these three runs are shown in Figure 6-8 ("E1/3 125W" refers to having 125 W/CPE on the pumps of plates 1 and 3, as described for run one). There are a number of significant aspects to note about these data. First, the data point for run two (E1/3 250W) at 1250 W/CPE is probably incorrect since a pump on plate 3 deprimed at this load. The depriming appeared to be a result of factors other than just the heat load because the majority of the heat was being applied to plate 2, not 3. The flow rate through the plate 3 pump may have been low enough to have caused some type of low power deprime, but this does not seem likely since that type of deprime would have more likely with the 125 W/CPE load than the 250 W/CPE load. There is no way of determining the exact cause.

Secondly, the capillary pressure rise is greater for run one, when the increasing heat was applied to plate 2, than for run three, when plate 3 received the majority of the heat. Assuming the data is accurate, this is probably due to the change in the flow characteristics of the system. In run one, most of the flow was through the pumps on plate 2, since it was receiving the greatest heat load. In run three, most of the flow was through the pumps on plate 3. Since most of the flow in run one circulated a larger distance than in run three, the pressure drops associated with a loop which has most of its flow through plate 2 would be higher than a loop with most of its flow through plate 3. The capillary pressure rise across the capillary pumps would reflect this difference, since the rise is only as great as the pressure drop in the system. As shown in Figure 6-8, the pressure rise for run three was less than that for run one, implying that the system pressure drop for the former was smaller.

Lastly, the capillary pressure rise at 1250 W/CPE for run one and at 1000 W/CPE for run two are almost equal (about 0.17 psi). The total system heat load at each of these points was 6 kW. The rise at 1250 W/CPE for run three, which also has a total system heat load of 6 kW, was lower (0.11 psi), but this was probably due to the difference in the flow characteristics associated with plate 3, as explained in the previous paragraph. Unfortunately, there was no accurate data for run two at 7 kW, but, taking into account the difference in system pressure drop, the pressure rises for runs one and three agree at 1500 W/CPE,

which corresponds to a system heat load of 7 kW. Thus, when dealing with an nonuniform system, the capillary pressure rise seems to be mostly dependent on the total system heat load, as opposed to the distribution of heat loads on the individual plates, except with respect to how that distribution may affect the system pressure drop. In the HPSTM system, since most of the pressure drop occurred in the liquid return line, the pressure drop in the rest of the system, including the evaporators, was only a secondary factor.

## 6.7 Nonuniform Test Data, Simulation

The same conditions used in the experiment were input to the SINFAC model, and the results of the simulation are shown in Figure 6-9. The simulation and actual data from run one are almost identical. For example, at 1250 W/CPE the capillary pressure rises were 0.165 and 0.166 psi for the experiment and simulation, respectively. For run two, the first points in the capillary-pumping region at 1000 W/CPE for both sets are almost the same (0.175 psi experimental; 0.166 psi simulation), but the second points differed due to the deprime mentioned earlier. The main divergence occurs when run three results are compared. The simulation data shows almost no difference when the higher heat load was placed on pump 3 as compared to pump 2. The main reason for this is that the two pumps in the model are identical and, even though the majority of the flow may be diverted to a another pump, the pressure drop of the system remains essentially the same. Since no two capillary pumps can be made identical in reality, this is not true for the experiment; changing the heat load distribution will affect the system pressure drop. One last point of comparison is the incipience of capillary pumping, which is the same in both the simulation and the experiment.

As mentioned earlier, one of the reasons for the developing the simulation was to try obtain a better understanding of the flow characteristics during nonuniform heating. One question raised during the nonuniform testing was how can one plate (four pumps) begin capillary pumping without creating an uphill pressure gradient for the flow on the outlet side, especially when either plate 2 or 3 is receiving the majority of the heat? At each node in the loop, the simulation lists all the fluid and thermodynamic properties including quality, flow rate, and pressure. It was found that the exit quality of the pump receiving the higher heat loads, in this case pump 2, would climb to around 94% or just short of that needed for capillary pumping (95%), while the exit qualities of the other two pumps were still relatively low. Then, as the heat load was further increased to pump 2, its flow rate would increase at the expense of those in pumps 1 and 3. As their flow rates would decrease, the exit qualities of pumps 1 and 3 would increase. Then, when the total heat load was sufficient, the exit qualities of all three pumps would exceed 95%, and all three would begin capillary pumping simultaneously. Thus, since all the exit pressures would increase together, there was no uphill pressure gradient. This

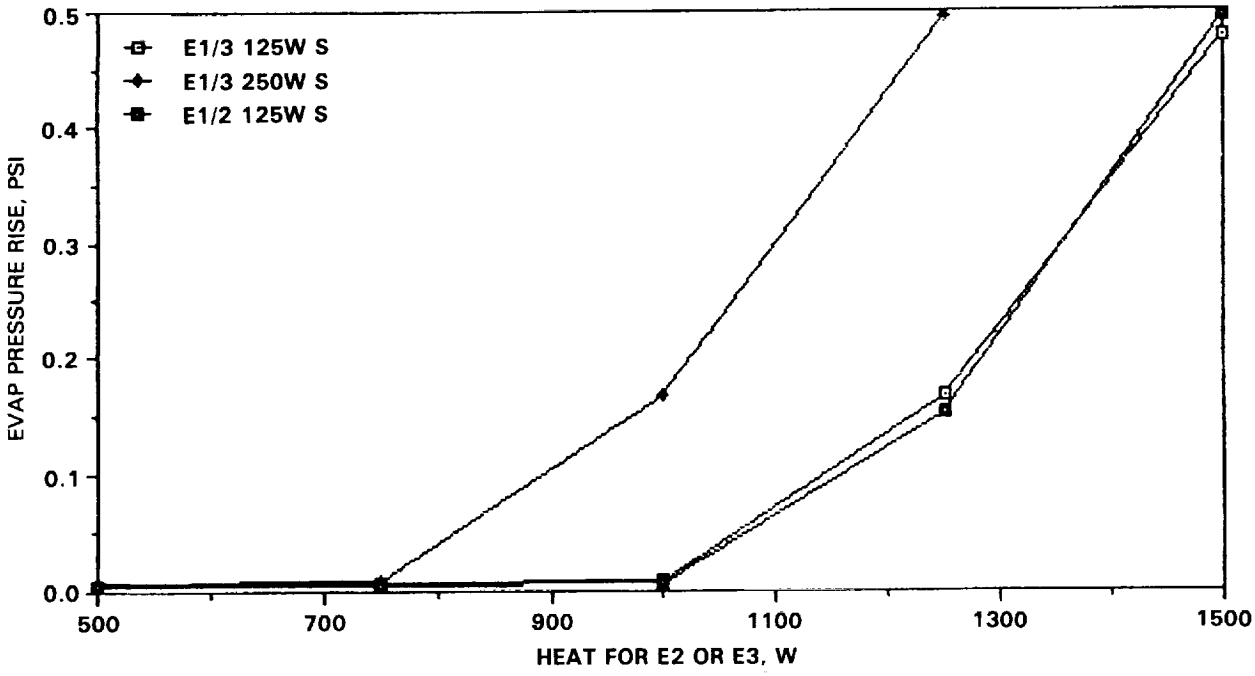


Figure 6-9. Nonuniform Data (Simulation)

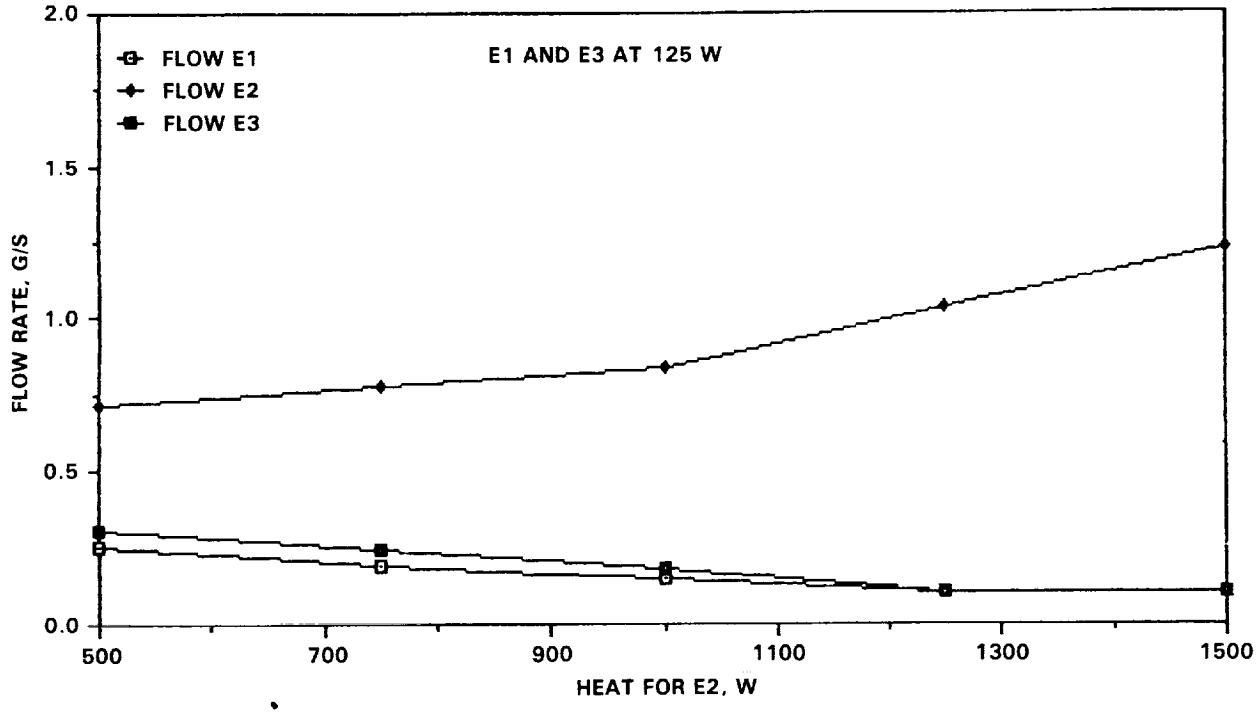


Figure 6-10. Nonuniform Data (Simulation)

may not always be the case though. As mentioned earlier in this report, the capillary pumps on the upstream, outlet side of a pump that begins capillary pumping must begin capillary pumping as well in order to maintain the correct pressure profile. In this case, pump 1 would transition to capillary pumping at the same time as pump 2. But, if there had been sufficient pressure drop between the outlets of pumps 2 and 3, capillary pump 3 could have remained in the forced flow region while pumps 1 and 2 were in the capillary-pumping region. Some preliminary tests were made with the model that tended to support this supposition, but more test runs were needed to adequately substantiate this.

Figure 6-10 shows the simulation flow rates of all three pumps for run one. Note that the flow rate in pump 2 begins to increase more rapidly when the capillary pumping starts (between 1000 and 1250 W/CPE), while the flow rates in pumps 1 and 3 continue to decrease. The increase in overall flow rate, seen in the capillary-pumping region, is due to the total heat load on the system but is manifested in that of pump 2.

## 6.8 SINFAC Simulation Conclusions

Even though the experimental data was somewhat sparse in some areas, the SINFAC model was able to closely reproduce what data was available, in a few cases obtaining an almost one-to-one correspondence. This does seem to indicate that the model is reliable and can be used to predict the response of the HPSTM system. But, more data should be obtained before the model can be considered more reliable. Experimental runs are planned to obtain more data that will go toward refining the model. In reciprocation, the experimental data was used to help improve the performance of the SINFAC model as well as test the flexibility of the SINFAC program by applying it to a type of system not previously simulated.

The model results also gave insight into some of the flow and thermodynamic relationships that could not be obtained during the experiment. This information is very useful in providing a better understanding of the mechanisms involved in a hybrid system such as the HPSTM.

Once the SINFAC model's reliability has been proven more conclusively by additional data, it is hoped that the model can be used to select future testing programs for the HPSTM and to predict the response of the HPSTM system to conditions that may

# 7 HPSTM TESTING SUMMARY AND CONCLUSIONS

The design and testing of a hybrid capillary pumped loop have been described. Test results have demonstrated the feasibility and practicality of a hybrid CPL system, consisting of a mechanical pump in series with 12 capillary evaporator pumps, as a two-phase device for temperature control and heat transport.

## 7.1 Capillary-Mode

Significant test results of the HPSTM system operating in the capillary- mode are summarized as follows:

A. Start-Up: System start-up tests were performed with nine different power input schemes to the evaporator plates. Power inputs ranged from 200 W/plate to 2000 W/plate, and included both uniform and nonuniform powers. The new elements in this system, which include the location of the reservoir feed line, multiple parallel plates with separate isolators, and 0.61 meter capillary pumps, had no adverse effect on the start-up performance. No evaporator deprimed in all of the start-up tests. In addition, a reliable start-up scenario was defined and repeated 10 times without failure.

B. Transport Limit: The system demonstrated a transport limit of between 21.5 and 24 kW for operating temperatures of 25, 35, and 45°C. The failure mode at the system transport limit was an inlet deprime of the evaporators on plate 1. While evaporator E11 was always the first pump to deprime, apparently, conduction from the inlet tube of E11 to the isolators of the other evaporators on plate 1 resulted in the deprime of all pumps on plate 1. The isolators did prevent vapor from flowing back into the liquid return line. The duration of the transport limit testing was restricted by the condenser heat-dissipating capability, which was limited to 9 kW of steady-state cooling. A long-duration operation of 10 kW of heat input for 5 hours was demonstrated without any pumps depriming.

C. Low Power Limit: A low power limit of 300 W total system power (25 W per pump) was demonstrated without any pumps depriming. At this level, however, the reservoir could not maintain thermal control of the saturation point in the loop because of a lack of liquid in the accumulator. This was attributed to vapor condensation in the vapor line. When the total system power level reached 700 W, individual pumps could operate with as little as 25 W per evaporator, with the reservoir controlling the saturation temperature in the loop. Testing demonstrated that the system could operate at a lower power level with the reservoir in control when the condenser was operating at a warmer temperature. The system has demonstrated normal operations with 600 W on the evaporator section (50 W per pump)

for seven hours with the condenser running at 10°C.

D. Pressure Priming: Pressure priming was successfully demonstrated on three occasions as a means of recovering a deprimed evaporator pump. The new elements in the HPSTM system had no affect on the effectiveness of this method of evaporator repriming.

## 7.2 Hybrid-Mode

The hybrid-mode testing has made significant contributions to better understanding the performance characteristics of a hybrid CPL system. The important test results are summarized below:

A. Liquid Inventory Requirement: Test results showed that a completely flooded system was not necessary for proper hybrid-mode operations. For the reservoir to operate as the thermal control device in the system, the ammonia inventory in the loop must not be made so great that the reservoir becomes fully flooded during normal operations. This means that when operating in the hybrid-mode, the pump speed must be adjusted to control the exit quality of fluid leaving the capillary pumps. To prevent cavitation of the mechanical pump, the pump speed could not be increased until the system power input was set at a minimum value. This value varied with each pump speed, but for higher pump speeds, a greater power input was required.

B. Start-Up: Start-up of the HPSTM system during hybrid-mode testing followed the same procedures used for the baseline capillary-mode start-up. Whenever ammonia vapor was seen to reach the condenser section, the mechanical pump was started at a speed of 10% full scale. For tests at pump speeds greater than 20%, power input to the evaporators was increased to 6 kW before the mechanical pump speed was increased. This start-up procedure was used in all the hybrid-mode tests and no cavitation of the mechanical pump was seen.

C. Capillary Heat Transport Augmentation: When the mechanical pump could no longer deliver enough mass flow rate to meet the demand of the evaporators which were subjected to increasing power inputs, capillary pumping action in the evaporator wicks was initiated. The net effect was that the mass flow rate in the loop would meet the heat transport requirement in the evaporator section, and the pressure heads developed by the capillary wicks and the mechanical pump would balance the total pressure drop in the loop. Capillary pumping in the evaporator was initiated when the vapor exit quality reached 100%, and was indicated by a pressure rise across the evaporators and an increase in the total mass flow rate in the loop. The system transport limit at a given mechanical pump speed was reached when the required pressure rise across the evaporators

exceeded the capillary pumping capability of the wicks. Once the evaporator deprimed, the system could not be reprimed until the total power input was reduced below that of the capillary pumping initialization point. Transport limits for mechanical pump speeds of 10, 15, and 20% full scale were 8, 19, and 36 kW, respectively. The large impedance of the thermal flowmeter in the liquid line bypass resulted in smaller heat transport capacities at the lower pump speeds than what would be attained in the capillary-mode of operation.

D. Capillary Flow Distribution Control: The ability of the capillary wicks to regulate fluid flow between evaporators with nonuniform power inputs was demonstrated. This flow control function eliminates the need for regulating valves, thus reducing the complexity and increasing the reliability of the system. Successful flow control by the capillary evaporators under nonuniform evaporator heat loads has been demonstrated for a power ratio up to 20:1.

E. Steady-State and Transient Operation: A steady-state capillary-mode of operation with a power input of 10 kW and a transient hybrid-mode operation with a 52 kW power input were demonstrated. The transition between operating modes was made by turning a bypass valve to the mechanical pump section.

F. Heat Load Sharing: Unlike the capillary-mode of operation, heat load sharing between evaporators in the hybrid-mode of operation is only possible under certain conditions. If the evaporator with power applied has initiated capillary pumping and the pressure distribution in the evaporator section allows for flow-reversal through the evaporator without a heat input, then heat sharing will occur. The heat load sharing function was demonstrated in the hybrid-mode testing under various mechanical pump speeds and evaporator heat loads.

## 8 RECOMMENDATIONS FOR FUTURE WORK

Some physical changes could be made to the system which should improve the overall operation of the hybrid CPL system. First, the reservoir size should be optimized so that the entire vapor line plus condenser volumes could be displaced into the reservoir bottle. The reservoir should also be re-oriented so that the effects of vapor compression on the system saturation temperature could be minimized. Since the reservoir during this latest test program was always fixed in a vertically upright position, the reservoir could be mounted horizontally. This would increase the surface area between the vapor and liquid interface, and thus decrease the work that could be done when liquid is forced into the reservoir.

Another change to the system which should improve performance would be the removal of the thermal flowmeter in the liquid line bypass. Though a flowmeter is crucial in measuring the system flow rate, an improved flowmeter which has a much lower impedance to the fluid flow should be installed in the loop. The large impedance of the current flowmeter made the system characteristics during hybrid-mode operations considerably different from those during capillary-mode testing.

A third change in the system which would be desirable in improving the performance would be to build and install an isolator header which would eliminate thermal cross-talk between individual isolators. It was seen in all of the high power tests in which deprimes occurred that when E11 deprimed, enough heat was conducted from the plate to the E11 isolator, and then from the E11 isolator to the isolators of pumps 2,3, and 4, in that order, to cause inlet deprimes in the other pumps. Though no vapor flowed back to the liquid return line, a buffer to prevent conduction to individual isolators is required so that an entire plate will not deprime if an individual pump deprimes at the high heat loads.

The evaporator plates should be modified to allow for a direct measurement of temperatures on the heating surface of the evaporators. Pressure- contact thermocouples should be installed on the evaporators so that the evaporative heat transfer coefficient for various power inputs could be measured.

The capacity of the cooling system was only 9 kW. To obtain steady-state temperature data at higher heat loads requires an improved cooling system. Ideally, one with a cooling capacity of 25 kW would suffice for the verification of long-term HPSTM operations at higher heat loads.

In addition to these hardware modifications, more tests are required in order to characterize and better evaluate the performance of the hybrid CPL system. The following tests could answer some of the questions raised by this latest test program, would provide a greater data base for future hybrid capillary systems.

## 8.1 Capillary-Mode

A. Low Power Limit Test: Tests should be performed to determine the lowest power levels each plate can handle while keeping the operating temperature under the reservoir's control. This can be accomplished by applying a constant heat load to one plate of 500 W, and running the low power limit test on the other plates.

B. Isolator Temperature/ Differential Pressure Oscillations: Some slight temperature and pressure oscillations were seen at the 10 kW system power level which disappeared after

the mechanical pump was run for 15 minutes. Further tests should be conducted to help understand this phenomenon.

C. Steady-State High Power Operation: A high-capacity condenser is required to run the system at the 24 kW power range for a substantial period of time. A steady-state power test of 20 kW should be run to verify the transport limit data and to better investigate the effects of subcooling on the overall system performance at high powers in both capillary and hybrid-modes.

## 8.2 Hybrid-Mode

A. Mechanical Pump Characterization Test: The relationship between the pressure head developed and the flow rate delivered by the mechanical pump should be characterized . Because of the high flow impedance of the thermal flowmeter in the current system, such a test could not be performed.

B. Heat Load Sharing Test: The heat dissipating capacity of the cold plates in the present system is limited to that of free convection between the plates and the environment. At least one of the plates should be facilitated with a forced-convection type of heat sink so that the upper limit of the heat load sharing can be demonstrated. This data would be useful in the design of a bidirectional heat exchanger where capillary evaporators can be used as evaporators as well as condensers.

C. Steady-State and Transient Operation: With an improved condenser, the hybrid steady-state and transient operations test could be run with a much higher power level. It will be desirable to demonstrate 25 to 50 kW steady state operation, and 75 to 100 kW in the transient hybrid test.

D. Transition from Mechanical to Capillary Pumping: The incipience of capillary pumping during hybrid-mode operations needs to be more carefully determined at a variety of pump speeds, and the capillary pressure rise curve needs to be characterized better for both uniform and nonuniform conditions.

9. References.

E.J. Kroliczek, J. Ku, and S. Ollendorf, "Design, Development and Test of a Capillary Pump Loop Heat Pipe," Paper No. 84-1720, AIAA 14th Thermophysics Conference, Snowmass, Colorado, June 25-28, 1984.

J. Ku, E. Kroliczek, W.J. Taylor and R. McIntosh, "Functional and Performance Tests of Two Capillary Pumped Loop Engineering Models," Paper No. 86-1248, AIAA/ASME 4th Thermophysics and Heat Transfer Conference, June 2-4, 1986, Boston, Massachusetts.

J. Ku, E. Kroliczek,, and R. McIntosh, "Capillary Pumped Loop Technology Development," 6th International Heat Pipe Conference, May 25-29, 1987, Grenoble, France.

J. Ku, E. Kroliczek, D. Butler, R. Schweikhart, and R. McIntosh, "Capillary Pumped Loop GAS and Hitchhiker Flight Experiments," Paper No. 86-1249, AIAA/ASME 4th Thermophysics and Heat Transfer Conference, June 2-4, 1986, Boston Massachusets.

A.E. Bergles, "Instabilities in Two-Phase Systems," From "Two-Phase Flows and Heat Transfer," 1981, Hemisphere Publishing Corp., Washington.

F.A. Jeglic and T.M. Grace, "Onset of Flow Oscillations in Forced Flow Subcooled Boiling," NASA-TN-D 2821, 1965.

J.G. Wallis and J.H. Heasley, "Oscillations in Two-Phase Flow Systems," Journal of Heat Transfer, 83, pgs 363-369, 1961.

F.A. Costello, "SINFAC Users Manual, Version 2.2," developed for NASA/GSFC, Greenbelt, MD, 1988.

APPENDIX A: SINFAC Input File Listing

```
        BCD 3THERMAL SPCS
        BCD 8FILE TITLE:  HPSTM
        END
        BCD 3NODE DATA
            30,70.,1.              $DUMMY NODE
            -103,70.0,0.01          $EVAPORATOR PLATE TEMPERATURES
            -105,70.0,0.01
            -107,70.0,0.01
            -109,40.0,0.01           $CONDENSER
C FLUID NODES (ENTERED AS BOUNDARY NODES, AFTER ALL OTHER NODES)
            -200,70.0,1.0           $ACCUMULATOR NODE
        GEN -1,18,1,70.,1.          $FLUID NODES
        END
        BCD 3SOURCE DATA
        END
        BCD 3CONDUCTOR DATA
            1,30,1,0.
        END
        BCD 3CONSTANTS DATA
            TIMEO=0.0
C FAC CHANGED TIMEND FROM 0.3 TO 0.1 TO SAVE COMPUTER TIME
            TIMEND=0.3
            OUTPUT=0.1
        END
        BCD 3ARRAY DATA
        END
        BCD 3EXECUTION
C NOTES TO USER:
C 1.  ALL LINES HAVING # AS THE FIRST CHARACTER REQUIRE INPUT SPECIFIC
C     TO YOUR PROBLEM.  THE INPUT REQUIRED IS EXPLAINED IN THE COMMENT
C     LINE IMMEDIATELY PRECEDING THE LINE(S) WITH THE #.
C 2.  ALL LINES WITHOUT A # NEED NOT BE CHANGED.
C 3.  WHEN FINISHED ENTERING INPUT SPECIFIC TO YOUR PROBLEM, REPLACE
C     THE # WITH A NULL CHARACTER.
C INCLUDE SINDA'S MANDATORY DIMENSIONING OF THE X ARRAY.  Typically the
C required dimension is 10 times the number of nodes.
F     DIMENSION X(5000)
C DIMENSION THE ARRAYS OF INITIAL CONDITIONS.  The dimension must be
C equal to or greater than the number of fluid nodes, including the
C reservoir nodes.  The initial conditions may be conveniently specified
C in a DATA statement, as is done in this example.
F     DIMENSION FLOW1(25),P1(25),EN1(25),QUAL1(25)
C COMMON BLOCKS NEEDED FOR FLUIDS SIMULATIONS.  DIMENSION of the arrays
C P, FLOW, EN, QUAL, PWR, WM, and the second dimension of WF MUST BE AT
C LEAST EQUAL TO THE NUMBER OF FLUID NODES (NFN) IN THE SYSTEM
C (including the reservoir nodes).
F     COMMON/PRESS/P(25)
F     COMMON/FLOWS/FLOW(25)
F     COMMON/ENTH/EN(25)
F     COMMON/QUAL/QUAL(25)
F     COMMON/POWER/PWR(25)
F     COMMON/WEIGHT/WM(25)
F     COMMON/WFLUID/WF(5,25)
C MNX IS DIMENSIONED equal to or greater than the NUMBER OF FLUID NODES
C IN THIS PROBLEM.  No other changes are needed in the following line.
```

```
C MNX, the inverse of INNODE, is the array of external fluid station
C numbers:  I=INNODE(MNX(I))
F     COMMON/IO/IDER,ISOL,ISOLX,IDUMP,NOUT,ISTOP,IDAMP,MNX(29)
C COMMON BLOCKS FOR STATE AND ERROR VARIABLES.  The dimension of each
C array in the next two lines must be equal to or greater than the
C number of state variables (NSV) in the users simulation (see Section
C 3.1.2)
F     COMMON/ERR1/EV(7)/ERR2/EVS(7)/ERR3/IEV(7)/ERR4/PE(7)
F     COMMON /SV1/SV(7)/ SV2/SVS(7)/ SV3/ISV(7)
C COMMON BLOCK TO TRANSFER REFRIGERANT NUMBER, NO. OF FLUID NODES,
C NUMBER OF NON-FLUID NODES, the number of controller variables, the
C number of state variables, the flag IK1, and the (internal) node
C numbers corresponding to the loop start and loop end for each
C loop.  Sensor station numbers can also be transferred in
C this COMMON block.  The order of all variables in this block up
C to and including IK1 must be as shown.  Thereafter, the order
C need only be consistent with VARIABLES 1, VARIABLES 2, and OUTPUT
C CALLS.
F     COMMON/SYSDEF/LREF,NFN,NNFN,NCTRL,NSV,IK1,LOOPS1,
F    &              LOOPE1
C SCRATCH ARRAY THAT IS ALWAYS DIMENSIONED AT 30
F     COMMON/SCRATCH/SCR(30)
C COMMON BLOCK FOR TRANSFERRING CONSTANTS, ALWAYS DIMENSIONED AT 5
F     COMMON/CONST/CONS(5)
C SINDA COMMON BLOCK NEEDED TO DEFINE THE NUMBER OF NODES
F     COMMON/POINTN/LNODE,LCOND,LCONS,LARRY,ICOMP
C COMMON BLOCKS TO TRANSFER COMPUTED DATA FROM FLUIDS SIMULATION.
C CURRENTLY SET FOR A MAXIMUM NUMBER OF STATE VARIABLES (MNSV) = 49.
C DIM'S MUST BE: SM(MNSV+1,MNSV+2),LR(MNSV+1),LC(MNSV+2),SE(MNSV,MNSV),
C EE(MNSV,MNSV),DX(MNSV,3),DR(MNSV,3),ER(2),XX(MNSV),MNX(MNSV)
F     COMMON/SOL1/SM(50,51),LR(50),LC(51),SE(49,49),EE(49,49),DX(49,3),
F    * DR(49,3),ER(2),XMIN,XX(49)
F     EQUIVALENCE (NX(1),X(1))
C DATA STATEMENT TO DEFINE THE NO. OF CONTROLLERS (NCTRL), NO. OF STATE
C VARIABLES (NSV) in this problem.  The initial values of the flags
C ISTOP and IK1 are always 0 and -1, respectively.
F     DATA NCTRL,NSV,ISTOP,IK1/0,4,0,-1/
C DATA STATEMENT TO INITIALIZE FLOW, PRESSURE, ENTHALPY, QUALITY for
C every fluid station in the system.  The number of values must equal
C the number in the DIMENSION statement above.
F     DATA FLOW1,P1,EN1,QUAL1
F    &    /25*9.9,25*140.,25*90.,25*0./
C The following DATA STATEMENT defines XMIN, the convergence criterion
C for the COMPOSITE CHANGE IN THE CONTROLLER VARIABLES:
C   Composite change = SQRT(SUM OF SQUARES OF CHANGE IN CONTROLLER STATE
C                           VARIABLES FROM PREVIOUS ITERATION)
C                    divided by  (NO. OF CONTROLLER STATE VARIABLES)
C                    = SQRT(SUM(DX(I)**2)/NCTRL)
C SCX, THE SOLUTION ROUTINE, ASSUMES CONVERGENCE composite change is
C less than XMIN. The DATA statement also defines XX(I) = MAXimum
C allowable CHANGE IN CONTROLLER STATE VARIABLES in any one iteration.
C SCX LIMITS EACH DX(I) TO BE LESS THAN XX(I).  THE NUMBER OF VALUES
C ASSIGNED TO XX(I) MUST BE THE SAME AS MNSV.
F     DATA XMIN,XX/0.00001,2.,.05,0.015,0.015,45*.01/
C DATA STATEMENT TO SET UP PERMISSIBLE ERRORS IN ERROR VARIABLES.  SCX
C assumes that convergence has been attained if
C       SQRT( SUM((EVS(I)/PE(I))**2) / NSV ) is less than 1.0
```

C-2

```
C where EVS is the error variable at the end of a step (i.e., not at the
C end of a perturbation).
F     DATA PE/7*0.01/
C DATA STATEMENT TO DEFINE MAXIMUM NO. OF ITERATIONS TO MAKE IN FLUIDS
C SOLUTION (ISOLX), DEFINE THE unit number (NOUT) where the output data
C from SINDA will be printed, AND SET THE DAMPING FACTOR FOR SUCCESSIVE
C SCX ITERATIONS (IDAMP).  WE SET ISOLX=200 FOR FIRST TIME STEP, BECAUSE
C WE MIGHT BE FAR FROM THE SOLUTION.  WE DECREASE ISOLX TO 60 FOR LATER
C TIMES.  See Section 3.1.3 for an explanation of ISOLX and IDAMP.
C FAC CHANGED ISOLX FORM 200 TO 20 TO WATCH TRENDS
F     DATA ISOLX,NOUT,IDAMP/200,6,8/
C DATA STATEMENT TO SET UP CONVERSION CONSTANTS: PI,LBM/SLUG,FT-LB/BTU,
C SQ.IN./SQ.FT., STEPHAN-BOLTZMAN CONSTANT
F     DATA CONS/3.14159,32.17,778.,144.,0.1713E-08/
C INCLUDE THE USUAL SINDA EXECUTION STATEMENTS.  THESE MUST BE INCLUDED
C BEFORE THE SINFAC STATEMENTS SO THE X ARRAY IS FILLED PROPERLY.
C NDIM must be equal to the dimension of the X array.
F     NDIM=5000
F     NTH=0
F     NLOOP=200
C IFIRST must be set equal to the node number of the first fluid node as
C listed in the NODE DATA block.
F     IFIRST=200
C Set up the list of fluid nodes:
F     CALL NNREAD(1)
F     I=0
F  10 I=I+1
F     IF(NX(LNODE+I).NE.IFIRST) GO TO 10
F     NFN=NNT-I+1
F     NNFN=NNT-NFN
F     DO 11 I=1,NFN
F     J=LNODE+NNFN+I
F  11 MNX(I)=NX(J)
C IDENTIFY THE INTERNAL NODE NUMBERS (LOOPS,LOOPE) CORRESPONDING TO
C   THE EXTERNAL LOOP-START AND LOOP-END NODE NUMBERS.  We do this once
C for the entire simulation only because we thereby save computation
C time.
F     LOOPS1=INNODE(1)
F     LOOPE1=INNODE(18)
C SELECT THE REFRIGERANT (E.G., NREF FOR R-11).  NREF defines the
C working fluid in the user's system.  See the description of the
C REFRIG-routine parameters in Appendix B to determine what value to use
C for NREF.
F     NREF=717
C SET THE MINIMUM PRESSURE (psia) YOU WILL ALLOW FOR THIS REFRIGERANT.
C Limiting PMIN to realistic values prevents the iterations in the
C refrigerant-properties routines from returning with unrealistic
C values.  If PMIN is set equal to zero, REFRIG will automatically reset
C PMIN to 1 percent of the critical pressure.
F     PMIN=40.
C CALL THE REFRIGERANT INITIALIZATION ROUTINE WITH THIS NREF AND PMIN.
C LREF is the internal refrigerant number, as computed by REFRIG and
C used in all refrigerant-properties subroutines and functions.
F     CALL REFRIG(NREF,LREF,PMIN)
C INITIALIZE THE FLOWS, PRESSURES, ENTHALPIES, AND QUALITIES.
F     DO 247 I=1,NFN
F     FLOW(I)=FLOW1(I)
```

```
F      P(I)=P1(I)
F      EN(I)=EN1(I)
C MAKE THE INITIAL CONDITIONS CONSISTENT (IN CASE NOT DONE IN DATA
C STATEMENT).  Notice that the pressure and enthalpy are specified by
C the user and that the temperature is computed.  The user may call any
C of the refrigerant routines to obtain other properties of the fluid as
C well.
F      IF(I.EQ.LOOPS1) P(I)=140.0
F      IF(I.EQ.LOOPS1) EN(I)=90.
C SET ACCUMULATOR ENTHALPY IN TWO-PHASE REGION (for this type of
C accumulator)
F      IF(MNX(I).EQ.200) EN(I)=60.
F      QUAL(I)=VQUALH(LREF,P(I),EN(I))
F      LT=I+NNFN
F      IF(QUAL(I).LT.0.) T(LT)=VTLIQ(LREF,P(I),EN(I))
F      IF(QUAL(I).GT.1.) CALL VTAV2(LREF,T(LT),DUMMY,P(I),EN(I))
F      T(LT)=T(LT)-459.67
F 247 CONTINUE
C INITIALIZE STATE VARIABLES
C FOR A CPL, THE STATE- AND ERROR-VARIABLE PAIRS ARE:
C          SV                    EV
C    ENTHALPY              ENTHALPY MISMATCH
C    FLOW RATE             PRESSURE MISMATCH
C    SPLIT RATIO 1         MERGE PRESSURE MISMATCH 2
C    SPLIT RATIO 2         MERGE PRESSURE MISMATCH 1
C THE CPE OUTLET QUALITY WILL ADJUST ITSELF ACCORDING TO THE PUMPING
C NEEDED.  THE QUALITY WILL BE APPROXIMATELY 1.0.
F      SV(1)=90.
F      SV(2)=9.9
F      SV(3)=0.17
F      SV(4)=0.78
           CNFRWD
        END
        BCD 3VARIABLES 1
C Specify the variable TYPE (FOR EXAMPLE, REAL MCDAC OR MERGEA) AND
C DIMENSION ALL ARRAYS NEEDED TO DEFINE COMPONENT CHARACTERISTICS.  An
C array is needed for each system component, although one array may
C apply to more than one component.  The array names are user selected,
C but the array dimension is always equal to that required by the
C component (see Appendix B).
F      DIMENSION ACCUMA(2),OAO1(16),OAO2(16), OAO3(16),OAOI(8),PUMPA(7),
F     &TCONDA(9),SPLITA(4),SPLITB(4),XMRGA(4),XMRGB(4),PIPEA(6),PIPEB(6)
C DIMENSION THE ARRAYS GIVING THE LIMITS OF THE STATE VARIABLES.  SV is
C kept between SVL and SVU.  By specifying reasonable values, the user
C can prevent the iteration procedure from making unreasonable
C "guesses".  The DIMENSION MUST BE EQUAL TO OR LARGER THAN NSV
F      DIMENSION SVL(7),SVU(7)
C DIMENSION ARRAY TO SAVE THE MAXIMUM STEP SIZE.  The dimension must be
C the same as for XX.
F      DIMENSION XXS(49)
F      DIMENSION TWALL(25)
C INCORPORATE SAME COMMON STATEMENTS AS USED IN EXECUTION BLOCK
F      COMMON/PRESS/P(25)
F      COMMON/FLOWS/FLOW(25)
F      COMMON/ENTH/EN(25)
F      COMMON/QUAL/QUAL(25)
F      COMMON/POWER/PWR(25)
```

```
F      COMMON/WEIGHT/WM(25)
F      COMMON/WFLUID/WF(5,25)
F      COMMON/ERR1/EV(7)/ERR2/EVS(7)/ERR3/IEV(7)/ERR4/PE(7)
F      COMMON /SV1/SV(7)/ SV2/SVS(7)/ SV3/ISV(7)
F      COMMON/SYSDEF/LREF,NFN,NNFN,NCTRL,NSV,IK1,LOOPS1,
F     &              LOOPE1
F      COMMON/IO/IDER,ISOL,ISOLX,IDUMP,NOUT,ISTOP,IDAMP,MNX(29)
C INCLUDE THE COMMON TO TRACK ERROR MESSAGES THAT CAN BE USED TO
C TERMINATE THE SIMULATION
F      COMMON/ERRMSG/IERRP,IERRM
F      COMMON/SCRATCH/SCR(30)
F      COMMON/CONST/CONS(5)
F      COMMON/POINTN/LNODE,LCOND,LCONS,LARRY,ICOMP
F      COMMON/SOL1/SM(50,51),LR(50),LC(51),SE(49,49),EE(49,49),
F     * DX(49,3),DR(49,3),ER(2),XMIN,XX(49)
C ENTER THE ARRAYS OF DATA DESCRIBING THE components.
C Appendix B describes each of the component routines and
C defines the parameters for wich the user must supply values in the
C DATA lines.  The names given to the DATA arrays must be identical to
C those selected by the user in the DIMENSION statement above.
F      DATA ACCUMA/1.0,2./
F      DATA OAO1/6.0, 12.0, 12.0, 6.0, 0.5, 0.89, 0.1, 0.5, 0.89, 0.938,
F     &          3.E-9, 410000., 4.E-4, 40., 250., 0.12/
F      DATA OAO2/6.0, 12.0, 12.0, 6.0, 0.5, 0.89, 0.1, 0.5, 0.89, 0.938,
F     &          3.E-9, 410000., 4.E-4, 40., 1000., 0.12/
F      DATA OAO3/6.0, 12.0, 12.0, 6.0, 0.5, 0.89, 0.1, 0.5, 0.89, 0.938,
F     &          3.E-9, 410000., 4.E-4, 40., 250., 0.12/
F      DATA OAOI/4.0, 4.0, 0.1, 0.89, 0.938, 3.E-9, 4.E-4, 0.12/
F      DATA PUMPA/0.9575, 12.2, 1500., 0.6, 0.4, 0.00027, 60./
F      DATA SPLITA/0.0355, 0.0067, 170., 2/
F      DATA XMRGA/0.0355, 0.0067, 170., 1/
F      DATA SPLITB/0.0355, 0.0067, 170., 2/
F      DATA XMRGB/0.0355, 0.0067, 170., 1/
F      DATA TCONDA/0.01,0.02,10.0,360.,0.5,1.0,0.023,100.,25./
F      DATA PIPEA/5.,0.0155,4.0,0.0017,170.,100./
F      DATA PIPEB/5.,0.0155,4.0,0.0017,170.,100./
C DEFINE THE upper and lower LIMITS OF THE STATE VARIABLES.
C THE NUMBER OF UPPER AND LOWER LIMITS MUST BE THE SAME AS THE DIMENSION
C NUMBER FOR THE STATE VARIABLES.
F      DATA SVL,SVU/ -50.,    0.01,  0.0,  0.0,   0.0,  0.0,  0.0,
F     &              200.,    200.,  1.0,  1.0,   1.0,  1.0,  1.0/
C STORE THE ARRAY OF MAXIMUM STEP SIZES
F      DATA XXS/49*0./
C SET ISTART=1 TO GET A SINGLE PASS THROUGH THE COMPONENTS TO CHECK
C SIZES.  SET ISTART.LT.1 TO GET NORMAL SIMULATION.  ISTART.GT.1 GIVES
C THE NORMAL SIMULATION PLUS SV,EV OUTPUT.  It is recommended that
C ISTART be set to 1 for the initial SINFAC simulation of a new case.
C Once the resulting data have been checked for reasonableness,
C including reasonable sizes, ISTART can be set to 0 for a complete
C simulation.
F      ISTART=0
C SET IDUMP=10 TO have COMPONENT PERFORMANCE DATA printed.  IDUMP allows
C varying amounts of data to be written to the output file.  If IDUMP is
C 0, only the fluid states are written.  If IDUMP is 10, detailed
C performance data are written for the component.  If IDUMP is 40, the
C input data to the component is printed (the array, such as PIPEA).  If
C IDUMP is 50 or 60, debugging data are printed; 60 yields more data
```

```
C than 50.  IDUMP greater than 10 should be used with caution, because
C the output can be inconveniently large.
F      IDUMP=0
C Set the various parameters before starting the iteration:
C SET THE COUNTERS FOR THE NUMBER OF TIMES THE CLACULATED
C PRESSURE WAS LESS THAN PMIN AND FOR THE NUMBER OF ERRORS MESSAGES.
F      IERRP=0
F      IERRM=0
C CONVERT ALL TEMPERATURES TO DEGREES RANKINE TO CONFORM WITH THE
C REFRIGERANT-PROPERTIES SUBROUTINES
F      DO 10 I=1,NNT
F   10 T(I)=T(I)+459.67
C SET THE ITERATION COUNTER TO 0
F      ISOL=0
C RESET MAXIMUM STEP SIZE IN SCX TO ORIGINAL VALUE, BUT ALLOW FOR
C EXPERIENCE OF PREVIOUS SOLUTION TO CHANGE XX SLIGHTLY
F      IF(ISTOP.LE.0) THEN
F       DO 4 I=1,NSV
F    4  XXS(I)=XX(I)
F      ELSE
F       DO 6 I=1,NSV
F       XX(I)=0.9*XXS(I)+0.1*XX(I)
F    6  XXS(I)=XX(I)
F      END IF
C SET THE derivative COUNTER (IDER) TO ZERO.  RETURN TO 11 AFTER MAKING
C STEP TO NEW TRIAL SOLUTION (NEW SET OF STATE VARIABLES)
F   11 IDER=0
F      ISOL=ISOL+1
C ZERO THE MATRIX OF DERIVATIVES
F      DO 12 I=1,NSV
F      DO 12 J=1,NSV
F   12 SM(I,J)=0.
C FORCE THE STATE VARIABLES TO BE WITHIN THEIR LIMITS
F      DO 121 I=1,NSV
F      IF(SV(I).LT.SVL(I)) THEN
F        SV(I)=SVL(I)+(SV(I)-SVL(I))/1000.
F        WRITE(NOUT,9050) I
F      END IF
F      IF(SV(I).GT.SVU(I)) THEN
F        SV(I)=SVU(I)+(SV(I)-SVU(I))/1000.
F        WRITE(NOUT,9051) I
F      END IF
F  121 CONTINUE
F9050 FORMAT('  THE STATE VARIABLE SV(',I2,') WAS LESS THAN ITS
F     &LOWER LIMIT')
F9051 FORMAT('  THE STATE VARIABLE SV(',I2,') EXCEEDED ITS
F     &UPPER LIMIT')
F      GO TO 122
C RETURNS TO 13 TO EVALUATE DERIVATIVES BY PERTURBATION METHOD.
F   13 CONTINUE
C FORCE THE PERTURBED STATE VARIABLE TO BE WITHIN ITS LIMITS
F      IF(SV(IDER).LT.SVL(IDER)) THEN
F        SV(IDER)=SVL(IDER)+(SV(IDER)-SVL(IDER))/1000.
F        WRITE(NOUT,9050) IDER
F      END IF
F      IF(SV(IDER).GT.SVU(IDER)) THEN
F        SV(IDER)=SVU(IDER)+(SV(IDER)-SVU(IDER))/1000.
```

```
F       WRITE(NOUT,9051) IDER
F     END IF
C PUT THE STATE VARIABLES IN THE APPROPRIATE SINFAC VARIABLES
C RETURN HERE AFTER convergence HAS BEEN OBTAINED TO GET COMPONENT DATA
F 122 CONTINUE
F     EN(LOOPS1)=SV(1)
F     FLOW(LOOPS1)=SV(2)
F     SPL1=SV(3)
F     SPL2=SV(4)
C TO BE CONSISTENT, WE MUST COMPUTE THE TEMPERATURE
F     CALL VALLPH(LREF,T(NNFN+LOOPS1),V,QUAL(LOOPS1),HFG,HG,
F    &  P(LOOPS1),EN(LOOPS1))
C FOR THIS PROBLEM, WE USE TIME=0 AND THE FIRST TIME STEP TO CALCULATE
C THE CONDITIONS IN THE ACCUMULATOR AT THE BEGINNING OF THE PROBLEM OF
C INTEREST.  WE NEED THE FIRST TIME STEP SO THAT THE TEMPERATURES MATCH
C THE ENTHALPIES -- WE DON'T TRUST OURSELVES TO HAVE INPUT INITIAL
C TEMPERATURES THAT ARE CONSISTENT WITH THE PRESSURES AND ENTHALPIES.
C WE MAKE Q INTO EVAP BE A RAMP, TO MAKE THE PROBLEM MORE INTERESTING.
C IF IDER FLAG IS -1, SOLUTION HAS BEEN OBTAINED.  SET IDUMP=10 TO GET
C ALL COMPONENT PERFORMANCE DATA PRINTED.
F     IF(IDER.EQ.-1) IDUMP=10
F     IF(ISTART.EQ.1) IDUMP=40
C Call the component subroutines according to the directions in Appendix
C B.  The sequence of component calls should be in the direction of flow
C in the system so that the output of one component is the input of the
C next, at least to the extent possible.  Where this input-output
C relationship is not possible, use a LOOP-START and state and error
C variables to "guess" the input conditions.
M     CALL PUMP(LREF,1,1,2,PUMPA,1400.)
M     CALL RPIPE(LREF,1,2,3,PIPEA,530.,TWALL)
M     CALL SPLITR(LREF,1,3,4,5,SPLITA,SPL1)
M     CALL SPLITR(LREF,1,5,6,7,SPLITB,SPL2)
F     CALL OAOISOL(LREF,1,4,8,1,OAOI)
F     CALL OAOISOL(LREF,1,6,9,1,OAOI)
F     CALL OAOISOL(LREF,1,7,10,1,OAOI)
M     CALL OAOVAP(LREF,1,8,11,T103,OAO3,1.0)
M     CALL OAOVAP(LREF,1,9,12,T105,OAO2,1.0)
M     CALL OAOVAP(LREF,1,10,13,T107,OAO1,1.0)
M     CALL MERGE(LREF,1,13,12,14,XMRGA,DP12A)
M     CALL MERGE(LREF,1,14,11,15,XMRGB,DP12B)
M     CALL RPIPE(LREF,1,15,16,PIPEB,530.,TWALL)
M     CALL TCOND(LREF,1,16,17,TCONDA,T109,TWALL)
M     CALL ACCUM1(LREF,1,17,18,200,ACCUMA,DTIMEU,0.0)
C COMPUTE THE ERROR VARIABLES
F     EV(1)=EN(LOOPS1)-EN(LOOPE1)
F     EV(2)=P(LOOPS1)-P(LOOPE1)
F     EV(3)=DP12B
F     EV(4)=DP12A
C Use the following 4 lines to get a single pass for checking the input
C data and the equipment sizing:
F     IF(ISTART.GE.1) THEN
F       WRITE(NOUT,9000) ISOL,IDER,((I,SV(I),EV(I)),I=1,NSV)
F     IF(ISTART.EQ.1)THEN
F       CALL OUTCAL
F       CALL EXIT
F     END IF
F     END IF
```

```
F      IF(IDER.EQ.-1) GO TO 99
F9000 FORMAT(' ISOL:',I7,' IDER:',I7,/,
F     & ' I',5X,'SV(I)',10X,'EV(I)',7(/,I2,2E15.7))
C      IF(IDER.EQ.0) WRITE(NOUT,9000) ISOL,IDER,
C     &  ((I,SV(I),EV(I)),I=1,NSV)
C CALL THE SOLUTION ROUTINE.  Set the perturbation fraction (usually
C 0.0001) for computing the derivatives of the ev's with respect to the
C sv's.  Perturbation factors of 0.01 have been needed when the ev's are
C insensitive to the sv's (e.g., in capillary-pumped systems)
F      CALL SCX(0.005,RMS)
C The user can select from one or more of the following lines if he
C wants to stop the computation if any of the following error conditions
C occur (see the FORMAT statement for the error description).  We stop
C by making ISTART=1 so all flows, pressures, etc., will be printed.
F      IF(IERRP.GT.0) THEN
F        WRITE(NOUT,9111)
F9111    FORMAT(' COMPUTATIONS STOPPED BECAUSE A PRESSURE WAS LESS '
F     &  'THAN PMIN')
F        ISTART=1
F      END IF
C THE VARIOUS SINFAC ROUTINES WRITE ERROR MESSAGES (E.G., ITERATIONS
C EXCEEDED), TRY TO CORRECT THE ERRORS, AND CONTINUE COMPUTING.  THE
C USER CAN LIMIT THE NUMBER OF ERROR MESSAGES BEFORE STOPPING THE
C SIMULATION:
F      IERRMX=2000
F      IF(IERRM.GT.IERRMX) THEN
F        WRITE(NOUT,9112) IERRM,IERRMX
F9112    FORMAT(' COMPUTATIONS STOPPED BECAUSE NUMBER OF ERROR '
F     &  'MESSAGES PRINTED (',I5,'),'/,' EXCEEDS USER-SELECTED ',
F     &  'ALLOWABLE,',I5)
F        ISTART=1
F      END IF
F      DO 912 I=1,NSV
F      IF(SV(I).LT.SVU(I).AND.SV(I).GT.SVL(I)) GO TO 912
F      WRITE(NOUT,9121) I,SV(I),SVL(I),SVU(I)
F9121 FORMAT(' COMPUTATIONS STOPPED BECAUSE SV(',I5,')= ',E14.7,
F     & ', WHICH IS OUT',/,' OF YOUR SPECIFIED RANGE:',E14.7,' TO',
F     & E14.7)
F      ISTART=1
F 912 CONTINUE
C The following write statement is frequently useful in studying the
C cause for non-convergence.  Watch the progress of RMS, which should
C progress toward 1.0, then jump if the controller variables are
C adjusted.  The RMS after the jumps should also progress toward 1.0.
C      IF(IDER.EQ.0) WRITE(NOUT,1003) ISOL,RMS
C1003 FORMAT(' ISOL:',I5,' SCALED RMS:',E14.7)
C AFTER COMPLETING FIRST PASS ON ENTIRE SYSTEM, SET FLAG SO COMPONENT
C COMPUTATIONAL SEQUENCE IS NOT RE-COMPUTED FOR EACH ITERATION AND TIME
C STEP.  SCX USES ISTOP ALSO, SO ISTOP=1 MUST BE SET AFTER SCX
F      ISTOP=1
C RETURN TO VARIOUS STATEMENTS DEPENDING ON IDER FLAG.  IF IDER=-1,
C SOLUTION HAS BEEN OBTAINED.
F      IF(IDER) 122,11,13
M  99 CONTINUE
F      WRITE(6,1004)OAO1(15),OAO2(15),OAO3(15)
F1004 FORMAT(/,' Q1 = ',F12.1,'  Q2 = ',F12.1,'  Q3 = ',F12.1)
C The user many want to stop the computations if the number of
```

```
C iterations exceed the maximum number allowable
F      IF(ISOL.LT.ISOLX) GO TO 913
F      WRITE(NOUT,9131) ISOL,ISOLX,RMS
F9131 FORMAT(' COMPUTATIONS STOPPED BECAUSE NUMBER OF FLUIDS ',
F     &  'ITERATIONS, ',I5,/,' EXCEEDED YOUR LIMIT, ',I5,'.  RMS ',
F     &  '(ERROR/PERMISSIBLE ERROR) = ',E14.7)
F 913 CONTINUE
C In most cases, the heat-transfer between the fluid nodes and a solid
C node should be included via the heating rate, q, rather than the
C conductance, g, because q will preserve the global energy balance.
C Such flow-dependent heating rates are not needed for this problem but
C would be entered with statements such as the following:
CF      i=innode(2)
CF      j=innode(3)
CM      q20=flow(i)*(en(i)-en(j))
C Note that q20 is the heat into the solid node; the equation for q20 is
C based on node i being upstream of node j.
C In some cases, a one-way conductance may depend on the fluid flow.
C For example, the effluent from a SINFAC station may be the input to a
C detailed model of a pipe having single-phase flow.  In such a case,
C the one-way conductance would be entered with statements such as the
C following:
CF      i=innode(2)
CM      g10=flow(i)*vcpf(lref,p(i),t(nnfn+i))
C RECONVERT THE TEMPERATURES TO DEGREES F TO CONFORM WITH SINDA
F      DO 930 I=1,NNT
F 930 T(I)=T(I)-459.67
C RESET THE IK1 FLAG TO -1 SO FLUIDS SOLUTION ROUTINE (SCX) KNOWS
C THAT, AT NEXT CALL, IT IS SOLVING AT NEW TIME STEP.
F      IK1=-1
        END
        BCD 3VARIABLES 2
        END
        BCD 3OUTPUT CALLS
C INCORPORATE SAME COMMON STATEMENTS AS USED IN EXECUTION BLOCK
F      COMMON/PRESS/P(25)
F      COMMON/FLOWS/FLOW(25)
F      COMMON/ENTH/EN(25)
F      COMMON/QUAL/QUAL(25)
F      COMMON/POWER/PWR(25)
F      COMMON/WEIGHT/WM(25)
F      COMMON/WFLUID/WF(5,25)
F      COMMON/ERR1/EV(7)/ERR2/EVS(7)/ERR3/IEV(7)/ERR4/PE(7)
F      COMMON /SV1/SV(7)/ SV2/SVS(7)/ SV3/ISV(7)
F      COMMON/SYSDEF/LREF,NFN,NNFN,NCTRL,NSV,IK1,LOOPS1,
F     &              LOOPE1
F      COMMON/IO/IDER,ISOL,ISOLX,IDUMP,NOUT,ISTOP,IDAMP,MNX(29)
F      COMMON/SCRATCH/SCR(30)
F      COMMON/CONST/CONS(5)
F      COMMON/SOL1/SM(50,51),LR(50),LC(51),SE(49,49),EE(49,49),
F     & DX(49,3),DR(49,3),ER(2),XMIN,XX(49)
F      COMMON/POINTN/LNODE,LCOND,LCONS,LARRY,ICOMP
C USE THE EQUIVALENCE STATEMENT TO CARRY DATA FROM SINDA'S X ARRAY
F      EQUIVALENCE (NX(1),X(1))
C PRINT THE STATES AT EACH FLUID NODE
F      IF(DTIMEU.EQ.0.) THEN
F        WRITE(NOUT,88)
```

```
F       ELSE
F        WRITE(NOUT,89) TIMEO
F      END IF
F   88 FORMAT(/,' INITIAL CONDITIONS FOR FLUID LOOP.  TEMPERATURES',
F     & ' ARE INPUT VALUES.',/,' THEY MAY NOT BE CONSISTENT WITH',
F     & ' THE PRESSURE AND ENTHALPY.')
F   89 FORMAT(/,' FLUIDS SOLUTION.  SETS BOUNDARY NODES FOR TIME =',
F     & E14.7)
F      WRITE(6,90)
F   90 FORMAT('  NODE NO.       LB/HR        P(PSIA)     T(F)',
F     *'          EN(BTU/LB)  QUALITY')
F      WRITE(6,95)((NX(LNODE+I+NNFN),FLOW(I),P(I),T(I+NNFN),
F     *  EN(I),QUAL(I)),I=1,NFN)
F 95   FORMAT(I8,5X,5F12.5)
F      DELP1=P(14)-P(11)
F      DELP2=P(13)-P(10)
F      DELP3=P(12)-P(9)
F      DELPP=P(3)-P(2)
F      WRITE(6,1003)DELP1,DELP2,DELP3
F1003 FORMAT(/,' DELP1 = ',F12.5,'  DELP2 = ',F12.5,'  DELP3 = ',F12.5)
F      WRITE(6,1005)DELPP
F1005 FORMAT(' DELP PUMP = ',F12.5)
F      IF(ISOL.GE.ISOLX) GO TO 98
F      WRITE(6,97) ISOL
F 97   FORMAT(/,' FLUID LOOP WAS SOLVED IN',I5,' TRIES.',/)
F      GO TO 99
F 98   WRITE(6,981) ISOL
F 981 FORMAT(/,' FLUID LOOP WAS NOT SOLVED EVEN AFTER',I5,' TRIES.',/)
F 99   CONTINUE
C RESET ISOLX TO 60 FOR NEXT TIME STEPS
F      ISOLX=60
C THE FLUID COMPUTATIONS ARE FOR PREVIOUS TIME STEP IN CNFRWD,
C BECAUSE EXPLICIT INTEGRATION IS USED.
            TPRINT
F      WRITE(6,94)
F   94 FORMAT(//,' STARTING COMPUTATIONS FOR NEXT TIME PERIOD',//)
        END
        BCD 3END OF DATA
```

NASA
National Aeronautics and Space Administration

# Report Documentation Page

| 1. Report No. | 2. Government Accession No. | 3. Recipient's Catalog No. |
|---|---|---|
| NASA TM-4051 | | |

**4. Title and Subtitle**
Design and Testing of a High Power Spacecraft Thermal Management System

**5. Report Date**
June 1988

**6. Performing Organization Code**
732.2

**7. Author(s)**
Michael E. McCabe, Jr., Dr. Jentung Ku, and Dr. Steve Benner

**8. Performing Organization Report No.**
88B0167

**10. Work Unit No.**

**9. Performing Organization Name and Address**
Goddard Space Flight Center
Greenbelt, Maryland 20771

**11. Contract or Grant No.**
NAS5-28626

**13. Type of Report and Period Covered**
Technical Memorandum

**12. Sponsoring Agency Name and Address**
National Aeronautics and Space Administration
Washington, D.C. 20546-0001

**14. Sponsoring Agency Code**

**15. Supplementary Notes**
Dr. Ku is employed by the OAO Corporation, Greenbelt, Maryland; Dr. Benner is employed with TS Infosystems, Inc., Lanham, Maryland; Mr. McCabe is employed by NASA/GSFC, Greenbelt, Maryland.
A portion of this work was sponsored by the U.S. Air Force, AFWAL, Thermal Technology Group, Wright-Patterson Air Force Base, Dayton, Ohio.

**16. Abstract** This report presents the design and test results of an ammonia hybrid capillary pumped loop thermal control system which could be used for heat acquisition and transport on future large space platforms and attached payloads, such as those associated with the NASA Space Station. The High Power Spacecraft Thermal Management System (HPSTM) can operate as either a passive, capillary-pumped two-phase thermal control system, or, when additional pressure head is required, as a mechanically-pumped loop. Testing has shown that in the capillary-mode, the HPSTM evaporators can acquire a total heat load of between 600 W and 24 kW, transported over 10 meters, at a maximum heat flux density of 4.3 W/cm$^2$. With the mechanical pump circulating the ammonia, a heat acquisition potential of 52 kW (9 W/cm$^2$ heat flux density) has been demonstrated for 15 minutes without an evaporator failure. These results represent a significant improvement over the maximum transport capability previously displayed in other capillary systems. The HPSTM system still retains the proven capillary capabilities of heat load sharing and flow control between evaporator plates, rapid power cycling, and nonuniform heating in both the capillary and hybrid operating modes. A computer model confirmed pressure drop measurements in various operating scenarios.

| 17. Key Words (Suggested by Author(s)) | 18. Distribution Statement |
|---|---|
| Space Station Thermal Control, Capillary Pumped Loop, Two-Phase Heat Transfer, Hybrid Thermal Control Systems, Instrument Thermal Bus, Ammonia-Based Thermal Control Systems | Unclassified - Unlimited<br>Subject Category 18 |

| 19. Security Classif. (of this report) | 20. Security Classif. (of this page) | 21. No. of pages | 22. Price |
|---|---|---|---|
| Unclassified | Unclassified | 112 | A06 |